

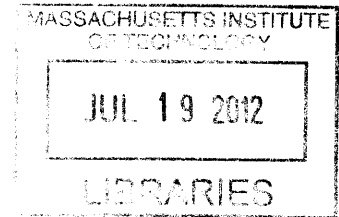
# Development of New Tools for the Production of Plasmid DNA Biopharmaceuticals

by

**Diana M. Bower**

B.S. Chemical Engineering  
The Pennsylvania State University, 2006

**ARCHIVES**



Submitted to the Department of Chemical Engineering  
in Partial Fulfillment of the Requirements for the Degree of

Doctor of Philosophy in Chemical Engineering

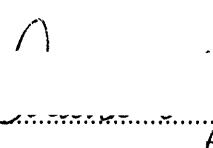
at the

Massachusetts Institute of Technology

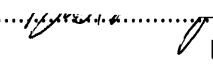
June 2012

©2012 Massachusetts Institute of Technology  
All rights reserved


Signature of Author .....

  
Diana M. Bower  
Department of Chemical Engineering  
May 16, 2012

Certified by .....

  
Kristala L. Jones Prather  
Associate Professor of Chemical Engineering  
Thesis Supervisor

Accepted by .....

  
Patrick S. Doyle  
Professor of Chemical Engineering  
Chairman, Committee for Graduate Students

# Development of New Tools for the Production of Plasmid DNA Biopharmaceuticals

by

**Diana M. Bower**

Submitted to the Department of Chemical Engineering on May 16, 2012  
in Partial Fulfillment of the Requirements for the Degree of  
Doctor of Philosophy in Chemical Engineering

## **Abstract**

DNA vaccines and gene therapies that use plasmid DNA (pDNA) as a vector have gained attention in recent years for their good safety profile, ease of manufacturing, and potential to treat a host of diseases. With this interest comes increased demand for high-yield manufacturing processes. Overall, this thesis aims to develop new, innovative tools for the production of plasmid DNA biopharmaceuticals.

As one part of this thesis, we designed a 1-mL fed-batch microbioreactor with online monitoring and control of dissolved oxygen, pH, and temperature, as well as continuous monitoring of cell density. We used the microbioreactors to scale down temperature-induced production of a pUC-based DNA vaccine vector, pVAX1-GFP. Scaled-down processes can facilitate high-throughput, low-cost bioprocess development. We found that the microbioreactors accurately reproduced the behavior of a bench-scale bioreactor as long as key process parameters, such as dissolved oxygen, were held constant across scales. The monitoring capabilities of the microbioreactors also provided enhanced process insight and helped identify conditions that favored plasmid amplification.

A second aspect of this thesis involved construction and characterization of a new DNA vaccine vector based on a runaway replication mutant of the R1 replicon. Runaway replication plasmids typically show increased amplification after a temperature upshift. However, we found that our new vector, pDMB02-GFP, gave higher yields during constant temperature culture at 30°C, reaching a maximum of 19 mg pDNA/g DCW in shake flasks. We gained mechanistic insight into this behavior by measuring RNA and protein expression levels of RepA, a plasmid-encoded protein required for initiation of replication at the R1 origin. Through these studies we found that RepA levels may limit plasmid amplification at 42°C, and relieved this limitation by increasing RepA translation efficiency via a start codon mutation. We also scaled up production of pDMB02-GFP at 30°C from 50-mL shake flasks to 2-L bioreactors. Initial scale up efforts resulted in increased growth rate compared to the shake flasks, accompanied by very low plasmid yields. Decreasing the growth rate by limiting dissolved oxygen increased plasmid specific yield and emerged as a viable strategy for maintaining productivity during scale up.

Thesis Supervisor: Kristala L. Jones Prather  
Title: Associate Professor of Chemical Engineering

# Acknowledgements

---

Without the guidance, support, and encouragement of a host of individuals this thesis would not have been possible. I would like to thank my thesis committee, Prof. Charles Cooney, Prof. Dane Wittrup, and Prof. Tony Sinskey for pushing me to look deeper into the phenomena observed in my research; the perspectives of both biologists and chemical engineers helped shape my thesis into a work that could be appreciated by both disciplines. I would also like to acknowledge the funding sources that made this project possible: the MIT-Portugal Program and Pfizer.

I am also grateful for my collaborators, Prof. Rajeev Ram and Dr. Kevin Lee. Kevin was a joy to work with on the microbioreactors project and I learned so much during our time working together. My undergraduate researcher Shan Tie laid the assay-development groundwork for the RNA expression analysis in this thesis, and her help was greatly appreciated.

I am very grateful for the mentorship and guidance of my thesis advisor, Kris Prather. During my time at MIT, her advice, encouragement, and enthusiasm kept me going, even during the toughest moments. She realized that grad school doesn't happen in a vacuum and always knew how to give me the perspective I needed.

Without my labmates, life in the Prather Lab would not have been nearly as memorable. I am incredibly grateful for our many conversations about both science and life, and will miss our pot-lucks, camping trips, and other lab outings. Kevin Solomon and Himanshu Dhamankar have been great sources of advice, as well as travel companions and gym buddies. I'd like to thank Geisa Lopes for being a great friend and co-author, for all of our talks about plasmid DNA, and for taking the strain engineering project and turning it into a great piece of science. Gwen Wilcox kept the lab running and kept all of us in line – she was great to work with and a huge asset to the group.

Last, but not least, I would like thank my family and friends for their support during my graduate school career. My mom, Kathy Wright, has always believed in me and her confidence that I will succeed is a constant source of inspiration. Finally, my fiancé, Trevor Ritz, was truly my rock during my years at MIT. I am forever grateful for his unwavering love and support.

DIANA M. BOWER

# Table of Contents

---

|   |    |
|---|----|
| <b>Abstract</b> .....   | 2  |
| <b>Acknowledgements</b> .....   | 3  |
| <b>List of Figures</b> .....  | 6  |
| <b>List of Tables</b> .....   | 10 |
| <b>Chapter 1: Introduction</b> .....  | 11 |
| Abstract.....   | 11 |
| 1.1 Engineering of bacterial strains and vectors for the production of plasmid DNA:<br>A literature review..... | 12 |
| 1.1.1 Background.....   | 12 |
| 1.1.2 Engineering to maintain sequence stability.....   | 15 |
| 1.1.3 Engineering to promote safety.....  | 18 |
| 1.1.4 Engineering to increase plasmid DNA yield.....  | 22 |
| 1.1.5 Engineering to address downstream processing and purification issues.....                                 | 24 |
| 1.1.6 Future directions.....  | 25 |
| 1.2 Motivation and thesis aims.....   | 26 |
| 1.3 Thesis organization.....  | 28 |
| <b>Chapter 2: Fed-batch microbioreactors</b> .....  | 29 |
| Abstract.....   | 29 |
| 2.1 Introduction.....   | 30 |
| 2.2 Materials and Methods.....  | 32 |
| 2.2.1 Plasmid and strain.....   | 32 |
| 2.2.2 Culture medium.....   | 32 |
| 2.2.3 Plasmid DNA production process.....   | 32 |
| 2.2.4 Microbioreactor device design.....  | 33 |
| 2.2.5 Microbioreactor cultures.....   | 34 |
| 2.2.6 Bioreactor cultures.....  | 35 |
| 2.2.7 Measurement of glycerol and acetate concentrations.....   | 36 |
| 2.2.8 Measurement of plasmid copy number.....   | 37 |
| 2.2.9 Measurement of plasmid DNA specific yield.....  | 37 |
| 2.2.10 pDNA quality analysis.....   | 38 |
| 2.3 Results and Discussion.....   | 38 |
| 2.3.1 Plasmid production in bench-scale bioreactors as a model system.....                                      | 38 |
| 2.3.2 Plasmid production in microbioreactors.....   | 41 |
| 2.3.3 Plasmid quality assessment.....   | 44 |
| 2.3.4 Impact of oxygen availability.....  | 45 |
| 2.3.5 Bench-scale bioreactors with oxygen supplementation.....  | 47 |
| 2.3.6 Oxygen-limited microbioreactors.....  | 49 |
| 2.4 Conclusions.....  | 51 |
| <b>Chapter 3: New plasmid DNA vaccine vectors with R1-based replicons</b> .....                                 | 53 |
| Abstract.....   | 53 |
| 3.1 Introduction.....   | 54 |
| 3.2 Materials and Methods.....  | 55 |
| 3.2.1 <i>E. coli</i> strains and plasmids.....  | 55 |



|  |            |
|--|------------|
| 3.2.2 Preparation of working seed banks .....                  | 57         |
| 3.2.3 Culture conditions .....                                 | 58         |
| 3.2.4 Measurement of plasmid copy number.....                  | 58         |
| 3.2.5 Measurement of plasmid DNA specific yield.....           | 59         |
| 3.2.6 Quantitative real-time PCR.....                          | 60         |
| 3.2.7 Immuno-detection of RepA protein .....                   | 61         |
| 3.2.8 Cloning and expression of <i>repA</i> .....              | 62         |
| 3.2.9 Plasmid quality assessment .....                         | 63         |
| <b>3.3 Results &amp; Discussion.....</b>                       | <b>63</b>  |
| 3.3.1 Characterization of plasmid yield .....                  | 63         |
| 3.3.2 Impact of seed growth phase on yield.....                | 66         |
| 3.3.3 Quantification of <i>repA</i> gene expression.....       | 67         |
| 3.3.4 Role of RepA protein expression levels.....              | 69         |
| 3.3.5 Plasmid quality .....                                    | 72         |
| <b>3.4 Conclusions.....</b>                                    | <b>73</b>  |
| <b>Chapter 4: Scale up of R1-based vector production .....</b> | <b>75</b>  |
| Abstract .....   | 75         |
| <b>4.1 Introduction.....</b>                                   | <b>76</b>  |
| <b>4.2 Materials and Methods .....</b>                         | <b>78</b>  |
| 4.2.1 Plasmid and strain .....                                 | 78         |
| 4.2.2 Preparation of working seed banks .....                  | 78         |
| 4.2.3 Culture medium.....                                      | 78         |
| 4.2.4 Shake flask cultures .....                               | 79         |
| 4.2.5 Fed-batch bioreactor cultures .....                      | 80         |
| 4.2.6 Batch bioreactor cultures .....                          | 81         |
| 4.2.7 Measurement of glycerol and acetate concentrations ..... | 81         |
| 4.2.8 Measurement of plasmid DNA specific yield.....           | 82         |
| <b>4.3 Results and Discussion .....</b>                        | <b>83</b>  |
| 4.3.1 Process medium design .....                              | 83         |
| 4.3.2 Scale up challenges.....                                 | 86         |
| 4.3.3 Batch bioreactor with growth rate control .....          | 87         |
| <b>4.4 Conclusions.....</b>                                    | <b>89</b>  |
| <b>Chapter 5: Conclusions &amp; Recommendations .....</b>      | <b>91</b>  |
| Abstract .....   | 91         |
| <b>5.1 Summary.....</b>  | <b>92</b>  |
| <b>5.2 Recommendations for future work.....</b>                | <b>93</b>  |
| <b>References .....</b>  | <b>96</b>  |
| <b>Appendix A .....</b>  | <b>105</b> |
| <b>Appendix B.....</b>   | <b>107</b> |

# List of Figures

---

**Figure 1-1.** Strain engineering strategies. The parent strain at the center of the diagram represents any *E. coli* K-12 strain, and the potential modifications to this strain are illustrated. The strain’s genome can be modified subtly by single gene knockouts or implementation of an antibiotic-free selection system. More dramatic modifications such as genome reduction can be used to remove mobile elements like insertion sequences. Other strategies aim to ease downstream processing, like expression of heterologous periplasmic nucleases to degrade host genomic DNA and RNA after cell lysis. Changing the parent strain from K-12 to B has also been investigated to improve pDNA production. Note that the engineering strategies are shown as independent of one another, but applying several strategies in parallel to a single strain is possible as well. ....13

**Figure 1-2.** Vector engineering strategies. A generic plasmid DNA vaccine or gene therapy vector is shown with the important features labeled. The bacterial elements required for propagation of the plasmid in *E. coli* are the selectable marker (kanamycin resistance gene, Kan<sup>R</sup>) and the pUC origin of replication. The eukaryotic elements of the vector required for *in vivo* efficacy include the eukaryotic promoter/enhancer (P<sub>euk</sub>), therapeutic or antigentic gene, and poly-adenylation signal (polyA). The goal of each vector engineering strategy is described next to the vector feature targeted for modification.....14

**Figure 2-1.** (A) Photograph of the fed-batch microbioreactor device with key features indicated. (B) Schematic of the microbioreactor highlighting details of the liquid flow path and valve design. The dotted boxes indicate that the valves are shared and act as a single unit. Valves are numbered V1 – V9. V1 controls flow from the solution input bottles (water, feed, and base); V2, V3, and V4 allow selection of output from pressurized reservoirs; V5, V6, and V7 comprise the peristaltic pumps; V8 and V9 control output from device. The reservoirs also have a shared valve for pressurization (not shown). .....34

**Figure 2-2.** (A) Optical density, (B) glycerol, (C) acetate, and (D) average plasmid copy number profiles for bench-scale fed-batch cultures with initial specific feed rates of 2.6 (■), 3.2 (○), 3.5 (▲), and 6.1 (◇) g glycerol/L/hr. In each plot, from left to right, the arrows indicate the start of feeding and the 30°C-to-42°C temperature shift, respectively. The plasmid copy number error bars represent the 95% confidence interval calculated from three replicate wells of the same sample.....40

**Figure 2-3.** (A) Growth curves for the microbioreactor cultures at feed injection rates of 0.536 (light gray), 0.664 (dark gray), and 0.868 (black) injections per minute. (B) Glycerol, (C) acetate, and (D) average plasmid copy number profiles for microbioreactor fed-batch cultures with feed injection rates of 0.536 (■), 0.664 (○), and 0.868 (▲) injections per minute. In each plot, from left to right, the arrows indicate the start of feeding and the 30°C-to-42°C temperature shift, respectively. The plasmid copy number error bars represent the 95% confidence interval calculated from three replicate wells of the same sample. ....43

**Figure 2-4.** Agarose gel electrophoresis of plasmid DNA produced by the microreactors and bench-scale bioreactors. **Lane 1:** DNA ladder with DNA size in kilobases (kb) indicated to the left of the image, **Lane 2:** Linearized pVAX1-GFP, **Lane 3:** Nicked pVAX1-GFP, **Lane 4:** pVAX1-GFP from bench-scale reactor (3.5 g glycerol/L/hr), **Lane 5:** pVAX1-GFP from bench-scale reactor (2.6 g glycerol/L/hr), **Lane 6:** pVAX1-GFP from microreactor (0.868 inj/min), **Lane 7:** pVAX1-GFP from microreactor (0.536 inj/min). Only a representative set of pDNA samples is shown. pDNA from all feed rates had quality similar to or better than that shown. All samples were from the final timepoint of each culture (approximately 30 hours after inoculation). Note also that the pDNA in Lanes 4, 5, and 7 was purified from  $OD_{600} = 2$  pellets, whereas the number of cells used for the pDNA preparation in Lane 6 was not determined. ....44

**Figure 2-5.** Dissolved oxygen profiles from representative microreactor and bench-scale bioreactor cultures. (A) Dissolved oxygen profile from microreactor culture with 0.664 inj/min feed rate (black line). A moving average over a 20-point window is also shown for clarity (light gray line). The inset shows a zoomed-in version of the dissolved oxygen versus time plot overlaid with the feed injection profile. For each point in the feed injection profile, a value of 0 indicates that no feed injection took place at that time, while a value of 1 indicates that a feed injection took place. (B) Dissolved oxygen profiles from bench-scale bioreactor cultures at an initial specific feed rate of 3.2 g glycerol/L/hr with air only in the inlet gas (black line) and with oxygen supplementation (light gray line). ....46

**Figure 2-6.** (A) Optical density, (B) glycerol, (C) acetate, and (D) average plasmid copy number profiles for oxygen-supplemented bench-scale cultures with initial specific feed rates of 3.2 (○) and 6.1 (■) g glycerol/L/hr. In each plot, from left to right, the arrows indicate the start of feeding and the 30°C-to-42°C temperature shift, respectively. Error bars on the plasmid copy number values represent the 95% confidence level calculated from three replicate wells of the same sample. ....48

**Figure 2-7.** (A) Acetate and (B) plasmid copy number profiles from microreactor runs at a feed rate of 3.1 g glycerol/L/hr with air only (▲) or a maximum of 50% oxygen (□) in the inlet gas. In each plot, from left to right, the arrows indicate the start of feeding and the 30°C-to-42°C temperature shift, respectively. Error bars on the plasmid copy number values represent the 95% confidence level calculated from three replicate wells of the same sample. ....49

**Figure 2-8.** (A) Acetate and (B) plasmid copy number profiles from fed-batch bioreactor cultures with (○) and without (●) a pH downshift from 7.1 to 6.0 at  $t = 20$  hr. From left to right, arrows indicate the start of feeding and the 30°C-to-42°C temperature shift, respectively. Error bars represent the 95% confidence level calculated from three replicate wells. ....50

**Figure 3-1.** Feature map of pDMB02-GFP. DNA vaccine vector features: kanamycin resistance marker (KanR), human cytomegalovirus immediate-early promoter/enhancer (PCMV), superfolder GFP gene (sGFP), bovine growth hormone polyadenylation signal (BGH PolyA). R1 replicon features: copy number control genes (repA, copA, copB), origin of replication (R1 ori). The locations of the point mutations that confer the runaway replication phenotype are also indicated (RR1, RR2). ....56

- Figure 3-2.** Specific yield of pCP40 (parent plasmid), pVAX1-GFP (pUC-based DNA vaccine vector), and pDMB02-GFP (R1-based DNA vaccine vector) with and without a temperature shift from 30°C to 42°C. Times in the legend are hours after the temperature shift..... 64
- Figure 3-3.** (A) Growth of DH5 $\alpha$ [pDMB02-GFP] with a temperature shift at OD<sub>600</sub> = 0.5 and (B) OD<sub>600</sub> = 1.0. (C) Specific yield of pDMB02-GFP with a temperature shift at OD<sub>600</sub> = 0.5 and (D) OD<sub>600</sub> = 1.0. Data are shown for cultures shifted to 42°C (●) and cultures that remained at 30°C (Δ). 0 hr on the x-axis is the time of the temperature shift. .... 65
- Figure 3-4.** Specific yield of pDMB02-GFP as a function of inoculum growth phase after 24 hours of culture at 30°C in shake flasks (gray bars). The plasmid copy number of the seed cultures at each growth phase are also shown (■). Specific yield error bars represent one standard deviation calculated from duplicate flasks, and copy number error bars represent the 95% confidence interval calculated from three replicate wells of the same sample. .... 67
- Figure 3-5.** Schematic of the R1 replicon. .... 68
- Figure 3-6.** Western blot for RepA. The RepA band is indicated by the arrow to the right of the image. Except for the lane containing the protein marker, all lanes contained crude lysates from the cultures indicated. **Lane 1:** BL21 Star (DE3) [pETDuet-1], **Lane 2:** BL21 Star (DE3) [pETDuet-repA], **Lane 3:** DH5 $\alpha$  (no plasmid), **Lane 4:** DH5 $\alpha$ [pDMB02-GFP] t=0 hr, **Lane 5:** DH5 $\alpha$ [pDMB02-GFP] t=2 hr 30°C, **Lane 6:** DH5 $\alpha$ [pDMB02-GFP] t=2 hr 42°C, **Lane 7:** DH5 $\alpha$ [pDMB02-GFP] t=8 hr 30°C, **Lane 8:** DH5 $\alpha$ [pDMB02-GFP] t=8 hr 42°C, **Lane 9:** DH5 $\alpha$ [pDMB-ATG] t=0 hr, **Lane 10:** DH5 $\alpha$ [pDMB-ATG] t=2 hr 30°C, **Lane 11:** DH5 $\alpha$ [pDMB-ATG] t=2 hr 42°C, **Lane 12:** DH5 $\alpha$ [pDMB-ATG] t=8 hr 30°C, **Lane 13:** DH5 $\alpha$ [pDMB-ATG] t=8 hr 42°C, **Lane 14:** Protein marker. Times indicate hours after the temperature shift. All lanes contained 2  $\mu$ g total protein except for Lane 2, which contained 0.4  $\mu$ g total protein. Results are shown for a single set of flasks, but the same trends in RepA expression were observed for the second replicate samples as well.. .... 71
- Figure 3-7.** Agarose gel electrophoresis of pDMB02-GFP and pDMB-ATG produced in DH5 $\alpha$  with and without a mid-exponential phase temperature shift from 30°C to 42°C. **Lane 1:** DNA ladder with DNA size in kilobases (kb) indicated to the left of the image, **Lane 2:** pDMB02-GFP t=2 hr 30°C, **Lane 3:** pDMB02-GFP t=2 hr 42°C, **Lane 4:** pDMB02-GFP t=4 hr 30°C, **Lane 5:** pDMB02-GFP t=4 hr 42°C, **Lane 6:** pDMB02-GFP t=8 hr 30°C, **Lane 7:** pDMB02-GFP t=8 hr 42°C, **Lane 8:** pDMB-ATG t=2 hr 30°C, **Lane 9:** pDMB-ATG t=2 hr 42°C, **Lane 10:** pDMB-ATG t=4 hr 30°C, **Lane 11:** pDMB-ATG t=4 hr 42°C, **Lane 12:** pDMB-ATG t=8 hr 30°C, **Lane 13:** pDMB-ATG t=8 hr 42°C, **Lane 14:** DNA ladder. Times indicate hours after the temperature shift..... 73
- Figure 4-1.** (A) Growth curves and (B) final OD<sub>600</sub> (cell density after 24 hours of incubation at 30°C) for cultures of DH5 $\alpha$ [pDMB02-GFP] in semi-defined medium containing either Bacto or soy peptone along with varying concentrations of MgSO<sub>4</sub>·7H<sub>2</sub>O in shake flasks. Growth of cultures in LB medium with no glycerol is also shown. OD<sub>600</sub> values are reported as the average of two replicates. For (A), the standard deviations are not shown because all were less than 0.13 OD<sub>600</sub> units. The error bars in (B) represent one standard deviation..... 84

**Figure 4-2.** Specific yield of pDMB02-GFP in semi-defined medium containing either Bacto or soy peptone along with varying concentrations of MgSO<sub>4</sub>·7H<sub>2</sub>O in shake flask scale culture. LB medium with no glycerol was also included. Cultures were grown at 30°C for 24 hours; the flasks containing semi-defined medium were supplemented with 5 g/L glycerol at the start of the experiment and 10 hours after inoculation. Error bars represent one standard deviation calculated from two replicate cultures.....85

**Figure 4-3.** Dissolved oxygen (gray line) and growth (●) profiles from a batch culture of DH5α[pDMB02-GFP]. The agitation rate was increased gradually throughout the run as indicated at the top of the figure. ....88

**Figure 4-4.** Specific yield (■) and volumetric yield (O) from a batch culture of DH5α[pDMB02-GFP] with controlled growth rate. ....88

**Figure B-1.** Plasmid feature maps. pVAX1-GFP is a pUC-based DNA vaccine vector used in the microbioreactor studies described in Chapter 2, as well as for comparison to the R1-based DNA vaccine vectors described in Chapter 3. pCP40 (Remaut et al., 1983) was used in Chapter 3 as the source of the runaway R1 replicon. pDMB02-GFP is the runaway R1-based DNA vaccine vector that was constructed and characterized in Chapters 3 and 4. A derivative of pDMB02-GFP with a GTG-to-ATG mutation in the start codon of *repA* was also constructed (feature map not shown). Finally, pETDuet-*repA* was constructed by cloning *repA* into the expression vector pETDuet-1 (EMD Millipore; feature map not shown) to overexpress RepA protein as a positive control for the Western blots in Chapter 3. ....107

# List of Tables

---

|  |     |
|--|-----|
| <b>Table 3-1.</b> Specific yield, plasmid copy number, and <i>repA</i> expression from pDMB02-GFP with and without a temperature shift. Error bars represent the standard deviation of duplicate samples.....  | 69  |
| <b>Table 3-2.</b> Specific yield, plasmid copy number, and <i>repA</i> gene expression in cultures of DH5 $\alpha$ [pDMB-ATG] with and without a temperature shift. Error bars represent the standard deviation of duplicate samples.....                  | 70  |
| <b>Table 4-1.</b> Combinations of hydrolysate source and MgSO <sub>4</sub> ·7H <sub>2</sub> O concentration tested during development of semi-defined medium.....  | 79  |
| <b>Table 4-2.</b> Glycerol and acetate concentrations measured in the supernatants of cultures containing either Bacto or soy peptones and various concentrations of MgSO <sub>4</sub> ·7H <sub>2</sub> O .....  | 86  |
| <b>Table 4-3.</b> Summary of maximum values of specific growth rate ( $\mu_{max}$ ), doubling time ( $t_D$ ), OD <sub>600</sub> , specific yield, and volumetric yield observed under various culture conditions at shake flask and bioreactor scales..... | 87  |
| <b>Table B-1.</b> Abbreviations used in plasmid feature maps .....   | 108 |

# Chapter 1

---

## Introduction

### Abstract

The demand for plasmid DNA (pDNA) is anticipated to increase significantly as DNA vaccines and non-viral gene therapies enter Phase 3 clinical trials and are approved for use. This increased demand, along with renewed interest in pDNA as a therapeutic vector, has motivated research targeting the design of high-yield, cost-effective manufacturing processes. An important aspect of this research is engineering bacterial strains and plasmids that are specifically suited to the production of plasmid biopharmaceuticals. This chapter begins with a survey of recent innovations in strain and vector engineering that aim to improve plasmid stability, enhance product safety, increase yield, and facilitate downstream purification. Following this in-depth description of the state of the field, the motivation for pursuing this thesis as well as the thesis aims will be presented. Finally, an outline of the thesis organization will be discussed.

### Parts of this chapter have been published in:

Bower DM, Prather KLJ. 2009. Engineering of bacterial strains and vectors for the production of plasmid DNA. *Appl Microbiol Biotechnol* 82: 805-813.

## 1.1 Engineering of bacterial strains and vectors for the production of plasmid DNA: A literature review

### 1.1.1 Background

In recent years, great strides have been made toward the development of safe and effective gene therapies and DNA vaccines for many infectious, acquired, and genetic diseases. Gene therapies act by transferring DNA to a patient to correct a genetic defect or overexpress a therapeutic protein, while DNA vaccines use genes to express antigens that elicit a protective immune response. The use of naked plasmid DNA (pDNA) as a vector for gene-based therapies has been gaining attention in the medical and biotechnology communities. Currently, 18.5% of gene therapy clinical trials use plasmid DNA as a vector ([www.wiley.co.uk/genmed/clinical](http://www.wiley.co.uk/genmed/clinical)). Four veterinary pDNA therapies have been licensed in the US, Canada, and Australia (Kutzler and Weiner, 2008). As more pDNA-based therapies enter late-stage clinical trials and are approved for clinical use, the demand for high-quality, pharmaceutical-grade plasmid DNA is anticipated to increase significantly. Interest in non-viral gene therapy has also been bolstered by disappointing results from a Phase 2 clinical trial of an adenovirus-based HIV DNA vaccine (Moore et al., 2008), along with recent advances in delivery vehicles and adjuvants that have increased the potency of naked pDNA (Saade and Petrovsky, 2012; Sardesai and Weiner, 2011).

From a manufacturing standpoint, the increasing demand for plasmid DNA is coupled to a need for high-yield, cost-effective production processes. Currently, plasmid DNA is often produced using “off the shelf” strains of *Escherichia coli* and plasmid backbones that are known to be effective producers of recombinant proteins. However, these choices may not be the most favorable when plasmid DNA is the final product. As a result, significant research efforts are in progress to rationally design bacterial strains and plasmids specifically suited to the production of plasmid biopharmaceuticals.

The motivation to design new bacterial strains for plasmid DNA production is due in part to the realization that many common laboratory strains like DH5 $\alpha$  and DH10B have undergone a high degree of



mutagenesis to improve their performance in cloning, library construction, and/or recombinant protein production applications. The complex genotypes of many *E. coli* strains in industrial use today also greatly hinder the ability to reliably predict the plasmid yield based on the genotype alone. In a survey of 17 strains of *E. coli* harboring plasmids ranging in size from 5.8 kb to 20 kb, Yau and colleagues (2008) found little correlation between strain genotype and plasmid yield. With these factors in mind, many researchers have used the strategies outlined in Figure 1-1 to develop well-characterized strains for pDNA production. These strain engineering efforts often seek to preserve the sequence fidelity of both the plasmid and host genome and to address upstream and downstream process issues.

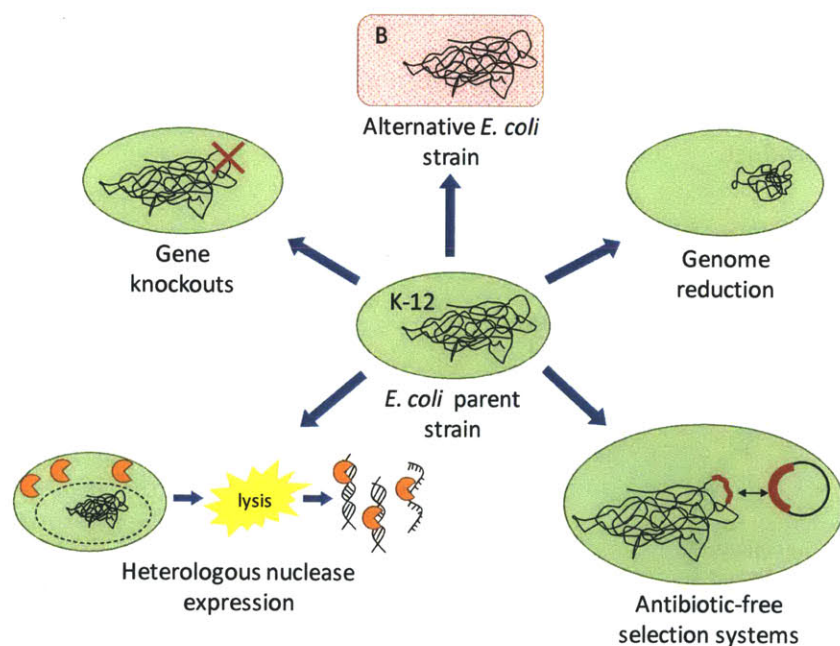


**Figure 1-1.** Strain engineering strategies. The parent strain at the center of the diagram represents any *E. coli* K-12 strain, and the potential modifications to this strain are illustrated. The strain’s genome can be modified subtly by single gene knockouts or implementation of an antibiotic-free selection system. More dramatic modifications such as genome reduction can be used to remove mobile elements like insertion sequences. Other strategies aim to ease downstream processing, like expression of heterologous periplasmic nucleases to degrade host genomic DNA and RNA after cell lysis. Changing the parent strain from K-12 to B has also been investigated to improve pDNA production. Note that the engineering strategies are shown as independent of one another, but applying several strategies in parallel to a single strain is possible as well.

Complementing these efforts are alterations in the vector backbone designed to enhance characteristics such as copy number, genetic fidelity, and segregational stability. Typical plasmid

backbones used for gene therapeutics have several common features that fall into two categories: features required for propagation in *E. coli* and features required for therapeutic efficacy. Elements in the first category include a bacterial origin of replication, such as the ColE1 origin, and a selective marker, such as a kanamycin resistance gene. Kanamycin resistance is preferred over a marker that requires addition of  $\beta$ -lactam antibiotics to the culture medium, as these could potentially induce an allergic response in patients (Butler, 1996). The second category of plasmid features includes the therapeutic gene and the associated sequences required for its expression *in vivo* such as a eukaryotic promoter and poly-adenylation signal. Many vector engineering efforts focus on modifications to the basic therapeutic backbone as illustrated in Figure 1-2. These modifications aim to improve the production process by increasing yield, improving product homogeneity and quality, and/or ensuring the sequence fidelity of the final plasmid product.

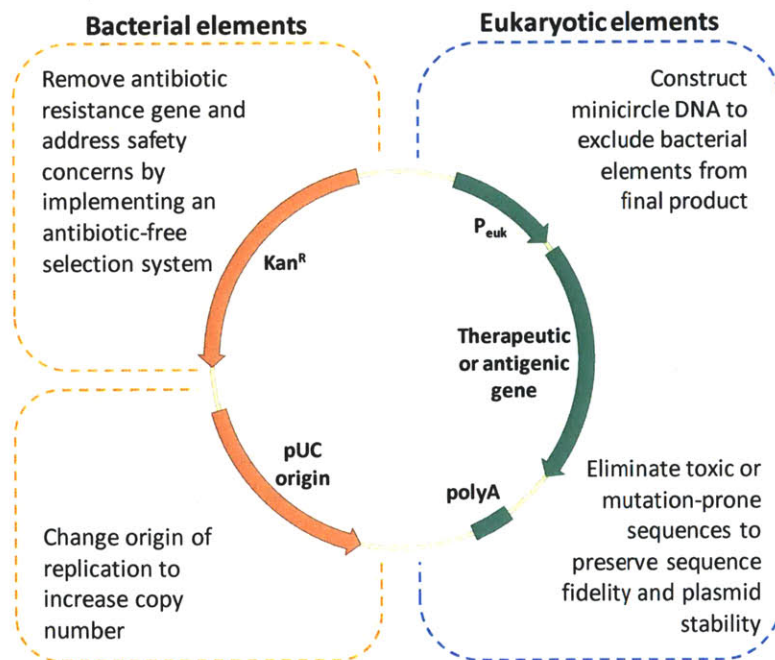


**Figure 1-2.** Vector engineering strategies. A generic plasmid DNA vaccine or gene therapy vector is shown with the important features labeled. The bacterial elements required for propagation of the plasmid in *E. coli* are the selectable marker (kanamycin resistance gene, Kan<sup>R</sup>) and the pUC origin of replication. The eukaryotic elements of the vector required for *in vivo* efficacy include the eukaryotic promoter/enhancer (P<sub>euk</sub>), therapeutic or antigenic gene, and poly-adenylation signal (polyA). The goal of each vector engineering strategy is described next to the vector feature targeted for modification.

This literature review will describe recent developments in strain and vector engineering for the production of pDNA-based therapies. The state of the field from a clinical perspective has recently been reviewed (Kutzler and Weiner, 2008). Reviews of vector and insert engineering strategies (Mairhofer and Grabherr, 2008; Williams et al., 2009a) as well as a review of strain engineering from a metabolic perspective have also been published recently (Gonçalves et al., 2012). This section will survey recent innovations in strain and vector engineering that aim to improve plasmid stability, enhance product safety, increase yield, and facilitate downstream purification. While these innovations all seek to enhance pDNA production, they can vary in complexity from subtle alterations of the host genome or vector backbone to the investigation of non-traditional host strains for higher pDNA yields.

### **1.1.2 Engineering to maintain sequence stability**

The sequence integrity of a plasmid vector must be controlled during the production process because of its enormous impact on product safety, yield, and quality. Modifications in the strain and vector used for production of pDNA can ensure that the sequence and structure of the plasmid is maintained throughout the duration of the process. The complete sequence of *E. coli* DH10B was recently published (Durfee et al., 2008) and underscores the need for re-evaluation of strains used for pDNA production. For example, DH10B was found to have a mutation rate 13.5-fold higher than wild-type *E. coli* (strain MG1655), mostly due to a significantly higher rate of insertion sequence (IS) transposition. When compared to MG1655, the DH10B genome contains five additional copies of IS1A (IS1E)-type transposons which are known to insert into plasmid DNA (Chen and Yeh, 1997). These findings are especially relevant for pDNA production where the integrity of the final plasmid preparation is paramount. Contamination of plasmid DNA by mobile elements is a serious regulatory concern, as these elements can alter the biological properties and safety profile of the vector DNA. This concern is not purely theoretical – IS1-mediated mutagenesis was recently reported in an industrial process for

selection of HIV plasmid DNA vaccine candidates. An IS1 insertion in the *E. coli* DH5 genome was postulated to be the cause of the presence of a significant population of low plasmid-producing clones (Prather et al., 2006). Insertion of both an IS1 and an IS5 sequence in the neomycin resistance gene of the therapeutic plasmid was also observed. Prolonged cultivation in minimal medium may have caused the high incidence of IS insertion detected in this study, as transposon activity can often be induced by environmental stressors such as nutrient limitation (Twiss et al., 2005). The population of low-producers was detrimental to process efficiency by necessitating extensive screening for high-producing clones for use in master seed banks.

To address the problem of IS-mediated genetic instability, researchers have constructed multiple-deletion series (MDS) strains of *E. coli* which contain a significantly reduced genome that is about 15% smaller than that of the parent strain, MG1655 (Posfai et al., 2006). These strains have all of the mobile elements removed, and showed no detectable transposon activity when compared to MG1655 and DH10B. Neither the growth rate of the MDS strains nor their capacity for recombinant protein production was compromised by the genome reduction. Without insertion sequences, MDS strains were able to stably maintain plasmids coding for recombinant ectopic fusion proteins and adeno-associated virus-based plasmids that contain hammerhead secondary structure. Both of these vector types are often highly unstable in *E. coli* K-12 strains. Evaluation of the MDS strains in a pDNA production process has not yet been reported, but the advantages of using these strains is clear and they have great potential to streamline the production of high-quality, stable pDNA.

Contamination of gene therapeutics by insertion sequences has also been addressed using vector design solutions. For instance, a plasmid containing the human cystic fibrosis transmembrane conductance regulator (CFTR) gene for cystic fibrosis therapy showed a high level of segregational instability due to the expression of toxic peptides from a cryptic *E. coli* promoter present in the gene (Boyd et al., 1999). An IS1-containing variant of the vector was discovered in high amounts in some

fermentations, presumably due to increased fitness via suppression of toxic peptide expression. To remedy these issues, the researchers inserted an intron near the site of the cryptic promoter that reduced expression of toxic gene products, thus substantially increasing plasmid stability and decreasing contamination by IS1 elements.

Changes in plasmid sequence can also be mediated by factors other than IS elements, even in recombination deficient *recA*<sup>-</sup> strains. For example, vectors that contain direct sequence repeats are especially vulnerable to *recA*-independent recombination and can form monomers that have lost one of the direct repeats and the intervening sequence, as well as head-to-tail combinations of two or three recombined monomers (Bi and Liu, 1996). This type of *recA*-independent recombination is thought to occur through a pathway involving strand mispairing at a stalled replication fork or replication slippage (Bi and Liu, 1996). A report by Ribeiro et al. (2008) and a follow-up study by Oliveira et al. (2009) observed this type of recombination in pCIneo as well as in a pCIneo-derived rabies DNA vaccine candidate cultivated in cells exposed to kanamycin. Both plasmids contained two 28-bp direct repeats, and all three recombination products described above were observed. This recombination conferred kanamycin resistance, possibly by reducing the distance between the neomycin phosphotransferase gene and a cryptic *E. coli* promoter. The kanamycin resistance gene should not have been expressed in *E. coli* because it was under the control of the eukaryotic SV40 promoter. These changes in plasmid structure and aberrant expression of an antibiotic resistance gene represent an obvious safety hazard, and emphasize the need for detailed sequence analysis of therapeutic vectors to identify and eliminate mutational hot spots. To aid in this work, Oliveira et al. (2008) have developed an algorithm to predict the recombination frequency of a plasmid containing a given set of direct repeats. A recent report has also identified hot spots for repeat-mediated recombination in commonly-used mammalian and bacterial expression vectors (Oliveira et al., 2010).

### 1.1.3 Engineering to promote safety

As discussed in the previous section, it is essential to ensure the sequence fidelity of gene-based therapeutics that will ultimately be administered to humans. Two other product safety concerns that can significantly affect the design of a pDNA production process include the use of antibiotics for plasmid selection and the potential for the therapeutic vector to be transferred to other organisms in the environment.

In terms of antibiotics, the FDA has long recommended that  $\beta$ -lactam antibiotics be avoided, as residual contamination in the final product could potentially cause an allergic reaction in sensitive individuals (Butler, 1996). Also, antibiotics that are in wide clinical use should be avoided. With these concerns in mind, the development of antibiotic-free selection systems is desirable from both a cost and safety perspective – especially as the emergence of antibiotic-resistant pathogens becomes more common. Several researchers have addressed these concerns by modifying the vector, host, or both to develop alternative plasmid selection systems. These advances have been reviewed recently (Vandermeulen et al., 2011), and some key examples are highlighted below.

Several groups have chosen to manipulate essential *E. coli* genes to ensure efficient killing of plasmid-free cells. One group chose to target *dapD*, an essential gene for diaminopimelate and lysine biosynthesis (Cranenburgh et al., 2001). The endogenous *dapD* locus was disrupted, and an ectopic copy of *dapD* under the control of a *lac* promoter was integrated into the chromosome. Transforming this strain with a high copy plasmid containing the *lac* operator resulted in sufficient titration of *lac* repressor away from *dapD* to give expression of the essential gene. As a result, only cells containing pDNA with the *lac* operator sequence survived in culture. This protocol was later adapted to medium copy number plasmids, like pBR322 (Cranenburgh et al., 2004), and was successfully applied to a plasmid DNA production process for an HIV DNA vaccine candidate (Hanke and McMichael, 2000). In other work, Hägg et al. (2004) created a host/vector system where the chromosomal *infA* gene, coding

for an essential translation initiation factor, was deleted, and was complemented by a copy of the gene on the expression vector of interest. A similar system was developed by Vidal et al. (2008) using *glyA*, an essential gene for glycine biosynthesis, which allowed only plasmid-bearing cells to grow in minimal medium without glycine. In both of these studies, the implementation of the antibiotic-free selection system did not significantly affect the growth rate of the strains.

Goh and Good (2008) overexpressed the essential *fabI* gene (enoyl ACP reductase) from a plasmid, and selected for plasmid-bearing cells using triclosan, a biocide that chemically inhibits *fabI*. A DNA vaccine vector for bovine viral diarrhea virus containing the *fabI*/triclosan selection system showed comparable immunogenicity to a vector with traditional antibiotic selection (El-Attar et al., 2012). In the same study, triclosan was also found to be efficiently removed during plasmid purification to levels below the assay detection limit. Use of an antidote/poison system has also been investigated in the context of antibiotic-free recombinant protein or DNA production. Szpirer and Milinkovitch (2005) constructed an *E. coli* B strain carrying a chromosomal copy of the *ccdB* poison gene and selected for plasmid-bearing cells using vectors containing the *ccdA* antidote gene. (*E. coli* B strains are non-pathogenic laboratory strains that can be used for many of the same applications as K-12 strains, and the differences between the two strains that are relevant to pDNA production will be discussed below.) The *ccd* system is an example of a class of natural plasmid maintenance strategies, known as post-segregational killing systems, which have been reviewed by Zielenkiewicz and Ceglowski (2001).

Alternative selection systems based on antisense RNA have also recently been investigated. Dryselius et al. (2003) used a synthetic peptide-nucleic acid complex to inactivate the mRNA from the chromosomal copy of the essential *acpP* gene. The strain was rescued by a plasmid containing a copy of *acpP* with a mutation that rendered it resistant to the antisense nucleic acid, thus allowing for selection of plasmid-bearing cells. This selection technique was effective, but is likely to be cost prohibitive at the large scale owing to the expense of synthesizing the peptide nucleic acid. Mairhofer and colleagues

(2008) avoided the issue of expense by developing a system that uses the RNA I antisense transcript that is produced during ColE1 plasmid replication to regulate expression of an essential host gene. They integrated an expression cassette containing the essential *murA* gene (UDP-N-acetylglucosamine enolpyruvyl transferase) under the control of the *pLtetO* operator into the chromosome of various *E. coli* strains. The *tet* repressor (*tetR*) was modified to contain a sequence complementary to RNA I. In the presence of a plasmid with a ColE1 replicon, *tetR* was inactivated, allowing expression of the essential gene. In the absence of a replicating ColE1 plasmid, *murA* expression was repressed, resulting in cell death. This selection system resulted in higher specific plasmid yields in a fed-batch process compared to a vector maintained by kanamycin selection (Mairhofer et al., 2010). A major advantage of these antisense-based systems is that the antibiotic resistance gene can be removed from the plasmid, resulting in a smaller vector and a reduction in the number of immunostimulatory unmethylated CpG sequences.

Antibiotic-free selection systems can also be used in conjunction with well-known natural plasmid stability systems that act by resolving multimers or facilitating plasmid partitioning instead of killing plasmid-free cells. For example, *cer* sequences present in natural plasmids like ColE1 act with *E. coli* host proteins to resolve plasmid multimers in order to prevent multimer accumulation which can significantly reduce plasmid segregational stability (Summers, 1998). Also, plasmids expressing Par-family partitioning proteins can help ensure that all daughter cells receive at least one plasmid (Pogliano, 2002).

A novel vector/host system developed by Soubrier and colleagues (1999) combined antibiotic-free selection with a plasmid replicon that is dependent on a specifically-engineered host for replication. This class of plasmids, called pCOR, contains an R6K-derived origin of replication that requires the  $\pi$  initiator protein encoded by the *pir* gene. In the system developed by Soubrier et al. (1999) the gene encoding  $\pi$  was removed from the plasmid and integrated into the *E. coli* genome. This host-dependent



replication improves the safety profile of the pCOR vectors by limiting the plasmid host range and thus significantly reducing the chance of plasmid dissemination to the environment. The pCOR plasmids also rely on an antibiotic-free, tRNA amber suppressor system for selection, along with a *cer* sequence to enhance plasmid stability. In terms of yield, the first-generation pCOR plasmids, which contain a point mutation in the *pir* gene to increase copy number, gave yields on the order of 100 mg pDNA/L (Soubrier et al., 1999). Later work increased the copy number further by additional mutagenesis of *pir*, producing yields of 421 mg pDNA/L in a 7-L fed-batch fermentation (Soubrier et al., 2005). The pCOR plasmids represent the only known published investigation of plasmids containing a non-ColE1 origin of replication for use in gene therapy or DNA vaccine applications.

Another method of addressing the safety concerns surrounding bacterial elements in plasmid biopharmaceuticals is the use of minicircle DNA. Minicircles contain only the transcription unit required for expression of the therapeutic gene(s), with the bacterial backbone sequences required for propagation in *E. coli* removed by site-specific, intramolecular recombination. The construction of minicircle DNA has been studied for about a decade (Darquet et al., 1997), but feasible production processes for these vectors have only recently been proposed and with them a new category of vector and strain engineering challenges. The vector must be engineered to contain the elements necessary for efficient intramolecular recombination. Two recombination systems currently under investigation include the phage  $\Phi$ C31 integrase gene (Chen et al., 2005) and the *parA* resolvase (Mayrhofer et al., 2008) with their associated recognition sites. Both of these systems have the sequence for the required enzyme integrated into the backbone of the parent plasmid. However, Kay et al. (2010) have recently reported a variation of their  $\Phi$ C31-based system that has the genes for all required enzymes integrated into the *E. coli* genome. Tolmachov et al. (2006) have designed a minicircle production system consisting of an *E. coli* strain with an arabinose-inducible copy of the Cre recombinase gene integrated into the chromosome along with a plasmid vector with *loxP* sites flanking the eukaryotic transcription

unit. Overall, minicircle DNA represents an attractive alternative to plasmid DNA, especially for gene therapy applications, because minicircles lack immunostimulatory CpG motifs (and an antibiotic resistance gene). However, until the production of minicircle DNA can be scaled up and streamlined, plasmid DNA is likely to remain the preferred vector for non-viral gene therapies.

#### **1.1.4 Engineering to increase plasmid DNA yield**

The art of high-density cell culture for pDNA production has been an active area of process research, often focusing on the development of seed trains (Okonkowski et al., 2005), media (Danquah and Forde, 2008; O’Kennedy et al., 2000; Wang et al., 2001), and induction strategies (Carnes et al., 2006). However, strain engineering efforts have also recently begun to address upstream process issues such as increasing plasmid DNA yield. In an attempt to design an organism better suited to production of plasmid DNA, researchers have investigated both *E. coli* B and K-12 strains. B and K-12 strains are genetically similar, but analysis of mobile elements in a particular B strain showed a very different profile of insertion sequences. Notably, *E. coli* B lacks a copy of IS5, and contains 20 copies of IS1 versus the six to eight usually found in K-12 (Schneider et al., 2002). The lipopolysaccharides (LPS) of K-12 and B strains both lack the O-antigen. B strains also lack the distal part of the LPS core consisting of D-galactose, D-glucose, and N-acetyl-D-glucosamine residues (Nikaido, 1996). However, we are not aware of any studies demonstrating that this difference in polysaccharide content significantly affects the endotoxin levels in a pDNA production process. Metabolically, derivatives of *E. coli* B differ from *E. coli* K-12 in that B strains typically produce significantly less acetate, even when grown in medium with a high glucose concentration. This phenomenon has been attributed to a more active glyoxylate shunt and consequently, more active acetate uptake pathways (Phue et al., 2005).

BL21, a B strain derivative, has been used with great success for overexpression of recombinant proteins. However, until recently, BL21 has not been considered to be a viable host for pDNA

production because its genome contains intact *endA* and *recA*, resulting in sub-optimal plasmid preparations. Deleting *recA* in BL21(DE3) has been shown to improve plasmid segregational stability (Zhao et al., 2007), but this investigation was conducted in the context of recombinant antibody production. A recent communication from Phue et al. (2008) reported that with glucose as the carbon source, BL21 $\Delta$ *recA* and BL21 $\Delta$ *recA* $\Delta$ *endA* produced more pDNA than DH5 $\alpha$ . Under these conditions, BL21-derived strains showed significantly less acetate production and improved glucose utilization, as expected for a B strain. With glycerol as a carbon source, BL21 $\Delta$ *recA* $\Delta$ *endA* performed significantly better than DH5 $\alpha$  in terms of volumetric yield (1904 mg/L versus 991 mg/L), but the differences were less substantial in terms of specific yield (10.07 mg versus 7.03 mg pDNA per g wet cell weight).

While the study described above found that a strain possessing a more active glyoxylate shunt (BL21) fared better in high density cell culture and produced more pDNA than a K-12 strain, other groups have found that disrupting a positive regulator of the glyoxylate shunt, the global transcriptional regulator *fruR*, also led to increased pDNA production. Ow et al. (2006) conducted global transcription and proteomic analyses to study the differences in metabolism between plasmid-bearing and plasmid-free *E. coli* DH5 $\alpha$  cells. As expected, they found that plasmid-bearing cells had a slower growth rate and an altered profile of central metabolic gene expression when compared to plasmid-free cells. Based on this work, Ow and colleagues (2007) chose to disrupt the *fruR* gene in DH5 $\alpha$  and found that this modification increased growth rate and glycolytic enzyme activity of plasmid-bearing cells along with a concomitant reduction in gluconeogenesis. The ability to recover a growth rate comparable to plasmid-free cells is particularly useful in pDNA production, as it reduces the selective pressure against plasmid-bearing cells and thus increases plasmid stability. In the context of pDNA production, a recent study by the same group (Ow et al., 2009) found that disruption of *fruR* led to a 21% increase in specific pDNA yield from a fed-batch fermentation. Additional strategies for altering host metabolism to improve pDNA yield have been extensively reviewed by Gonçalves et al. (2012).

### 1.1.5 Engineering to address downstream processing and purification issues

A key challenge in the development of cost-effective manufacturing processes is improving the yield of downstream purification steps. Large-scale purification of pDNA is difficult due to the complex, dynamic structure of pDNA (Prazeres and Ferreira, 2004), viscous process streams (Ciccolini et al., 1998), and the presence of impurities (e.g. RNA, genomic DNA) with similar properties to the desired product (Ferreira et al., 2000). One method to improve downstream purification yields is the development of fermentation processes with high specific pDNA yields which improve overall process yield by increasing the ratio of plasmid DNA to contaminating biomass. Recent studies have reported yields of 49.1 (Danquah and Forde, 2008) and 51.1 mg/g DCW (Williams et al., 2009b) – significant improvements over earlier reported values.

Several researchers have taken a different approach and sought to improve downstream purification by engineering the *E. coli* host strain to reduce the amount of contaminating genomic DNA (gDNA) and RNA in the cell lysate. The FDA has yet to set formal lot release criteria for gene-based therapeutics; however, a generally-accepted specification for product purity is that any residual RNA is not present in a high enough concentration to be visualized on a 0.8% agarose gel (Horn et al., 1995). The separation of RNA from DNA is particularly challenging because of the similar physicochemical properties of both nucleic acids. One strategy for RNA removal is digestion of cell lysates with bovine RNase A, which allows the resulting small RNA fragments to be more easily separated from DNA. However, recent concerns surrounding prion-based diseases have precluded the use of animal-derived enzymes. Cooke et al. (2001) addressed this problem by integrating the gene coding for RNase A into the chromosome of *E. coli* JM107 under the control of an IPTG-inducible promoter. After induction, pre-RNase A was targeted to the periplasm where it folded into its active form and was sequestered from host nucleic acids. Upon cell lysis, the enzyme was released and efficiently degraded host RNA. This

strategy was particularly successful because the RNase A enzyme is robust enough to withstand the conditions of high pH encountered during alkaline lysis.

To address removal of host genomic DNA as well as RNA, Nature Technology Corporation has developed *E. coli* hosts expressing periplasmic chimeric proteins that degrade both nucleic acids (Hodgson and Williams, 2006). These chimeras include the plasmid-safe phage T5 D15 exonuclease linked to RNase A or S. The exonuclease is “plasmid-safe” in that it specifically degrades linear and denatured DNA while not affecting the fidelity of supercoiled plasmid DNA. The chimeric proteins can be reintroduced into the cytoplasm before lysis by inner membrane permeabilization techniques, or can begin to degrade host nucleic acids immediately after being released by cell lysis. Both of these schemes significantly reduce the viscosity of the lysate, easing the later stages of purification. This approach to strain engineering also incorporated autolytic host strains, which have been used previously for recombinant protein production applications.

While efforts to improve downstream processing focus on strain engineering, they have addressed many of the major challenges of pDNA production, like separating plasmids from genomic DNA and host RNA contamination. Continued work in this area has the potential to lower manufacturing costs by increasing the yield from downstream purification steps.

#### **1.1.6 Future directions**

This section described a wide range of strain and vector engineering solutions to problems facing the production of plasmid DNA for gene therapies and DNA vaccines. As these technologies mature, they are likely to continue to positively impact the way gene-based therapeutics are produced. However, there are several other interesting options for improved strains and vectors that have yet to be investigated. For example, a potential strategy for increasing pDNA yield at an early stage in the manufacturing process is to increase plasmid copy number. However, surprisingly little work has been

reported in this area with respect to strain or vector engineering. With the exception of the work on pCOR (Soubrier et al., 1999; Soubrier et al., 2005) published pDNA production processes exclusively use high copy number pUC-based plasmids with ColE1 origins of replication. Often, plasmid copy number is modulated using external factors such as temperature (Carnes et al., 2006) to balance the metabolic burden effects of maintaining high copy number plasmids with the desire for high-yield fermentations. These external, sometimes resource-intensive, modulations could potentially be eliminated through rational engineering of the plasmid backbone to increase copy number, or by investigating alternative origins of replication. In terms of strain engineering, areas of research that could improve production include removing auxotrophies of existing high pDNA producing strains, as well as engineering a strain that can maintain high concentrations of supercoiled pDNA. Engineering the structure of the bacterial outer membrane to reduce endotoxin contamination could also have a significant impact on streamlining downstream purification of pDNA.

Overall, the strain and vector engineering efforts described in this section demonstrate the improved processes that can result from re-evaluation of existing technologies and consideration of process concerns during the basic research phase of product development. While much of the infrastructure is similar for both recombinant protein and pDNA production, there are many issues that are specific to a plasmid DNA final product and these issues have been addressed in many original and innovative ways. As new, engineered strains and vectors continue to be characterized and gain greater acceptance, implementation of these technologies has great potential to result in more productive plasmid DNA manufacturing processes.

## **1.2 Motivation and thesis aims**

For nearly two decades, researchers have sought to realize the potential of gene-based therapies to provide specific and effective treatment for a variety of both infectious and acquired

diseases. Renewed interest in pDNA-based vaccines has recently been spurred by approval of four veterinary pDNA-based therapies (Kutzler and Weiner, 2008) and improvement of pDNA delivery via novel methods such as electroporation (Sardesai and Weiner, 2011). With this renewed interest comes the need for rationally-designed, high-yield fermentation processes for the production of pDNA. The overall goal of this thesis is to develop new tools for the production of plasmid DNA biopharmaceuticals.

One crucial aspect of pDNA production is design of the plasmid vector. As demonstrated by the literature reviewed in the previous section, current manufacturing processes and development efforts almost exclusively use pUC-based plasmid backbones. This is mostly due to the fact that these vectors are known to have high copy numbers. There is also a wealth of experience with pUC plasmids from recombinant protein production. However, it is possible that better alternatives exist, and to this end, one aspect of this thesis focuses on design of a new DNA vaccine vector. We investigated the potential of runaway R1-based plasmids for production of plasmid DNA. This class of plasmids contains replicon mutations that confer a temperature-induced increase in copy number. The high copy numbers reported at the shake flask scale (Uhlen et al., 1979) suggest that these vectors could produce yields that exceed those typically produced by pUC-based plasmids. However, these plasmids have yet to be investigated in the context of plasmid DNA production.

In the preceding section, we have discussed recent innovations in using engineering approaches to design strain-vector platforms for plasmid DNA production. With these innovations comes the need for an effective way to screen new strains and vectors for high productivity. In parallel, there is increased pressure in the biopharmaceutical industry for faster discovery-to-launch timelines and reduced research and development costs. To meet these needs, we have designed a process development tool that combines the high-throughput, low-cost nature of micro-well plates and shake flasks with the process monitoring and control capabilities of bench-scale bioreactors – a fed-batch,

micro-scale bioreactor. More specifically, we have used this microbioreactor to scale down and analyze production of a pUC-based DNA vaccine vector.

**Overall, this thesis aims to**

- Demonstrate that micro-scale bioreactors can be used as an effective process design tool for a complex, temperature-inducible process like pDNA production
- Construct a plasmid DNA vaccine vector containing the R1-based, runaway replication origin and gain mechanistic insight into its replication
- Develop a bench-scale process for production of the R1-based vector

### **1.3 Thesis organization**

This thesis is divided into five chapters. **Chapter 1** includes a review of the literature describing recent advances in bacterial strain and vector engineering for improved production of plasmid DNA, as well as the specific motivation and aims for this thesis work. **Chapter 2** describes scale down of production of a pUC-based DNA vaccine vector using a fed-batch microbioreactor device. We demonstrated that the 1-mL microbioreactor was a good proxy for a bench-scale bioreactor, and identified key process parameters that must be held constant to achieve reproducibility across scales. **Chapter 3** presents construction of a new DNA vaccine vector, pDMB02-GFP, containing the runaway R1 replicon and characterization of specific yield profiles of the new vector under various temperature conditions. We also conducted RNA and protein expression analyses of a key replication control gene to identify possible factors limiting pDNA yield. In **Chapter 4**, scale up of pDMB02-GFP production from the 50-mL to 2-L scale is described, including medium development, key scale-up challenges encountered, and our efforts to mitigate these challenges. Finally, the thesis ends with **Chapter 5** which includes conclusions and recommendations for future work.



# Chapter 2

---

## Fed-batch microbioreactors

### Abstract

The rising costs of bioprocess research and development emphasize the need for high-throughput, low-cost alternatives to bench-scale bioreactors for process development. In particular, there is a need for platforms that can go beyond simple batch growth of the organism of interest to include more advanced monitoring, control, and operation schemes such as fed-batch or continuous. We have developed a 1-mL microbioreactor capable of monitoring and control of dissolved oxygen, pH, and temperature. Optical density can also be measured online for continuous monitoring of cell growth. To test our microbioreactor platform, we used production of a plasmid DNA vaccine vector (pVAX1-GFP) in *Escherichia coli* via a fed-batch temperature-inducible process as a model system. We demonstrated that our platform can accurately predict growth, glycerol and acetate concentrations, as well as plasmid copy number and quality obtained in a bench-scale bioreactor. The predictive abilities of the micro-scale system were robust over a range of feed rates as long as key process parameters, such as dissolved oxygen, were kept constant across scales.

### Parts of this chapter have been published in:

Bower DM, Lee KS, Ram RJ, Prather KLJ. 2012. Fed-batch microbioreactor platform for scale down and analysis of a plasmid DNA production process. *Biotechnol Bioeng* *In press*. DOI: 10.1002/bit.24498.

## 2.1 Introduction

There is increasing pressure in the pharmaceutical industry to accelerate the discovery-to-launch timelines for therapeutics and to reduce the cost of research and development. It can be difficult to realize cost savings when dealing with biological therapeutics, as their development often entails extensive process design and scale-up studies using bench-top bioreactors. Other cheaper, more high-throughput process development tools exist (shake flasks, micro-well plates), but they often sacrifice process monitoring and control capabilities for cost and throughput savings.

With these challenges in mind, many researchers have sought to design mini- and microbioreactors that maintain the control and monitoring capabilities of bench-scale units while increasing throughput and decreasing capital and labor costs. These developments typically occur in one of several forms: miniaturized stirred-tank reactors with working volumes on the order of milliliters, micro-well plates that have been modified to allow online process monitoring and/or nutrient feeding, or flat-form microfluidic devices with microliter-scale working volumes. The state-of-the-art in microbioreactor development has been reviewed recently, with articles focusing on the breadth of available reactor configurations (Betts and Baganz, 2006), as well as advances in process monitoring and fabrication techniques (Schapper et al., 2009). Another recent article reviewed all of the available small-scale process development tools and outlined the features that an ideal scale-down system should contain to meet current biopharmaceutical process development needs (Bareither and Pollard, 2011).

However, only recently have more complex process strategies, such as fed-batch operation, been investigated at the microscale. Fed-batch processes are common in industrial fermentation and cell culture as they facilitate a significant increase in biomass under controlled-growth-rate conditions, often leading to increased productivity. Reports of fed-batch processes at the microscale vary in their complexity. Isett et al. (2007) achieved feeding in the twenty-four-well  $\mu$ -24 system (Applikon Biotechnology Inc.; Foster City, CA) by manually removing the reactor cassette and adding substrate

aseptically in a biosafety cabinet. Other devices at both the microliter and milliliter scale have used robotics to intermittently add feed solution to the microreactor cultures (Legmann et al., 2009; Vester et al., 2009). Siurkus et al. (2010) sought to achieve more continuous feeding using the Enbase controlled-release technology (Panula-Perala et al., 2008) to mimic a fed-batch process in 96-well plates used for high-throughput library screening. Implementing a fed-batch process early on allowed the group to not only select a high-producing cell line, but to ensure that the associated conditions would maintain productivity upon scale-up. Microfluidics have also been used for nutrient feeding as demonstrated by Funke et al. (2010). These researchers coupled microfluidic channels to the microtiter plates in the BioLector system (m2p-labs GmbH; Baesweiler, Germany) to achieve a fed-batch process.

In this work, we have adapted a microbioreactor system originally designed for continuous culture (Lee et al., 2011) for fed-batch cultivation of *Escherichia coli* bearing a plasmid DNA vaccine vector. We chose to study a plasmid production process in the microbioreactors because of its complexity – plasmid amplification is induced by a temperature shift, and plasmid DNA is an intracellular product that can only be measured offline. Our microbioreactor is capable of real-time monitoring and control of pH, dissolved oxygen, and temperature, as well as online measurement of optical density. Substrate feeding can also be accurately controlled by the system. A working volume of 1000  $\mu\text{L}$  allows periodic sampling for offline analysis of metabolites and the plasmid DNA product. This work characterizes the features of our fed-batch microbioreactor and demonstrates its utility as a process design tool in the context of plasmid DNA production.

## 2.2 Materials and Methods

### 2.2.1 Plasmid and strain

This study used *E. coli* DH5 $\alpha$  [F  $\phi$ 80*lacZ* $\Delta$ M15  $\Delta$ (*lacZYA-argF*)U169 *deoR recA1 endA1 hsdR17*(r<sub>k</sub><sup>-</sup>, m<sub>k</sub><sup>+</sup>) *phoA supE44 thi-1 gyrA96 relA1*  $\lambda$ ] as a host for the plasmid pVAX1-GFP. pVAX1-GFP is a 3642-bp, kanamycin-resistant plasmid constructed by cloning the superfolder green fluorescent protein gene (Pedelacq et al., 2006) into the multi-cloning site of pVAX1 (Invitrogen; Carlsbad, CA), a pUC-based DNA vaccine vector backbone. DH5 $\alpha$ [pVAX1-GFP] frozen seed banks were prepared from mid-exponential-phase shake flask cultures grown at 30°C and stored at -80°C in 15% glycerol.

### 2.2.2 Culture medium

A semi-defined culture medium was adapted from Listner et al. (2006a). The basal cultivation medium contained 3 g/L (NH<sub>4</sub>)<sub>2</sub>SO<sub>4</sub>, 3.5 g/L K<sub>2</sub>HPO<sub>4</sub>, 3.5 g/L KH<sub>2</sub>PO<sub>4</sub>, 10 g/L yeast extract, and 10 g/L Bacto peptone. 5 g/L glycerol, 8.3 mL/L seed supplement solution, 1 mL/L trace elements solution, and 25  $\mu$ g/mL kanamycin were added as supplements to the basal medium. The seed supplement solution contained 60 g/L MgSO<sub>4</sub>·7H<sub>2</sub>O and 24 g/L thiamine hydrochloride. The trace elements solution contained 16.2 g/L FeCl<sub>3</sub>, 2 g/L ZnCl<sub>2</sub>, 2 g/L CoCl<sub>2</sub>·6H<sub>2</sub>O, 2 g/L Na<sub>2</sub>MoO<sub>4</sub>·2H<sub>2</sub>O, 1 g/L CaCl<sub>2</sub>·2H<sub>2</sub>O, 1.27 g/L CuCl<sub>2</sub>·2H<sub>2</sub>O, and 0.5 g/L H<sub>3</sub>BO<sub>3</sub> dissolved in 1.2 N hydrochloric acid. The pH of the basal medium was adjusted to 7.1 using NaOH. The feed solution for all fed-batch cultures contained 321.4 g/L glycerol and 79.3 g/L yeast extract.

### 2.2.3 Plasmid DNA production process

pVAX1-GFP was produced in a process adapted from Carnes et al. (2006) that consisted of three phases: (1) batch growth on 5 g/L glycerol at 30°C, (2) feeding of a concentrated glycerol/yeast extract solution at 30°C, and (3) plasmid amplification at 42°C with continued feeding.

#### 2.2.4 Microbioreactor device design

The fed-batch microbioreactor device used in this study (Figure 2-1) was a modified version of the continuous culture device designed by Lee et al. (2011). In contrast to the continuous device, the fed-batch microreactor has three 15- $\mu\text{L}$  fluid reservoirs connected to the growth chamber via peristaltic pumps, each with an injection volume of 240 nL. The pumps share the three valves required for operation (Lee et al., 2011), while the input to the pumps is selected by independent upstream valves (Figure 2-1B: V2, V3, and V4). In another key adaptation from the continuous culture device, each reservoir was given a direct connection to the growth chamber by removing the pass-through channel and combiner before the peristaltic pump. This reduced the time delay between performing an injection and the injected plug of liquid reaching the growth chamber. As in the continuous device, the growth chamber consists of three interconnected sections, each with a 500- $\mu\text{L}$  liquid capacity. Using a working volume of 1000  $\mu\text{L}$  ensured that at most only two of the sections were full at a given time to facilitate mixing. Oxygenation of the growth chamber was provided by gas diffusion through the PDMS membrane and was enhanced by mixing (Lee et al., 2006b). Samples for offline analysis were collected via one of two output ports connected to the growth chamber (Figure 2-1).

Heating was performed at the base of the device using a resistive heater and a digital temperature sensor calibrated against the temperature of water inside the reactor. Dissolved oxygen and pH sensing were performed as described by Lee et al. (2011). Optical density was measured through a 100- $\mu\text{m}$  path length at a wavelength of 590 nm by positioning an LED and photodetector in-line in a connecting microchannel between two of the growth chamber sections. A smaller path length enabled linear optical density measurements up to at least  $\text{OD}_{600} = 50$  as measured offline by a DU800 Spectrophotometer (Beckman Coulter; Indianapolis, IN). All optical sensors were measured using fiber optic probes and data was analyzed in MATLAB to extract measured values. Oxygen and temperature

control algorithms were implemented using PID control (Lee et al., 2011) while pH control was implemented using a threshold and estimation algorithm (Lee et al., 2004).

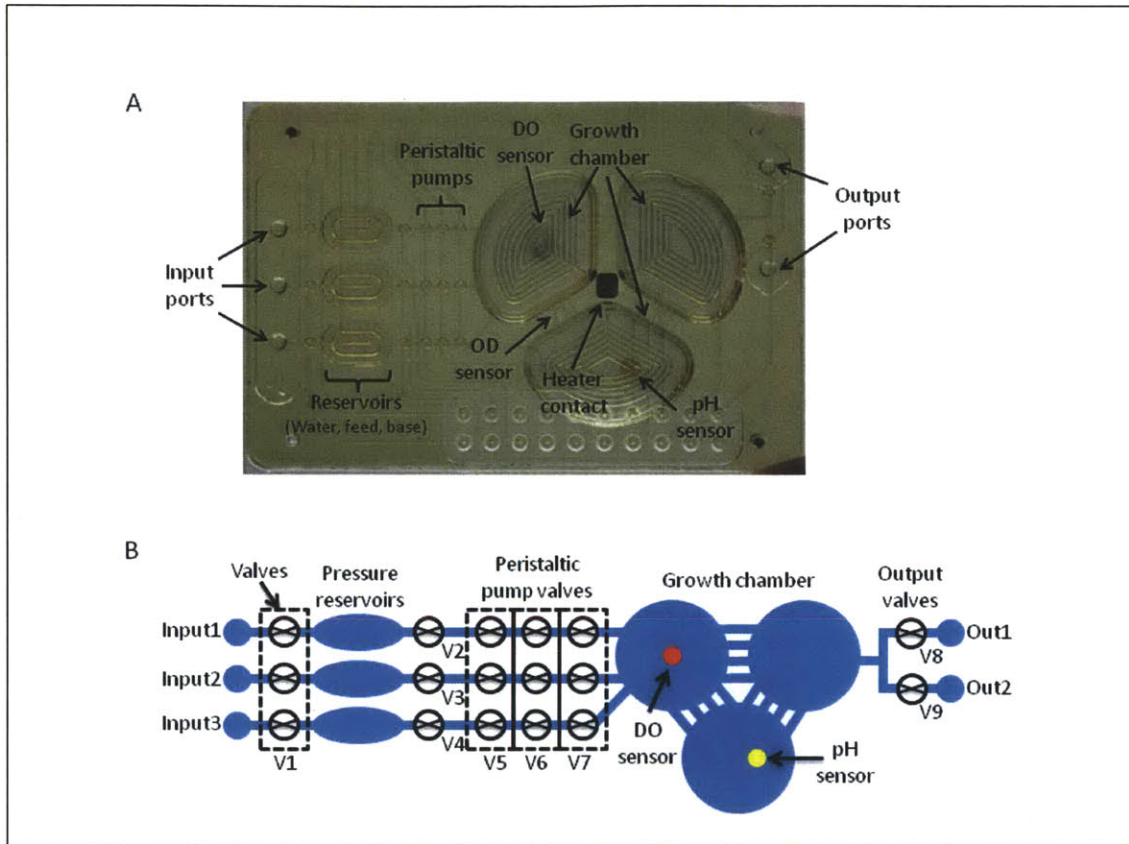


**Figure 2-1.** (A) Photograph of the fed-batch microbioreactor device with key features indicated. (B) Schematic of the microbioreactor highlighting details of the liquid flow path and valve design. The dotted boxes indicate that the valves are shared and act as a single unit. Valves are numbered V1 – V9. V1 controls flow from the solution input bottles (water, feed, and base); V2, V3, and V4 allow selection of output from pressurized reservoirs; V5, V6, and V7 comprise the peristaltic pumps; V8 and V9 control output from device. The reservoirs also have a shared valve for pressurization (not shown).

### 2.2.5 Microbioreactor cultures

Prior to use, the microbioreactors were placed in heat-sealable PVC bags and sterilized by gamma-irradiation at 18 kGy. To prepare inoculum for the microbioreactors, 3 mL of semi-defined medium was inoculated with 0.4% seed bank and grown overnight at 30°C. The next day, 3 mL semi-defined medium was inoculated to an initial OD<sub>600</sub> of 0.3 using the overnight culture; 1000 µL of the

resultant culture was used to fill the microbioreactor. Dissolved oxygen was controlled by varying the ratio of oxygen and helium in the inlet gas. Helium was used as the inert gas instead of nitrogen because its low solubility in water helped to control foaming. pH was controlled at 7.1 using 4 M NaOH. To better mimic the conditions in the bench-scale reactor, the temperature was slowly increased from 30°C to 42°C over a period of 30 minutes during the temperature induction phase of the plasmid production process. An evaporation control scheme was used to compensate for volume lost to evaporation and sampling. Before the start of feeding, the chip entered evaporation refill mode (Lee et al., 2011) every 30 minutes. After a sample was taken, the reactor was manually set to evaporation refill mode to add sterile distilled, de-ionized water until the culture reservoir was full. Evaporation refill was turned off after the start of feeding (approximately 8 hr after inoculation) to help maintain the reactor volume at or below 1 mL. Working volumes above 1 mL could result in reduced mixing efficiency. During the 30°C feeding phase, the feed addition helped compensate for volume lost due to evaporation; however, evaporation control was turned back on after the temperature shift (at approximately 20 hr) to compensate for the higher evaporation rate at the elevated temperature. While this scheme may have resulted in some transient changes in nutrient concentration, it helped alleviate the large volume losses observed in runs without any compensation for evaporation. At the end of the process, the chip could be discarded or gamma-irradiated and re-used.

### **2.2.6 Bioreactor cultures**

Bench-scale bioreactor cultures were performed using a Labfors 3 bioreactor (Infors; Bottmingen, Switzerland) with a maximum working volume of 2.3 L. The bioreactor was equipped with a D140 OxyProbe dissolved oxygen sensor (Broadley-James; Irvine, CA) and an F-695 FermProbe pH electrode (Broadley-James). To prepare the bioreactor inoculum, 3 mL of semi-defined medium was inoculated with 0.4% seed bank and grown overnight at 30°C. The next day, 100 mL of semi-defined

medium was inoculated with 100  $\mu$ L of overnight culture in a 500-mL baffled shake flask and incubated overnight at 30°C.

To set up the bioreactor, 1.3 to 1.8 L of basal cultivation medium was autoclaved in the reactor. On the day of inoculation, medium supplements and 0.2 mL Antifoam 204 (Sigma-Aldrich; St. Louis, MO) were added, and the reactor was inoculated to an initial OD<sub>600</sub> of 0.3 using overnight seed culture. The dissolved oxygen setpoint was controlled at 35% using a cascade to agitation (250 rpm to 800 rpm), and air was provided at an initial flow rate of 1 vvm. For oxygen supplementation studies, pure oxygen was automatically added to the air flow at 0.4 to 0.6 LPM as needed to maintain the DO setpoint. In all runs, the air flow was increased to 1.2 vvm when the temperature was increased to 42°C. pH was controlled at 7.10  $\pm$  0.05 using 4 M NaOH and 2.25 M H<sub>3</sub>PO<sub>4</sub>. Online data was logged using IRIS fermenter log and control software (Infors). Antifoam was manually added in 0.2-mL increments as needed. Samples were taken periodically to measure OD<sub>600</sub> offline using a DU800 Spectrophotometer (Beckman Coulter). Samples for glycerol, acetate, and plasmid DNA concentration measurements were stored at -30°C until analysis.

### **2.2.7 Measurement of glycerol and acetate concentrations**

Glycerol and acetate concentrations in culture supernatants were determined using an Agilent 1200 Series HPLC (Agilent Technologies; Santa Clara, CA) equipped with an Aminex HPX-87H column (Bio-Rad; Hercules, CA). A 5 mM sulfuric acid mobile phase was run at 0.6 mL/min for 25 minutes at 50°C. Glycerol and acetate peaks were detected by refractive index at approximate retention times of 13.4 and 15.2 minutes, respectively.



### 2.2.8 Measurement of plasmid copy number

Plasmid copy number was measured using a quantitative PCR (qPCR) assay adapted from the relative quantitation method described by Lee et al. (2006a). Total DNA (genomic and plasmid) was isolated from 25-50  $\mu\text{L}$  of culture using the DNeasy Blood & Tissue kit (Qiagen; Valencia, CA). qPCR was performed using a 7300 Real-Time PCR system (Applied Biosystems; Carlsbad, CA) with primers targeting the plasmid-based kanamycin resistance gene (forward primer: 5'-TCGACCACCAAGCGAAACA-3', reverse primer: 5'-CGACAAGACCGGCTTCCAT-3') and *dxs*, a single-copy gene on the *E. coli* chromosome encoding 1-deoxyxylulose-5-phosphate synthase (forward primer: 5'-CGAGAACTGGCGATCCTTA-3', reverse primer: 5'-CTTCATCAAGCGGTTTACA-3'). Each 25- $\mu\text{L}$  qPCR reaction contained 1X Brilliant II SYBR Green High ROX Master Mix reagent (Agilent Technologies), 200 nM each of the forward and reverse primers, and the total DNA sample diluted 10- to 100-fold in order to be within the linear range of the assay. The thermal profile consisted of a 10-minute hold at 95°C followed by 40 cycles of 95°C for 30 s and 60°C for one minute. Plasmid copy number was calculated using the  $\Delta\Delta C_T$  method (Livak and Schmittgen, 2001) which included normalization to a calibrator plasmid, pVAX1-*dxs*, containing single copies of both the kanamycin resistance gene and *dxs*.

### 2.2.9 Measurement of plasmid DNA specific yield

Plasmid DNA was quantified from crude lysates prepared from  $\text{OD}_{600} = 10$  cell pellets using the method described by Listner et al. (2006a). Typically, volumes ranging from 0.2 to 2.5 mL were required to form a pellet of the appropriate density. The lysis method was modified slightly: cell pellets were harvested by centrifugation at 5000  $\times g$  for 15 minutes, the 37°C incubation took place with 250 rpm shaking, and 5  $\mu\text{L}$  of 10 mg/mL RNase A solution was used per mL of lysate. The pDNA content of the lysates was measured using a Gen-Pak FAX anion-exchange column (Waters Corporation; Milford, MA) on an Agilent 1100 Series HPLC system (Agilent Technologies). Three buffers were used: Buffer A (25

mM Tris-HCl, 1 mM EDTA, pH 8.0), Buffer B (25 mM Tris-HCl, 1 mM EDTA, 1 M NaCl, pH 8.0), and Buffer C (0.04 M H<sub>3</sub>PO<sub>4</sub>). The LC method was run at a constant flow rate of 0.75 mL/min and consisted of the following steps: (1) linear ramp from 70%:30% A:B to 34%:66% A:B over 10 min., (2) 100% B for 5 min., (3) 100% C for 4.5 min., and (4) 70%:30% A:B for 10 min. Plasmid DNA eluted at a retention time of approximately 11.5 min as detected by absorbance at 260 nm. A standard curve of pVAX1-GFP (2 µg/mL to 50 µg/mL) was prepared using pDNA purified using the Hi-Speed QIAfilter Plasmid Maxi Kit (Qiagen) and quantified using a NanoPhotometer (Implen; Westlake Village, CA). A standard curve was used to calculate the µg of pDNA per mL of lysate prepared from each pellet. Specific yield was calculated using the correlation that 1 OD<sub>600</sub> unit = 0.4 g DCW/L culture.

#### **2.2.10 pDNA quality analysis**

Plasmid DNA purified using the Zymoply Plasmid Miniprep Kit (Zymo Research Corporation; Irvine, CA) was run on a 0.7% agarose gel and stained with ethidium bromide to visualize the relative quantities of linear, nicked, and supercoiled species. Linear and nicked pDNA standards were made by digesting pVAX1-GFP with the restriction enzyme XhoI or the nicking endonuclease Nt.BstNB1, respectively.

## **2.3 Results and Discussion**

### **2.3.1 Plasmid production in bench-scale bioreactors as a model system**

A key property of microbioreactors is the ability to predict the behavior of larger scale fermentations. To evaluate the performance of our fed-batch microbioreactor we used production of a pUC-based DNA vaccine vector via temperature-induction as a model system. Specifically, we compared *E. coli* growth, glycerol consumption, acetate production, and plasmid copy number across scales.

At the bench-scale, initial specific feed rates of 2.6, 3.2, 3.5, and 6.1 g glycerol/L/hr were investigated. Growth curves show that fed-batch cultures of DH5α[pVAX1-GFP] typically reached OD<sub>600</sub>

values between 40 and 60 under the conditions tested (Figure 2-2A). As the feed rate increased, the final  $OD_{600}$  decreased, likely due to the increased duration of oxygen limitation at higher feed rates. With air as the only oxygen source, the dissolved oxygen setpoint could not be maintained for the duration of the run. Higher feed rates led to increased oxygen demand due to increased substrate availability, and as a result, cultures with higher feed rates became oxygen-limited earlier in the run.

In all bench-scale experiments, the 5 g/L of batched glycerol was consumed before the start of feeding (Figure 2-2B). At all but the highest feed rate tested, there was no glycerol accumulation in the medium after the start of feeding. Acetate was produced to varying degrees during the feeding phase, with the amount of acetate produced increasing with increasing feed rate (Figure 2-2C).

Production of pVAX1-GFP was quantified by measuring the number of plasmid copies per chromosome (Figure 2-2D). As expected, temperature-induced amplification of pVAX1-GFP occurred in the bench-scale bioreactor. For the moderate feed rates (3.2 and 3.5 g glycerol/L/hr), the plasmid copy number remained below 50 copies/chromosome until the temperature shift from 30°C to 42°C, after which the copy number steadily increased until the end of the fermentation, reaching maximum values of 351 and 434 copies/chromosome, respectively. At the highest feed rate, the copy number was about 2-fold higher when the temperature was shifted, but clear temperature-induced amplification still occurred. At the lowest feed rate, the plasmid copy number only increased from 39 to 62 copies/chromosome over the course of the temperature-induction phase of the culture. Possible explanations for this phenomenon will be discussed below.

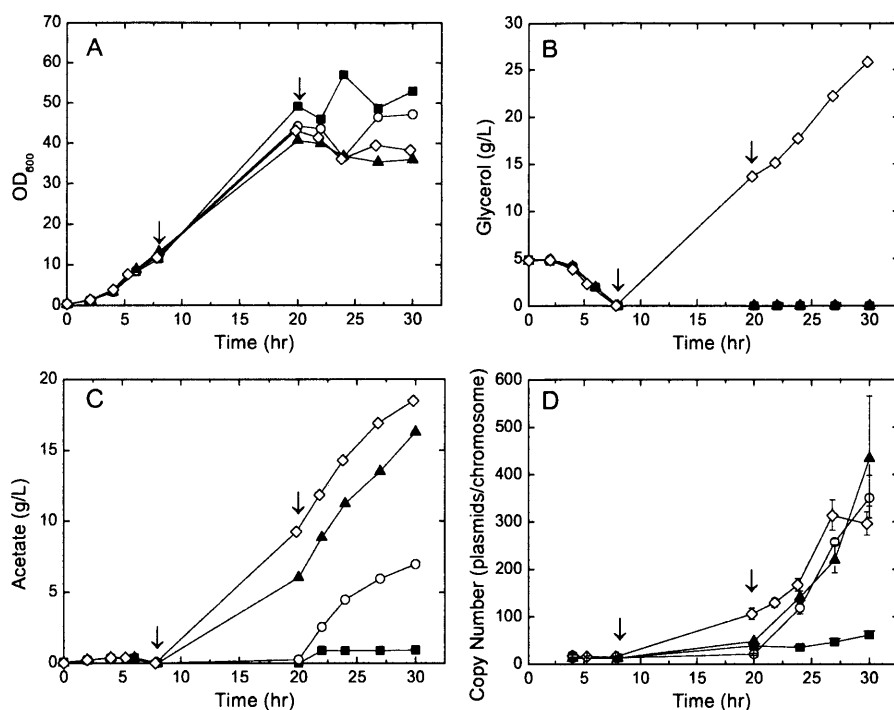


**Figure 2-2.** (A) Optical density, (B) glycerol, (C) acetate, and (D) average plasmid copy number profiles for bench-scale fed-batch cultures with initial specific feed rates of 2.6 (■), 3.2 (○), 3.5 (▲), and 6.1 (◇) g glycerol/L/hr. In each plot, from left to right, the arrows indicate the start of feeding and the 30°C-to-42°C temperature shift, respectively. The plasmid copy number error bars represent the 95% confidence interval calculated from three replicate wells of the same sample

At the bench scale, we were also able to measure specific pDNA yield from crude lysates. The final specific yields were 2.9, 4.5, 1.3, and 0.4 mg pDNA/g DCW at initial specific feed rates of 2.6, 3.2, 3.5, and 6.1 g glycerol/L/hr, respectively. There are several possible explanations for the apparent discrepancies between the copy number and specific yield trends. First, conversion between copy number and specific yield involves several assumptions, including the cellular chromosomal content and the number of intact cells contributing to optical density measurements. The average *E. coli* cell is typically cited to contain 2.1 chromosomes, however, this value was measured for *E. coli* B/r during balanced growth at 37°C, and is not likely to be valid under other growth conditions or for different strains (Neidhardt and Umberger, 1996). Chromosomal content changes with growth rate (Bipatnath et

al., 1998) and growth phase (Akerlund et al., 1995) and a two-fold change in the number of chromosomes/cell will result in a two-fold change in the expected specific yield calculated from a given copy number. Due to the complex nature of cell physiology during non-balanced growth, we cannot calculate the number of chromosomes per cell expected during our fed-batch process. It is also possible that at higher feed rates, cell debris or partially intact cells containing no pDNA contributed to optical density measurements, resulting in an artificial lowering of the specific yield. This is supported by the fact that discrepancies were more prevalent under high-stress culture conditions (oxygen limitation and high acetate concentration) under which cell morphology likely undergoes the most dramatic change. Along these lines, it is also possible that stress-induced physiological and morphological changes reduced the effectiveness of the lysis protocol. Conversely, it is also possible that these physiological changes resulted in partial occlusion of the genomic DNA such that the qPCR primers could not efficiently bind, resulting in reduced detection of the chromosomal target. However, gel electrophoresis analysis of samples from the highest feed rate run showed evidence of increased pDNA concentration with time (data not shown), lending credence to the idea that the specific yield measurements may not be accurately capturing pDNA concentrations.

The apparent discrepancy between the trends in copy number and specific yield observed at the higher feed rates highlights one of the key challenges of microreactor technologies – analytics. The small sample volumes available from the microreactors preclude the use of the specific yield assay. However, the qPCR-based copy number assay can be performed at both scales so we chose to make this our standard for comparison of productivity in the sections that follow.

### **2.3.2 Plasmid production in microbioreactors**

Microbioreactor feed rates of 0.536, 0.664, and 0.868 injections per minute were investigated to determine the ability of the microreactors to predict trends in growth, metabolite concentration, and

product yield at the bench scale. The volume of each feed injection was approximately 240 nL, but this number varied by roughly 20% due to small deviations in the device fabrication process. The injection rates studied corresponded to specific feed rates of approximately 2.5, 3.1, and 4.0 g glycerol/L/hr.

The growth curves at each feed rate (Figure 2-3A) demonstrate that the microbioreactors can support cell densities of at least  $OD_{600} = 40-60$ . These cell densities are in the range of those observed at the bench scale. Note that the trend in optical density with respect to feed rate is inverted for the microreactors when compared to the bench-scale bioreactor. This is likely due to differences in oxygen availability. The inlet gas stream to the microreactors was supplemented with oxygen, allowing the dissolved oxygen level to be maintained at approximately 30% for all feed rates investigated. Therefore, at higher feed rates, more substrate was available for biomass production and its utilization was not restricted by the oxygen limitation observed at the bench scale.

The glycerol profiles from the microreactor experiments (Figure 2-3B) show that, in contrast to the bench-scale runs, there was some glycerol present at the time feeding began. The highest feed rate resulted in glycerol accumulation, suggesting that the cells were unable to utilize all of the glycerol being fed. However, the glycerol concentration decreased after the temperature shift, suggesting an increase in glycerol uptake rate. This is in contrast to the bench-scale reactor in which glycerol accumulated in the medium monotonically.

The acetate accumulation profiles (Figure 2-3C) highlight a major difference observed between the micro and bench scales. With the exception of the highest feed rate tested, less than 1 g/L acetate was produced in the microreactors. This is in stark contrast to the bench-scale reactor in which acetate accumulated under all conditions tested (Figure 2-2C).

Temperature-induced amplification of pVAX1-GFP was observed at feed rates of 0.536 and 0.664 injections/minute in the microreactors (Figure 2-3D). The final copy number values were about 2-fold lower than those observed at the bench scale; however, a comparison by agarose gel

electrophoresis shows comparable pDNA content across the reactor scales (Figure 2-4: Lanes 4, 5, and 7). At a feed rate of 0.868 injections/minute there was a slight increase in copy number after the temperature shift, but the increase was not nearly as dramatic as that observed at the lower feed rates or at the bench scale.

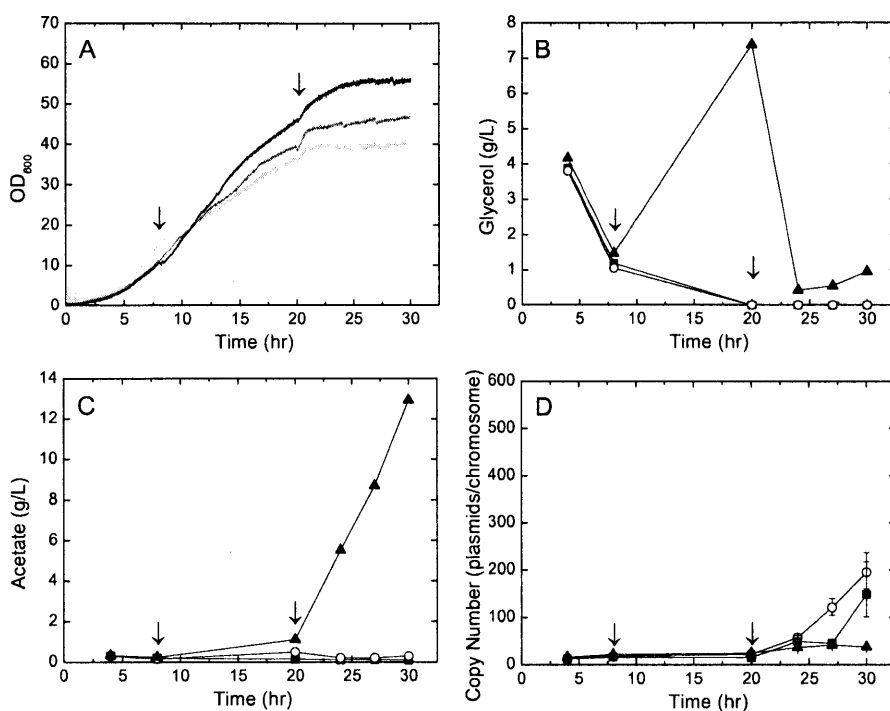


**Figure 2-3.** (A) Growth curves for the microbioreactor cultures at feed injection rates of 0.536 (light gray), 0.664 (dark gray), and 0.868 (black) injections per minute. (B) Glycerol, (C) acetate, and (D) average plasmid copy number profiles for microbioreactor fed-batch cultures with feed injection rates of 0.536 (■), 0.664 (○), and 0.868 (▲) injections per minute. In each plot, from left to right, the arrows indicate the start of feeding and the 30°C-to-42°C temperature shift, respectively. The plasmid copy number error bars represent the 95% confidence interval calculated from three replicate wells of the same sample.

Additional experiments demonstrated that the residual glycerol present at the time of feed initiation in the microreactor did not impact plasmid copy number (data not shown). Delaying feeding resulted in a slight increase in the maximum acetate concentration (1.3 g/L compared to 0.5 g/L, both at 20 hr), but the final acetate concentrations with both feeding schemes were nearly identical.

Another factor that could be contributing to the differences observed between scales is that in the microreactors the volume was kept approximately constant at 1000  $\mu\text{l}$  throughout the run, and as a result the specific feed rate remained the same. This is in contrast to the bench-scale reactor in which the specific feed rate decreased over the course of the fermentation due to the increasing culture volume.

### 2.3.3 Plasmid quality assessment

Plasmid DNA quality was evaluated using gel electrophoresis to demonstrate that the microreactor could produce both comparable quantity and quality (*i.e.*, degree of supercoiling) of the product. The plasmid produced at both scales was predominantly in the supercoiled form with traces of the nicked (open-circular) form (Figure 2-4). We can conclude that the microreactor cultivation does not negatively impact plasmid quality, and that the device can be used to evaluate product quality, in addition to product yield, under a variety of culture conditions.

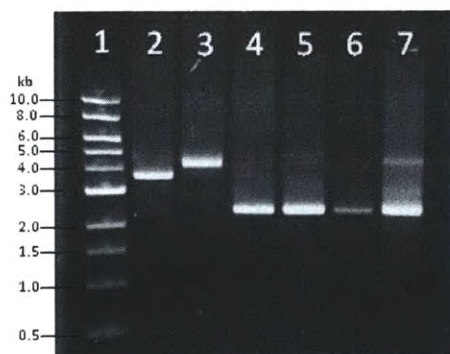


**Figure 2-4.** Agarose gel electrophoresis of plasmid DNA produced by the microreactors and bench-scale bioreactors. **Lane 1:** DNA ladder with DNA size in kilobases (kb) indicated to the left of the image, **Lane 2:** Linearized pVAX1-GFP, **Lane 3:** Nicked pVAX1-GFP, **Lane 4:** pVAX1-GFP from bench-scale reactor (3.5 g glycerol/L/hr), **Lane 5:** pVAX1-GFP from bench-scale reactor (2.6 g glycerol/L/hr), **Lane 6:** pVAX1-GFP from microreactor (0.868 inj/min), **Lane 7:** pVAX1-GFP from microreactor (0.536 inj/min). Only a representative set of pDNA samples is shown. pDNA from all feed rates had quality similar to or better than that shown. All samples were from the final timepoint of each culture (approximately 30 hours after inoculation). Note also that the pDNA in Lanes 4, 5, and 7 was purified from  $\text{OD}_{600} = 2$  pellets, whereas the number of cells used for the pDNA preparation in Lane 6 was not determined.



#### 2.3.4 Impact of oxygen availability

One of the most marked differences between the microreactor and bench-scale bioreactor studies was acetate production. In the microreactors, acetate production was only observed when glycerol accumulated in the medium, which points to metabolic overflow as the primary cause. In contrast, acetate was produced in all of the bioreactor runs despite an absence of glycerol accumulation at all but the highest feed rates. Two common causes of acetate production are metabolic overflow (*i.e.*, carbon flux that exceeds the capacity of the TCA cycle) and oxygen limitation (Wolfe, 2005). Elevated temperature has also been shown to induce increased acetate production (Luders et al., 2009). The degree of metabolic overflow is related to feed rate rather than scale, and the cultures were exposed to the same temperature extremes at both scales. Therefore, the most plausible explanation for the differences in acetate production likely involves the oxygen transport properties of each system. The oxygen mass transfer rate ( $k_La$ ) in microbioreactors with the same growth chamber geometry as those used in this work has been measured previously to be approximately  $58 \text{ hr}^{-1}$  (Lee et al., 2011), which is an order of magnitude lower than values typically achieved in stirred-tank vessels (Bareither and Pollard, 2011; Islam et al., 2008). To compensate for the lower  $k_La$ , the microreactors were always supplemented with up to 100% oxygen, resulting in different dissolved oxygen profiles at each scale (Figure 2-5).

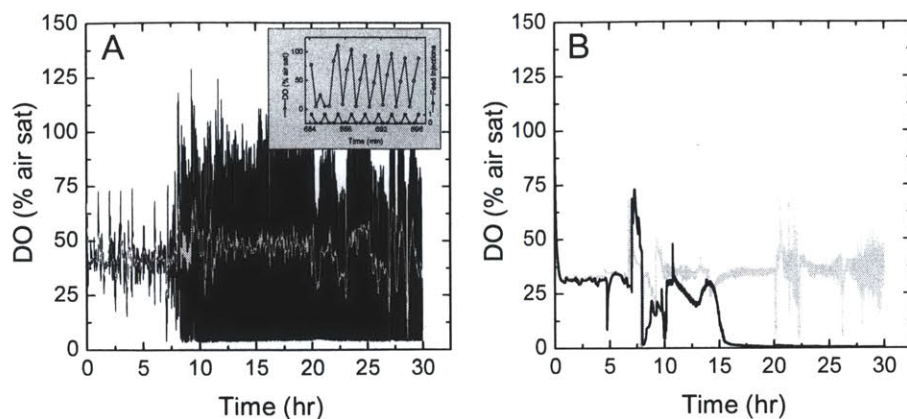


**Figure 2-5.** Dissolved oxygen profiles from representative microreactor and bench-scale bioreactor cultures. (A) Dissolved oxygen profile from microreactor culture with 0.664 inj/min feed rate (black line). A moving average over a 20-point window is also shown for clarity (light gray line). The inset shows a zoomed-in version of the dissolved oxygen versus time plot overlaid with the feed injection profile. For each point in the feed injection profile, a value of 0 indicates that no feed injection took place at that time, while a value of 1 indicates that a feed injection took place. (B) Dissolved oxygen profiles from bench-scale bioreactor cultures at an initial specific feed rate of 3.2 g glycerol/L/hr with air only in the inlet gas (black line) and with oxygen supplementation (light gray line).

In the microreactors, the cultures were never oxygen limited for an extended period of time. Because of the intermittent nature of the feed injections, the dissolved oxygen dropped sharply immediately after the injection of substrate, but recovered before the next injection, resulting in an average dissolved oxygen concentration that was greater than zero (Figure 2-5A). The same was not true for the bioreactor cultures. At the bench-scale, the setpoint was maintained until the agitation reached its maximum, at which point the oxygen demand outstripped supply and the dissolved oxygen dropped to zero (Figure 2-5B). The differences in dissolved oxygen profiles across scales suggest that acetate accumulation at the bench scale could be due to the culture no longer being fully aerobic. Alexeeva et al. (2002) have shown that the acetate production rate of a culture increases dramatically during the transition from aerobic to anaerobic growth. Our hypothesis is also supported by the detection of fermentation products (formate, lactate, succinate, and ethanol) in the medium at the highest feed rate (*i.e.*, conditions in which the duration of zero dissolved oxygen was the longest).

### 2.3.5 Bench-scale bioreactors with oxygen supplementation

To test the impact of oxygen availability on acetate accumulation and plasmid yield, we supplemented the inlet air to the bench-scale bioreactor with oxygen in order to maintain the dissolved oxygen setpoint for the entire run (Figure 2-5B). Two conditions were tested: a moderate feed rate which did not result in glycerol accumulation (3.2 g glycerol/L/hr initial specific feed rate) and a high feed rate that resulted in significant glycerol accumulation (6.1 g glycerol/L/hr initial specific feed rate). The glycerol profile at the moderate feed rate with oxygen supplementation (Figure 2-6B) was the same as the profile with air only (Figure 2-2B). At the high feed rate, the glycerol profile (Figure 2-6B) resembled that observed in the microreactors at the highest feed rate tested (Figure 2-3B) -- glycerol accumulated after the start of the feed, but the concentration decreased after the 30°C-to-42°C temperature shift.

Interestingly, at the moderate feed rate with oxygen supplementation no acetate was produced after the start of feeding (Figure 2-6C), in contrast to the air-only run at the same feed rate that resulted in production of approximately 7 g/L acetate (Figure 2-2C). This suggests that oxygen limitation was the cause of the discrepancies in acetate production between scales. At the high feed rate with oxygen supplementation, acetate still accumulated in the medium (Figure 2-6C), likely due to metabolic overflow. This is consistent with the acetate profile seen in the microreactor at the highest feed rate (Figure 2-3C).

Oxygen supplementation of the bench-scale reactor led to significantly lower plasmid copy numbers (Figure 2-6D) when compared to the runs with air only in the inlet gas (Figure 2-2D). Some temperature-induced amplification was observed at both the moderate and high feed rates. The trends are consistent with those observed in the microreactor, in which the highest feed rate gave the lowest final copy number (Figure 2-3D). The phenomenon of lower plasmid copy number under non-limiting oxygen conditions is also consistent with the low copy number observed at the lowest feed rate in the

air-only bench-scale run (Figure 2-2D). In this run, the dissolved oxygen setpoint could not be maintained at 30%, but remained above zero for the duration of the run.

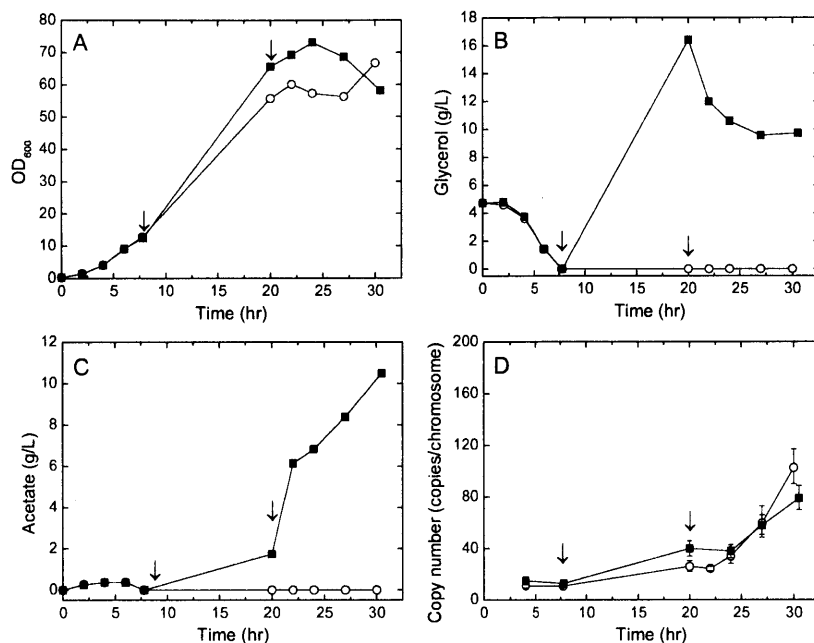


**Figure 2-6.** (A) Optical density, (B) glycerol, (C) acetate, and (D) average plasmid copy number profiles for oxygen-supplemented bench-scale cultures with initial specific feed rates of 3.2 (○) and 6.1 (■) g glycerol/L/hr. In each plot, from left to right, the arrows indicate the start of feeding and the 30°C-to-42°C temperature shift, respectively. Error bars on the plasmid copy number values represent the 95% confidence level calculated from three replicate wells of the same sample.

The data from the oxygen-supplemented bioreactors clearly demonstrate that our fed-batch microbioreactor platform can replicate a complex bench-scale fed-batch process as long as key process parameters (*i.e.*, oxygen availability) are held constant across scales. We have shown that the dissolved oxygen profiles under standard operating conditions can be quite different at the bench and micro-scale, and that results were only consistent across scales when these differences were accounted for. Thus, the microreactor system enabled the identification of oxygen availability as a key parameter affecting pDNA production.

### 2.3.6 Oxygen-limited microbioreactors

To simulate the oxygen limitations observed at the bench scale and further test our devices, we ran microbioreactors at a feed rate of 3.1 g glycerol/L/hr using air alone or helium containing a maximum of 50% oxygen as the inlet gas. We found that acetate accumulated to concentrations of about 17 g/L (Figure 2-7A). We expected a significant increase in plasmid copy number, similar to that observed in the air-only bench-scale runs, but only a slight amount of plasmid amplification was observed (Figure 2-7B). Careful analysis of the runs showed that the high concentrations of acetate resulted in a very low pH by the end of the run (5.8 – 6) due to a combination of technical problems with the pH sensor and the limited volume available for base addition.

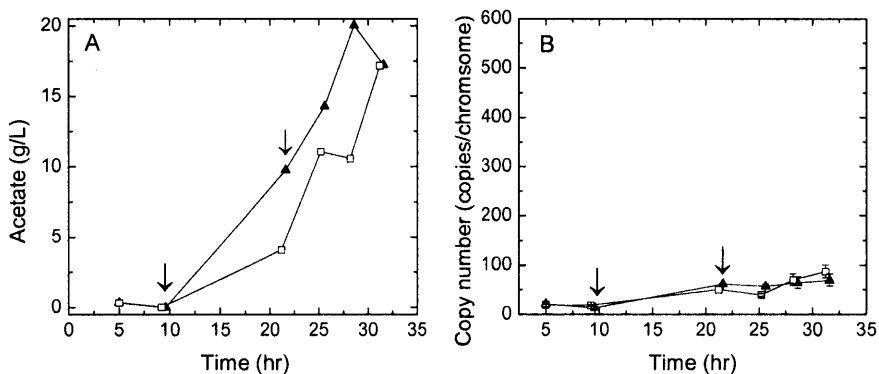


**Figure 2-7.** (A) Acetate and (B) plasmid copy number profiles from microbioreactor runs at a feed rate of 3.1 g glycerol/L/hr with air only (▲) or a maximum of 50% oxygen (□) in the inlet gas. In each plot, from left to right, the arrows indicate the start of feeding and the 30°C-to-42°C temperature shift, respectively. Error bars on the plasmid copy number values represent the 95% confidence level calculated from three replicate wells of the same sample.

To test the hypothesis that acidic pH was negatively affecting plasmid copy number, we ran two bench-scale fermentations at an initial specific feed rate of 5.5 g glycerol/L/hr. In one run, the pH was controlled at 7.1 for the entire experiment. In the other, the pH was controlled at 7.1 until the temperature shift, at which time the pH was shifted to 6.0. Under both pH conditions, acetate accumulation levels (Figure 2-8A) were comparable to those in the oxygen-limited microreactor experiments (Figure 2-7A). These similar profiles likely resulted from the higher feed rate used in the

bioreactor runs (and the resulting higher oxygen demand) counterbalancing the effects of the higher  $k_L a$  of the bioreactors. Metabolic overflow also likely contributed to acetate production in all runs, as glycerol accumulated in the medium at both scales (data not shown). In terms of plasmid production, the results show that acidic pH at the end of the process resulted in a significant decrease in plasmid copy number compared to the run controlled at a neutral pH (Figure 2-8B).

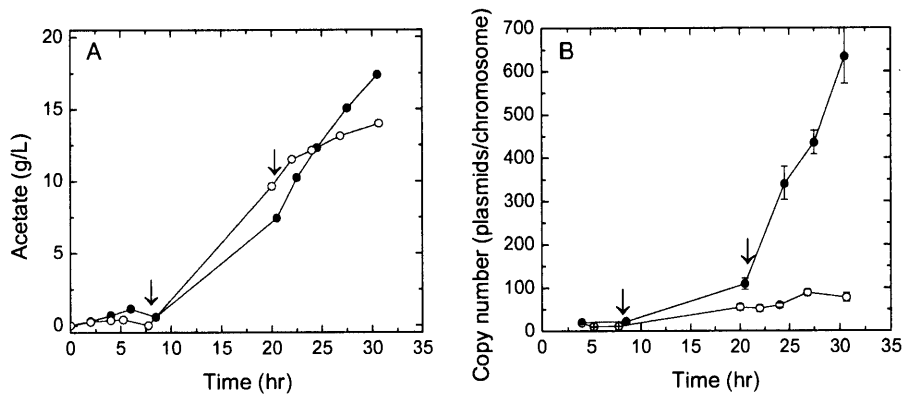


**Figure 2-8.** (A) Acetate and (B) plasmid copy number profiles from fed-batch bioreactor cultures with (○) and without (●) a pH downshift from 7.1 to 6.0 at  $t = 20$  hr. From left to right, arrows indicate the start of feeding and the 30°C-to-42°C temperature shift, respectively. Error bars represent the 95% confidence level calculated from three replicate wells.

There is some evidence in the literature that acidic pH can negatively impact plasmid yield, possibly due to a reduction in the proton motive force and the resulting drop in ATP production (Ongkudon et al., 2011). However, another study observed a modest improvement in plasmid titers at slightly acidic pH values (O'Mahony et al., 2007). Despite these conflicting results, the observations made in this work emphasize the importance of being vigilant about changes in all process parameters during a scale-down effort, as they may have a significant impact on productivity.

## 2.4 Conclusions

In this work, we demonstrated the design and implementation of a 1-mL microbioreactor for scale-down of a complex, fed-batch process. Our microreactor provided monitoring and control of dissolved oxygen, pH, and temperature, as well as continuous monitoring of optical density. Using the model system of temperature-induced production of a plasmid DNA vaccine vector in *E. coli* we showed that the microbioreactor can accurately reproduce the growth, metabolite profiles, and plasmid amplification observed at the bench-scale under comparable conditions. We varied the feed rate to demonstrate that the results were reproducible across scales under conditions in which the primary substrate (glycerol) was limiting or in excess. We also observed that plasmid copy number appeared to be higher under “non-optimal” conditions (low dissolved oxygen, acetate accumulation), and is negatively impacted by acidic pH. These key parameters would not have been identified without the use of the scale-down system. By extending our process monitoring beyond growth and including metabolites and product yields as indicators of scale-down accuracy, we were able to gain a better understanding of the process as a whole.

Over the course of our investigation, we identified several differences between scales, such as volume changes with feeding (or lack thereof). However, the qualitative agreement between the bench- and micro-scale data indicates that these differences are not critical for the utility of the microreactor system. In addition, oxygen availability emerged as a key parameter to achieve consistency during scale-down. The increased ease and safety of using oxygen supplementation at the microscale led us to uncover this key process requirement. Various input gas mixtures could be explored in the microreactors to further investigate the impact of oxygen availability on culture productivity.

Overall, we have demonstrated the successful scale down of a temperature-inducible, fed-batch process for plasmid DNA production in *E. coli* from 2 L to 1 mL. Our microbioreactor device includes many of the key features required to meet the current needs of microbial process development in the

biopharmaceutical, biomaterials, and biofuels industries. These features include advanced process monitoring and control capabilities, well-controlled feeding, sufficient oxygen transfer to achieve high cell densities, and rapid set-up and clean-up. Current and future work seeks to parallelize the devices to allow a single researcher to run multiple experiments simultaneously.



# Chapter 3

---

## New plasmid DNA vaccine vectors with R1-based replicons

### Abstract

There has been renewed interest in biopharmaceuticals based on plasmid DNA (pDNA) in recent years due to approval of several veterinary DNA vaccines, on-going clinical trials of human pDNA-based therapies, and significant advances in adjuvants and delivery vehicles that have helped overcome earlier efficacy deficits. In this work, we have constructed a new DNA vaccine vector, pDMB02-GFP, containing the runaway R1 origin of replication. The runaway replication phenotype should result in plasmid copy number amplification after a temperature shift from 30°C to 42°C. However, using *Escherichia coli* DH5 $\alpha$  as a host, we observed that the highest yields of pDMB02-GFP were achieved during constant-temperature culture at 30°C, with a maximum yield of approximately 19 mg pDNA/g DCW being observed. By measuring mRNA and protein levels of the R1 replication initiator protein, RepA, we determined that RepA may be limiting pDMB02-GFP yield at 42°C. A mutant plasmid, pDMB-ATG, was constructed by changing the *repA* start codon from the sub-optimal GTG to ATG. In cultures of DH5 $\alpha$ [pDMB-ATG], temperature-induced plasmid amplification was more dramatic than that observed with pDMB02-GFP, and RepA protein was detectable for several hours longer than in cultures of pDMB02-GFP at 42°C. Overall, we have demonstrated that R1-based plasmids can produce high yields of high quality pDNA without the need for a temperature shift, and have laid the groundwork for further investigation of this class of vectors in the context of plasmid DNA production.

**Parts of this chapter are in preparation for publication in:**

Bower DM, Prather KLJ. Development of new plasmid DNA vaccine vectors with R1-based replicons.

### 3.1 Introduction

Gene therapies and DNA vaccines have gained attention in recent years as potential treatments for a range of acquired and infectious diseases. In particular, plasmid-DNA-based therapies are attractive because they have a good safety profile and are relatively easy to manufacture using *Escherichia coli* as a host. Interest in the field has also been stimulated by the approval of several veterinary pDNA-based therapeutics and on-going clinical trials of plasmid-based human therapeutics (Kutzler and Weiner, 2008). In addition, a recent Phase 2 trial of an adenoviral-vectored DNA vaccine yielded disappointing results (Moore et al., 2008), fueling safety and efficacy concerns surrounding adenoviral vaccines. Finally, recent advances in delivery vehicles and adjuvants for use in concert with naked plasmid DNA have helped increase the efficacy of these therapies (Saade and Petrovsky, 2012). Gene delivery via electroporation has especially reinvigorated the field; early studies suggest that DNA delivered using electroporation devices may elicit immune responses on par with more traditional vaccines (Sardesai and Weiner, 2011).

Currently, plasmid DNA is produced almost exclusively using vectors containing the high-copy pUC replicon. pUC-based plasmids are derivatives of the ColE1 origin of replication that lack the RNA one modulator (Rom) protein and contain a point mutation in the RNA II sequence. These two mutations together give increasingly higher copy numbers as the culture temperature is increased from 30°C to 42°C (Lin-Chao et al., 1992). Extensive process development has resulted in the design of very high yield, fed-batch processes for the production of pUC vectors (Williams et al., 2009b). However, with the exception of the pCOR family of plasmids based on the R6K replicon (Soubrier et al., 1999; Soubrier et al., 2005), no other plasmid replicons have been investigated for pDNA production applications.

One promising alternative to the currently-available plasmids are vectors based on the so-called runaway R1 origin of replication. There are numerous reports in the early plasmid literature about these

high-copy mutants of the *E. coli* plasmid R1. Runaway replication plasmids lose control of their copy number at high temperatures (> 37°C), resulting in plasmid copy numbers as high as 2000 copies per chromosome (Uhlin et al., 1979). The mechanism of R1 replication has been described extensively elsewhere (Nordström, 2006). In short, two point mutations confer the runaway replication phenotype: one that decreases transcription of the antisense RNA repressor *copA*, and a second that increases transcription of the replication initiator protein gene, *repA*, in a temperature-dependent fashion (Givskov et al., 1987). Runaway R1-based plasmids have been used successfully for temperature-induced recombinant protein production (Ansorge and Kula, 2000; Hoffmann et al., 1987; Kidwell et al., 1995; Morino et al., 1988), but they have yet to be investigated in the context of plasmid DNA production for therapeutic applications.

This chapter describes the construction and characterization of a new DNA vaccine vector, pDMB02-GFP, containing the runaway R1 origin of replication that is capable of producing high plasmid DNA yields. The yield trends of our new vector were compared to the yields of both the replicon source plasmid and a pUC-based DNA vaccine vector at the shake flask scale in rich medium. We also monitored the mRNA and protein expression of the plasmid replication initiator, *repA*, to gain insight into the observed yield trends.

## 3.2 Materials and Methods

### 3.2.1 *E. coli* strains and plasmids

*E. coli* strain DH5 $\alpha$  [F $\phi$ 80*lacZ* $\Delta$ M15  $\Delta$ (*lacZYA-argF*)U169 *deoR recA1 endA1 hsdR17*(r $_k^-$ , m $_k^+$ ) *phoA supE44 thi-1 gyrA96 relA1*  $\lambda$ ] and the plasmid pVAX1 (2999 bp) were purchased from Invitrogen (Carlsbad, CA). pVAX1-GFP (3642 bp) was constructed by cloning the superfolder green fluorescent protein (sGFP) gene (Pedelacq et al., 2006) into the multi-cloning site of pVAX1. The sGFP gene was obtained from the plasmid pTrcsGFP, a gift from the Gregory Stephanopoulos laboratory. pCP40 (5029

bp) was constructed by Remaut et al. (1983) and was obtained from the Belgian Coordinated Collections of Microorganisms BCCM/LMBP plasmid collection (accession number LMBP 951).

To construct pDMB02-GFP, a 1938-bp fragment of pVAX1 containing the human cytomegalovirus (CMV) immediate-early promoter/enhancer, bovine growth hormone (BGH) polyadenylation signal, and kanamycin resistance gene was PCR-amplified using primers containing *AvrII* and *SbfI* restriction sites. A 3073-bp fragment of pCP40 containing the R1 origin of replication along with the *repA*, *copA*, and *copB* gene sequences was also PCR-amplified with the same restriction sites. The pVAX1 and pCP40 fragments were ligated to construct the plasmid pDMB02. The sGFP gene was cloned into the *NheI* and *XhoI* restriction sites downstream of the CMV promoter/enhancer. A Kozak sequence was also inserted at the start of the sGFP gene by adding the sequence ACC before the start codon and a valine codon (GTG) following the start codon. The Kozak sequence should help facilitate sGFP gene expression in mammalian cells (Kozak, 1987). The resulting vector, pDMB02-GFP, was 5668 bp in size (Figure 3-1). Correct construction was confirmed by restriction digests and sequencing.

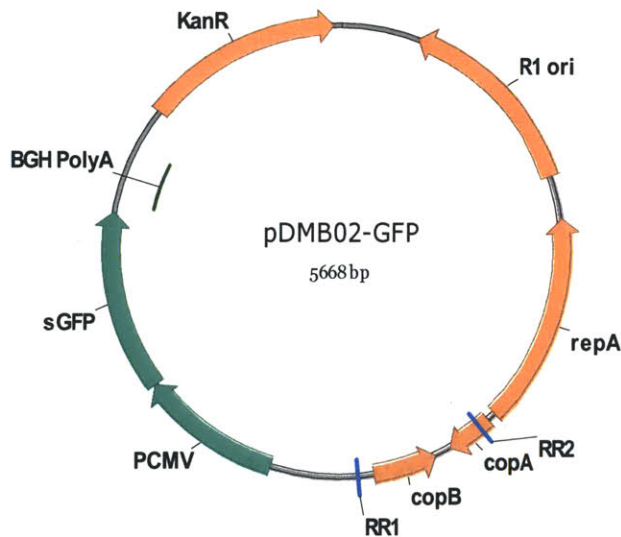


**Figure 3-1.** Feature map of pDMB02-GFP. DNA vaccine vector features: kanamycin resistance marker (KanR), human cytomegalovirus immediate-early promoter/enhancer (PCMV), superfolding GFP gene (sGFP), bovine growth hormone polyadenylation signal (BGH PolyA). R1 replicon features: copy number control genes (*repA*, *copA*, *copB*), origin of replication (R1 ori). The locations of the point mutations that confer the runaway replication phenotype are also indicated (RR1, RR2).

The start codon of *repA* in pDMB02-GFP was mutated from GTG to ATG using site-directed mutagenesis resulting in the plasmid pDMB-ATG. Primers containing the mutation were used to amplify pDMB02-GFP using 20 cycles of PCR with Phusion high-fidelity DNA polymerase (New England Biolabs; Ipswich, MA). The primers were purified using a reverse phase cartridge by the vendor (Sigma-Aldrich; St. Louis, MO) and their sequences are shown below:

5'-GTGAAGATCAGTCATACCATCCTGCACTTACAATGCG-3'

5'-GCAGGATGGTATGACTGATCTTCACCAAACGTATTACCG-3'

After PCR, the template plasmid was digested using DpnI, and after clean-up the reaction was used to transform ElectroMAX DH10B cells (Invitrogen). Positive transformants were selected on LB/agar plates containing 50 µg/mL kanamycin, and the presence of the start codon mutation was verified by sequencing.

### **3.2.2 Preparation of working seed banks**

Frozen working seed banks of DH5α[pDMB02-GFP] and DH5α[pDMB-ATG] were prepared by transforming subcloning-efficiency, chemically-competent DH5α (Invitrogen) with purified plasmid. Positive transformants were selected on LB/agar plates containing 25 µg/mL kanamycin. After overnight incubation at 30°C, a single colony was used to inoculate 3 mL of LB medium containing 25 µg/mL kanamycin. The culture was incubated overnight at 30°C. The next day, 500 µL of overnight culture was used to inoculate 50 mL of LB medium containing 25 µg/mL kanamycin in a 250-mL shake flask. The culture was incubated at 30°C until mid-exponential phase ( $OD_{600}$  approximately equal to 0.5), at which time 900 µL of culture was added to 900 µL of cold 30% (v/v) glycerol in a cryogenic vial and immediately stored at -80°C. Working seed bank vials were discarded after two freeze-thaw cycles.

### 3.2.3 Culture conditions

Difco LB Broth, Miller (BD; Franklin Lakes, NJ) was used for shake flask cultures and contained 10 g/L tryptone, 5 g/L yeast extract, and 10 g/L NaCl. Cell density was monitored using  $OD_{600}$  measurements on a DU800 spectrophotometer (Beckman Coulter; Indianapolis, IN). All cultures were mixed and aerated by agitation at 250 rpm unless otherwise specified.

#### *Temperature shift experiments*

Temperature-induced plasmid amplification was studied using temperature shift experiments as follows: 100 to 110 mL of LB medium containing 25  $\mu\text{g}/\text{mL}$  kanamycin was inoculated to an initial  $OD_{600} = 0.00025$  using a working seed bank. The very low initial  $OD_{600}$  was chosen to avoid glycerol carry-over from the working seed bank vial. The cultures were incubated in 500-mL baffled shake flasks at 30°C until the desired growth phase was achieved (typically  $OD_{600} = 0.5 - 1.0$ ) at which point half of the culture volume was transferred to a 250-mL baffled shake flask and incubated at 42°C. The remaining culture was transferred to a 250-mL shake flask and incubated at 30°C.

#### *Seed growth phase study*

5 mL LB containing 25  $\mu\text{g}/\text{mL}$  kanamycin was inoculated with 20  $\mu\text{L}$  of DH5 $\alpha$ [pDMB02-GFP] working seed bank and incubated at 30°C. Aliquots of the culture were collected in late exponential ( $OD_{600} = 1.1$ ), early stationary ( $OD_{600} = 2.3$ ), and late stationary ( $OD_{600} = 2.8$ ) growth phases and used to inoculate 50 mL LB containing 25  $\mu\text{g}/\text{mL}$  kanamycin to an initial  $OD_{600} = 0.01$ . The resulting cultures were incubated at 30°C for at least 24 hours. Samples were taken periodically to measure cell growth and plasmid production.

### 3.2.4 Measurement of plasmid copy number

Plasmid copy number was measured using a quantitative PCR (qPCR) assay adapted from the relative quantitation method described by Lee et al. (2006a). Total DNA (genomic and plasmid) was

isolated from 100  $\mu$ L of culture using the DNeasy Blood & Tissue kit (Qiagen; Valencia, CA). qPCR was performed using a 7300 Real-Time PCR system (Applied Biosystems; Carlsbad, CA) with primers targeting the plasmid-based kanamycin resistance gene (forward primer: 5'-TCGACCACCAAGCGAAACA-3', reverse primer: 5'-CGACAAGACCGGCTTCCAT-3') and *dxs*, a single-copy gene on the *E. coli* chromosome encoding 1-deoxyxylulose-5-phosphate synthase (forward primer: 5'-CGAGAACTGGCGATCCTTA-3', reverse primer: 5'-CTTCATCAAGCGGTTTCACA-3'). Each 25- $\mu$ L qPCR reaction contained 1X Brilliant II SYBR Green High ROX Master Mix reagent (Agilent Technologies; Santa Clara, CA), 200 nM each of the forward and reverse primers, and the total DNA sample diluted 5-fold (if necessary) in order to be within the linear range of the assay. The thermal profile consisted of a 10-minute hold at 95°C followed by 40 cycles of 95°C for 30 s and 60°C for one minute. Plasmid copy number was calculated using the  $\Delta\Delta C_T$  method (Livak and Schmittgen, 2001) which included normalization to a calibrator plasmid, pVAX1-dxs, containing single copies of both the kanamycin resistance gene and *dxs*.

### 3.2.5 Measurement of plasmid DNA specific yield

Plasmid DNA was quantified from crude lysates prepared from  $OD_{600} = 10$  cell pellets using the method described by Listner et al. (2006a). The lysis method was modified slightly: cell pellets were harvested by centrifugation at 5000 x *g* for 15 minutes, the 37°C incubation took place with 250 rpm shaking, and 5  $\mu$ L of 10 mg/mL RNase A solution was used per mL of lysate. The pDNA content of the lysates was measured using a Gen-Pak FAX anion-exchange column (Waters Corporation; Milford, MA) on an Agilent 1100 Series HPLC system (Agilent Technologies). Three buffers were used: Buffer A (25 mM Tris-HCl, 1 mM EDTA, pH 8.0), Buffer B (25 mM Tris-HCl, 1 mM EDTA, 1 M NaCl, pH 8.0), and Buffer C (0.04 M H<sub>3</sub>PO<sub>4</sub>). The LC method was run at a constant flow rate of 0.75 mL/min and consisted of the following steps: (1) linear ramp from 70%:30% A:B to 34%:66% A:B over 10 min., (2) 100% B for 5 min., (3) 100% C for 4.5 min., and (4) 70%:30% A:B for 10 min. Plasmid DNA eluted at a retention time of

approximately 11.5 min as detected by absorbance at 260 nm. A standard curve of pVAX1-GFP (2 µg/mL to 50 µg/mL) was prepared using pDNA purified using the Hi-Speed QIAfilter Plasmid Maxi Kit (Qiagen) and quantified using a NanoPhotometer (Implen; Westlake Village, CA). The standard curve was used to calculate the µg of pDNA per mL of lysate prepared from each pellet. Specific yield was calculated using the correlation that 1 OD<sub>600</sub> unit = 0.4 g DCW/L culture.

### 3.2.6 Quantitative real-time PCR

RNA was purified from OD<sub>600</sub> = 1 pellets using the Illustra RNAspin Mini RNA Isolation Kit (GE Healthcare; Piscataway, NJ). 1 g/L lysozyme was used for cell lysis in the first step of the protocol. Due to the high plasmid DNA content of the strains used in this work, an additional DNase digestion was required after the RNA purification step to remove contaminating DNA. 43 µL purified RNA was digested with 2 µL DNase I (New England Biolabs) in 5 µL of the supplied reaction buffer for 10 min. at 37°C. RNA was purified from the other reaction components using the RNA Cleanup protocol from the RNeasy Mini Kit (Qiagen). The RNA content of each sample was measured using a NanoPhotometer (Implen), and 800 ng of RNA was converted to cDNA using the QuantiTect Reverse Transcription Kit (Qiagen). Control reactions containing water instead of the reverse transcriptase enzyme were included for each sample.

Quantitative PCR was performed on a 7300 Real-Time PCR System (Applied Biosystems). The desired reference sample was diluted 2- to 1000-fold to prepare a standard curve. *repA* mRNA was detected using gene-specific primers (forward primer: 5'-CAGAGCTTAAGTCCCGTGAAT-3', reverse primer: 5'-TGACGTTCTCTGTTCGCATCA-3') designed by Primer Express 3.0 software (Applied Biosystems). Each 25-µL reaction contained 1X Brilliant II SYBR Green QPCR High ROX Master Mix, 200 nM each of the forward and reverse primers, and the experimental sample diluted 100-fold. The thermal cycling conditions were a 95°C hold for 10 min., followed by 40 cycles of 95°C for 30 sec. and



60°C for 1 min. Dissociation-curve analysis was also performed to check for the presence of primer dimers or non-specific products. Results were analyzed using the Applied Biosystems Sequence Detection Software (v. 1.3.1).

### **3.2.7 Immuno-detection of RepA protein**

#### *Removal of cross-reactive antibodies from RepA antiserum*

Polyclonal RepA antiserum was a generous gift from Prof. Rafael Giraldo (Centro de Investigaciones Biológicas, Madrid, Spain) and was prepared from rabbits as described by Giraldo-Suárez et al. (1993). To reduce background binding, the RepA antiserum was incubated with plasmid-free DH5 $\alpha$  lysate to precipitate non-specific *E. coli*-reactive antibodies. A lysate of plasmid-free DH5 $\alpha$  was prepared from 50 mL of mid-exponential phase culture grown in LB medium by freeze-thaw and sonication in buffer containing 10 mM Tris-HCl at pH 7.5, 140 mM NaCl, 1% Triton X-100, 1% BSA, 1% sodium deoxycholate, and 1 Complete Mini Protease Inhibitor Cocktail tablet (Roche; Indianapolis, IN) per 10 mL. The DH5 $\alpha$  lysate was added to an aliquot of RepA antiserum in a 1:1 ratio and incubated at room temperature for 5.5 hr with gentle rocking. After incubation, the antisera was centrifuged for 20 min. at 20000 x *g* and 4°C. The supernatant was recovered and stored in single-use aliquots at -80°C.

#### *Cell lysis*

Cell lysates were prepared by resuspending pellets from 4-5 mL of culture in 1 mL 10 mM Tris-HCl at pH 8.0. The 1-mL suspension was added to approximately 500  $\mu$ L of 0.1 mm glass beads (Scientific Industries; Bohemia, NY) in a 1.7-mL microcentrifuge tube. The suspension and glass beads were vortexed at maximum speed for 5 min. followed by centrifugation for 20 min. at 14000 x *g* and 4°C. The supernatant was recovered and stored at -30°C.

### *SDS-PAGE*

Total protein content of the lysates was measured using the modified Bradford assay described by Zor and Selinger (1996). A 7.5- $\mu$ L aliquot of each lysate containing 2  $\mu$ g total protein (balance water) was prepared. An equal volume of Laemmli buffer containing 5% (v/v)  $\beta$ -mercaptoethanol was added to each aliquot, and the samples were incubated at 100°C for 5 min. Samples were loaded on a 10% Mini-PROTEAN TGX Gel with 15 x 15- $\mu$ L wells (Bio-Rad; Hercules, CA) and run at 200 V for 30 min in tris/glycine/SDS buffer.

### *Western blots*

Protein separated by SDS-PAGE was transferred to a nitrocellulose membrane (Pall Corporation; Pensacola, FL) for 1 hr at 100 V using a Mini Trans-Blot Electrophoretic Transfer Cell (Bio-Rad) with transfer buffer containing 25 mM Tris, 192 mM glycine, and 20% (v/v) methanol at pH 8.3. After transfer, the membrane was blocked with a 5% (w/v) bovine serum albumin solution prepared in TBS (2.42 g/L Tris, 29.24 g/L NaCl, pH 7.5) at room temperature for 2 hr. After two 10-min. washes with TBST solution (TBS + 0.05% v/v Tween-20), the membrane was incubated with a 1:1000 dilution of RepA antiserum in TBS containing 10% glycerol for 2 hr at room temperature. The membrane was washed three times with TBST for 10 min. each, and was then incubated with a 1:5000 dilution of goat anti-rabbit IgG-HRP secondary antibody (Santa Cruz Biotechnology; Santa Cruz, CA) in TBS for 1 hr. After two 10-minute washes with TBST and one 10-minute wash with TBS, secondary antibody binding was visualized using Western Blotting Luminol Reagent (Santa Cruz Biotechnology) following the manufacturer's instructions.

### **3.2.8 Cloning and expression of *repA***

To verify that the band being detected on the Western blots was indeed RepA, a positive control vector was constructed by cloning the *repA* gene into the BamHI/HindIII sites of pETDuet-1 (EMD

Millipore; Billerica, MA), in-frame with an N-terminal 6X His tag. The resulting plasmid, pETDuet-repA, was used to express RepA-His in *E. coli* BL21 Star (DE3) (Invitrogen). 50-mL LB cultures of BL21 Star (DE3) containing either pETDuet-repA or pETDuet-1 and 100 µg/mL ampicillin were grown at 30°C with 250 rpm shaking and induced with 0.5 mM IPTG at an OD<sub>600</sub> of approximately 0.5. Six hours after induction, 20-mL aliquots of culture were harvested by centrifugation. Lysates were prepared from the pellets using disruption with 0.1 mm glass beads (Scientific Industries) in buffer containing 7 M urea, 0.1 M NaH<sub>2</sub>PO<sub>4</sub>, and 0.01 M Tris-HCl at pH 8.0.

### 3.2.9 Plasmid quality assessment

Plasmid DNA purified from OD<sub>600</sub> = 2 pellets using the Zyppy Plasmid Miniprep Kit (Zymo Research Corporation; Irvine, CA) was run on a 0.7% agarose gel at 90 V for 60 min. to separate the supercoiled, nicked (open-circle), and linear isoforms. The separated DNA was visualized by staining the gel with 0.5 µg/mL ethidium bromide.

## 3.3 Results & Discussion

### 3.3.1 Characterization of plasmid yield

We constructed a new DNA vaccine vector, pDMB02-GFP, containing the runaway R1 replicon as described in Section 3.2.1. The vector also carries the kanamycin resistance gene as well as the sequences necessary for expression of therapeutic genes in a eukaryotic host. For this work, we have included GFP as a placeholder for the therapeutic gene sequence. The specific yield of the new vector was compared to that of both the parent vector (pCP40) and a pUC-based DNA vaccine vector (pVAX1-GFP) after a mid-exponential phase temperature shift from 30°C to 42°C in LB medium (Figure 3-2). The pUC-based vector behaved as expected – the specific yield remained low (less than 1 mg/g DCW) at 30°C, and increased to about 4 mg/g DCW after temperature induction. Both of the R1-based plasmids

produced higher specific yields than the pUC-based plasmid. Interestingly, while temperature-induced amplification was observed for the R1 vectors at early time points (2 and 4 hours after the temperature shift), at later time points the yield at 30°C was higher than or the same as that at 42°C. Note also that the parent vector, pCP40, contains the phage lambda major leftward promoter ( $p_L$ ) upstream of the origin (Appendix B, Figure B-1). Despite using a host (DH5 $\alpha$ ) that does not contain the  $p_L$  repressor protein, we did not observe the plasmid instability alluded to by Remaut et al. (1983). The completely de-repressed phage promoter may not affect pCP40 stability because there is no recombinant protein sequence immediately downstream of  $p_L$ .

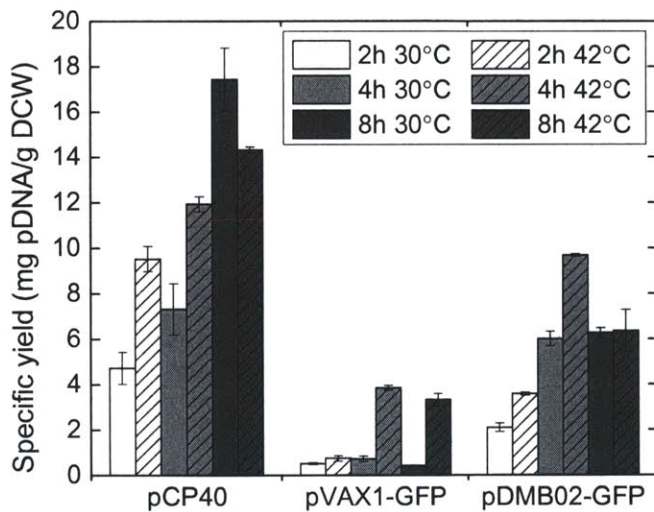


**Figure 3-2.** Specific yield of pCP40 (parent plasmid), pVAX1-GFP (pUC-based DNA vaccine vector), and pDMB02-GFP (R1-based DNA vaccine vector) with and without a temperature shift from 30°C to 42°C. Times in the legend are hours after the temperature shift.

To further investigate the production capabilities of pDMB02-GFP, the specific yield after a temperature shift later in exponential phase ( $OD_{600} = 1$ ) was compared to the yields obtained after a mid-exponential phase shift (Figure 3-3). Typically, the temperature-shifted cultures reached a lower final optical density than the cultures that remained at 30°C, likely due to heat stress (Figure 3-3A, 3-3B). A period of increased growth rate was observed between 0 and 2 hours post shift – possibly due to the

culture transiently being at optimal growth temperature for *E. coli* (37°C) – followed by growth arrest. The timing of the temperature shift did not significantly impact the yield of the 42°C cultures, but resulted in higher yields at 30°C, likely due to the increased elapsed culture time. Also, the maximum yield achieved in the experiments (Figure 3-3) was on par with the maximum yield produced by pCP40 (Figure 3-2), confirming that pDMB02-GFP did not lose any production capacity during the construction process.

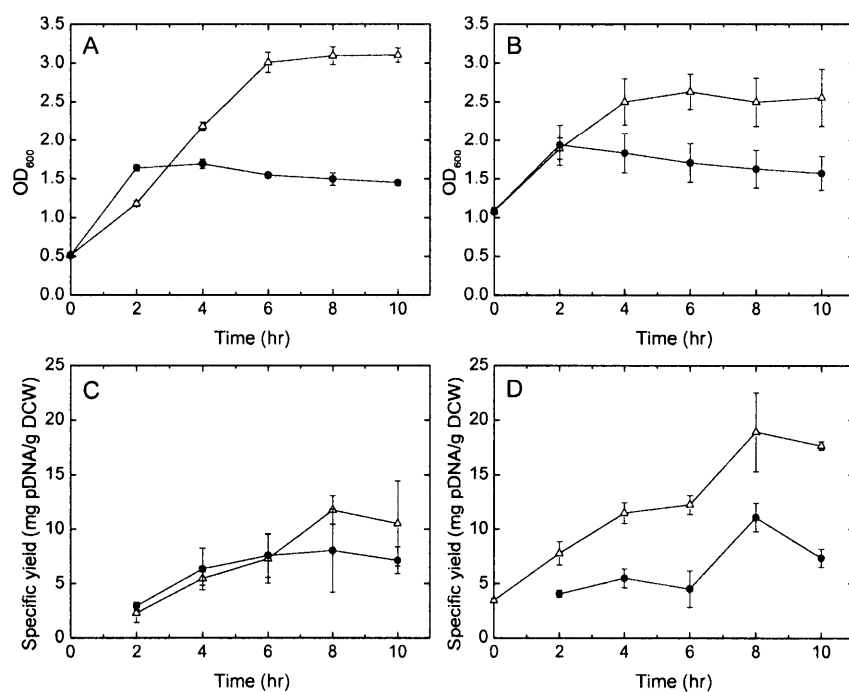


**Figure 3-3.** (A) Growth of DH5α[pDMB02-GFP] with a temperature shift at OD<sub>600</sub> = 0.5 and (B) OD<sub>600</sub> = 1.0. (C) Specific yield of pDMB02-GFP with a temperature shift at OD<sub>600</sub> = 0.5 and (D) OD<sub>600</sub> = 1.0. Data are shown for cultures shifted to 42°C (●) and cultures that remained at 30°C (△). 0 hr on the x-axis is the time of the temperature shift.

There are several possible explanations for the experiment-to-experiment variability observed in the maximum yield of pDMB02-GFP. The use of a rich medium (LB) may be partially responsible, as the exact medium composition can vary from run-to-run. However, the mechanism of R1 replication is not designed for tight control of plasmid copy number. Instead, the goal is to prevent the copy number

from dropping below one per cell – a concern that is more relevant for the low-copy, wild-type R1 plasmid (Nordström, 2006). This may result in increased clone-to-clone variability when the plasmid copy number is significantly higher than one, as observed in the runaway mutants.

### **3.3.2 Impact of seed growth phase on yield**

In all of the experiments described above, shake flask cultures were inoculated directly from working seed banks. However, it has been reported previously that the growth phase of the seed can significantly impact the productivity of resulting cultures when using runaway replication plasmids for recombinant protein production (Morino et al., 1988). To test the sensitivity of DH5 $\alpha$ [pDMB02-GFP] to seed age, we inoculated flasks using seeds in late exponential, early stationary, and late stationary phase and measured the specific plasmid yield after 24 hours at 30°C. The data show that the plasmid production capacity of DH5 $\alpha$ [pDMB02-GFP] cultures inoculated using late-stationary seeds was greatly reduced compared to cultures inoculated using seeds earlier in their respective growth phases (Figure 3-4). In addition, the reduction in culture productivity corresponded to an increase in the plasmid content of the seed culture, suggesting that high plasmid content in the seed negatively impacted the productivity of resulting cultures. These results are consistent with the findings of a previous report (Morino et al., 1988). Remaut et al. (1983) also alluded to the fact that runaway R1 plasmids can be unstable after prolonged growth, even at low temperatures. Direct inoculation from the working seed bank gave yields comparable to those obtained from late exponential/early stationary seeds, so we continued to use this as our standard protocol for maximum run-to-run consistency.

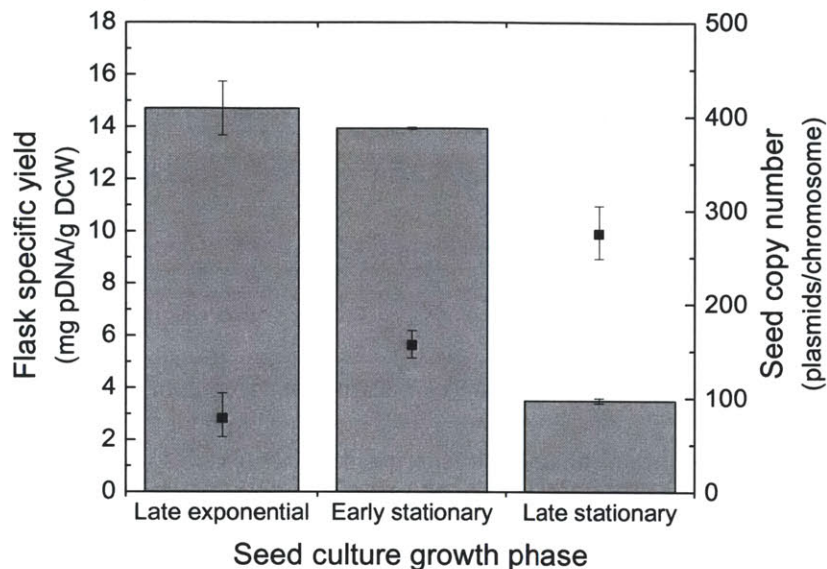


**Figure 3-4.** Specific yield of pDMB02-GFP as a function of inoculum growth phase after 24 hours of culture at 30°C in shake flasks (gray bars). The plasmid copy number of the seed cultures at each growth phase are also shown (■). Specific yield error bars represent one standard deviation calculated from duplicate flasks, and copy number error bars represent the 95% confidence interval calculated from three replicate wells of the same sample.

### 3.3.3 Quantification of *repA* gene expression

We were surprised to observe that pCP40 and pDMB02-GFP did not show the dramatic temperature-induced amplification reported in the early literature characterizing the runaway R1 replicon (Remaut et al., 1983; Uhlin et al., 1979). In particular, we expected greater copy number control before the temperature shift; however, we are not the first group to observe that runaway replication is not completely suppressed at 30°C (Mizutani et al., 1986; Morino et al., 1988). To further investigate the temperature-dependent behavior of pDMB02-GFP we pursued additional studies at the RNA and protein levels.

In the R1 replicon, the *repA* gene codes for a protein required for initiation of replication at the origin and is transcribed from both the  $P_{repA}$  and  $P_{copB}$  promoters (Figure 3-5). *copA* is an antisense RNA that binds to and inhibits translation of *repA* mRNA, and CopB is a tetrameric repressor of  $P_{repA}$ . The two point mutations that lead to the runaway replication phenotype reduce the efficiency of  $P_{copA}$  and cause



a temperature-dependent increase in transcription from  $P_{copB}$  (Givskov et al., 1987). The replication initiation protein, RepA, is likely the limiting factor in plasmid replication, owing to the fact that multiple copies of the protein are required for initiation of replication (Nordström, 2006). In the results that follow, we chose to focus our analysis exclusively on *repA*. Our experiments were all in the high-copy-number regime (compared to wild-type plasmid R1), and under these conditions, CopB is likely present in sufficiently high amounts to completely repress  $P_{repA}$  such that all *repA* mRNA is transcribed from  $P_{copB}$  (Light et al., 1985). Also, the antisense RNA control element, *copA*, is small and unstable (Nördstrom and Uhlin, 1992) and as such we were unable to obtain reliable measurements of its expression.

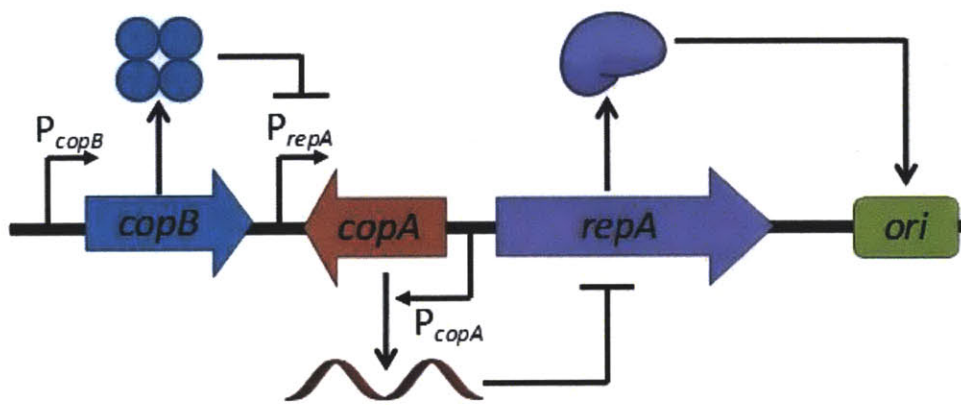


Figure 3-5. Schematic of the R1 replicon.

The expression of *repA* was calculated relative to one of two replicate flasks at the time of the temperature shift ( $t = 0$  hr). As an internal standard, the same amount of total RNA was used for all reverse transcriptase reactions in lieu of a housekeeping gene, since it is unlikely that transcription of a chromosomal target would remain unchanged under all temperature and growth conditions tested. Relative expression measurements of *repA* in cultures of pDMB02-GFP with and without a temperature shift showed that *repA* transcription increased by an order of magnitude after the temperature shift (Table 3-1). However, the pDNA specific yield did not increase in a similar manner, consistent with the observations made in previous experiments. The *repA* expression data suggest that the runaway R1



replicon is functioning as expected, in that there is clear temperature-induced expression of *repA* mRNA. However, as the plasmid copy number increases, the total amount of *repA* mRNA in the culture is also expected to increase. To account for this, we normalized *repA* expression to plasmid copy number to obtain an estimate of the relative *repA* expression level per plasmid (Table 3-1) and found that temperature-induced expression of *repA* was still evident.

**Table 3-1.** Specific yield, plasmid copy number, and *repA* expression from pDMB02-GFP with and without a temperature shift. Error bars represent the standard deviation of duplicate samples.

| Temperature | Time (hr) <sup>a</sup> | Specific Yield (mg pDNA/g DCW) | Plasmid copies/chromosome | <i>repA</i> expression <sup>c</sup> | <i>repA</i> expression/plasmid <sup>d</sup> |
|-------------|------------------------|--------------------------------|---------------------------|-------------------------------------|---|
| 30°C        | 0                      | ND <sup>b</sup>                | 42 ± 2                    | 1.07 ± 0.10                         | 1.07 ± 0.16                                 |
|             | 2                      | 1.5 ± 0.1                      | 90 ± 9                    | 0.69 ± 0.02                         | 0.32 ± 0.05                                 |
|             | 4                      | 4.4 ± 0.2                      | 144 ± 3                   | 0.77 ± 0.25                         | 0.22 ± 0.08                                 |
|             | 8                      | 7.0 ± 0.3                      | 212 ± 72                  | 1.40 ± 1.74                         | 0.27 ± 0.36                                 |
| 42°C        | 2                      | 2.2 ± 0.0                      | 153 ± 3                   | 12.50 ± 2.55                        | 3.40 ± 0.78                                 |
|             | 4                      | 4.2 ± 0.1                      | 105 ± 39                  | 28.15 ± 1.48                        | 11.21 ± 4.33                                |
|             | 8                      | 5.1 ± 0.6                      | 177 ± 29                  | 24.60 ± 0.14                        | 5.78 ± 1.12                                 |

<sup>a</sup>Time after temperature shift

<sup>b</sup>Not detected (below detection limit of HPLC assay)

<sup>c</sup>Normalized to *repA* expression at t = 0 in flask replicate 1

<sup>d</sup>*repA* expression multiplied by a factor of (t = 0 plasmid copy number)/(plasmid copy number of sample) to give an estimate of normalized *repA* expression per plasmid

### 3.3.4 Role of RepA protein expression levels

The *repA* mRNA expression data pointed to the possibility of a post-transcriptional limitation on plasmid yield at 42°C. One possible option for relieving this limitation is to increase expression of RepA. To this end, we changed the RepA start codon in pDMB02-GFP from GTG to ATG, resulting in the plasmid pDMB-ATG. There is evidence in the literature that genes with a GTG start codon are typically translated several-fold less efficiently than genes with an ATG start codon (Kozak, 2005). We chose a start codon mutation instead of a promoter replacement to minimize disruption of the other elements of the replicon. Also, since RepA is primarily *cis* acting (Masai and Arai, 1988), supplying RepA exogenously

from either the chromosome or an additional plasmid was not a viable strategy for increasing RepA availability.

In a mid-exponential phase temperature shift experiment, pDMB-ATG showed distinctly different plasmid yield profiles compared to pDMB02-GFP (Table 3-2). The specific yield at 30°C was lower than that typically observed for pDMB02-GFP, and there was an approximately five-fold increase in specific yield after temperature induction. *repA* RNA expression also showed temperature-induced amplification (Table 3-2); the fold difference between the 30°C and 42°C cultures containing pDMB-ATG was approximately the same order of magnitude as that observed for pDMB02-GFP (Table 3-1). However, when *repA* expression was normalized to plasmid copy number, temperature-induced transcription of *repA* was still evident but to a lesser degree; the mechanism responsible for this observation is unclear.

**Table 3-2.** Specific yield, plasmid copy number, and *repA* gene expression in cultures of DH5α[pDMB-ATG] with and without a temperature shift. Error bars represent the standard deviation of duplicate samples.

| Temperature | Time (hr) <sup>a</sup> | Specific yield (mg pDNA/g DCW) | Plasmid copies/chromosome | <i>repA</i> expression <sup>c</sup> | <i>repA</i> expression/plasmid <sup>d</sup> |
|-------------|------------------------|--------------------------------|---------------------------|-------------------------------------|---|
| 30°C        | 0                      | ND <sup>b</sup>                | 13 ± 3                    | 0.09 ± 0.01                         | 0.30 ± 0.09                                 |
|             | 2                      | 0.2 ± 0.1                      | 20 ± 4                    | 0.06 ± 0.00                         | 0.13 ± 0.03                                 |
|             | 4                      | 1.0 ± 0.0                      | 54 ± 1                    | 0.20 ± 0.02                         | 0.15 ± 0.02                                 |
|             | 8                      | 2.3 ± 0.3                      | 96 ± 27                   | 0.32 ± 0.02                         | 0.14 ± 0.04                                 |
| 42°C        | 2                      | 1.9 ± 0.1                      | 243 ± 32                  | 1.00 ± 0.08                         | 0.17 ± 0.03                                 |
|             | 4                      | 5.1 ± 1.9                      | 407 ± 210                 | 15.20 ± 1.13                        | 1.56 ± 0.83                                 |
|             | 8                      | 11.4 ± 1.7                     | 476 ± 176                 | 9.85 ± 0.64                         | 0.86 ± 0.34                                 |

<sup>a</sup>Time after temperature shift

<sup>b</sup>Not detected (below detection limit of HPLC assay)

<sup>c</sup>Normalized to *repA* expression from pDMB02-GFP at t = 0 in flask replicate 1 (Table 3-1)

<sup>d</sup>*repA* expression multiplied by a factor of (t = 0 pDMB02-GFP copy number)/(plasmid copy number of sample) to give an estimate of relative *repA* expression per plasmid

To qualitatively evaluate the expression of RepA protein in cultures of DH5α[pDMB02-GFP] and DH5α[pDMB-ATG] we used a Western blot to detect RepA using polyclonal antiserum obtained from

rabbits. For pDMB02-GFP, a band corresponding to RepA (33 kDa) was visible on the blot after 2 hr at 42°C and after 8 hr at 30°C, with the intensity of the RepA band being higher in the 30°C lysate (Figure 3-6: Lanes 6 and 7). This suggests that temperature-induced expression of RepA from pDMB02-GFP was occurring two hours post-shift, but by 8 hours, protein was either no longer being translated or was degraded, possibly by heat-shock-induced proteases (Gross, 1996). A higher molecular weight band is visible in all lanes, but since this band is also present in the negative control lanes (Figure 3-6: Lanes 1 and 3), it is likely due to cross-reaction with either the primary or secondary antibody rather than expression of RepA. As with specific plasmid yield, the trends in RepA expression were also different for pDMB-ATG. A RepA band is visible in the lanes corresponding to the 42°C samples at both 2 and 8 hours post-shift, and in the lane containing the 30°C sample at 8 hours post-shift (Figure 3-6: Lanes 11-13). The band for the 8 hr, 42°C sample is the most intense. It is clear that the kinetics of RepA expression are different for pDMB-ATG, and that RepA expression persists longer after the temperature shift when compared to expression from pDMB02-GFP.

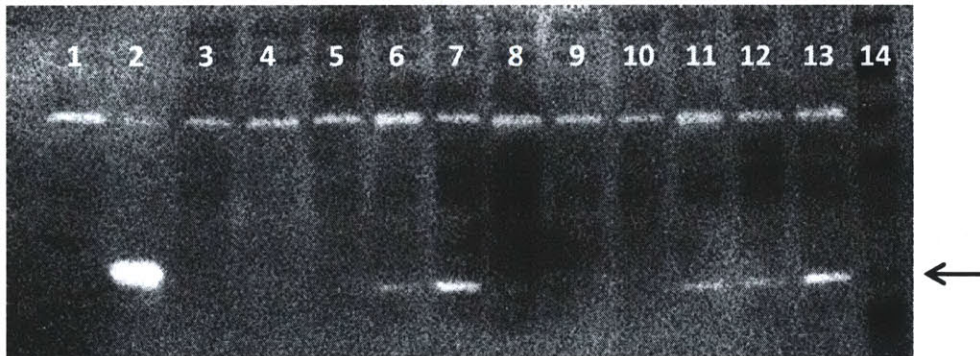


**Figure 3-6.** Western blot for RepA. The RepA band is indicated by the arrow to the right of the image. Except for the lane containing the protein marker, all lanes contained crude lysates from the cultures indicated. **Lane 1:** BL21 Star (DE3) [pETDuet-1], **Lane 2:** BL21 Star (DE3) [pETDuet-repA], **Lane 3:** DH5α (no plasmid), **Lane 4:** DH5α[pDMB02-GFP] t=0 hr, **Lane 5:** DH5α[pDMB02-GFP] t=2 hr 30°C, **Lane 6:** DH5α[pDMB02-GFP] t=2 hr 42°C, **Lane 7:** DH5α[pDMB02-GFP] t=8 hr 30°C, **Lane 8:** DH5α[pDMB02-GFP] t=8 hr 42°C, **Lane 9:** DH5α[pDMB-ATG] t=0 hr, **Lane 10:** DH5α[pDMB-ATG] t=2 hr 30°C, **Lane 11:** DH5α[pDMB-ATG] t=2 hr 42°C, **Lane 12:** DH5α[pDMB-ATG] t=8 hr 30°C, **Lane 13:** DH5α[pDMB-ATG] t=8 hr 42°C, **Lane 14:** Protein marker. Times indicate hours after the temperature shift. All lanes contained 2 μg total protein except for Lane 2, which contained 0.4 μg total protein. Results are shown for a single set of flasks, but the same trends in RepA expression were observed for the second replicate samples as well.

Taken with the RNA expression data, the protein expression data for pDMB02-GFP suggest RepA protein levels may be limiting replication at 42°C. While we cannot deconvolute whether more RepA expression is leading to higher copy number or vice versa, it is clear that RepA protein is depleted after 8 hours at 42°C for the wild-type plasmid, and that the start codon mutation increases RepA protein levels at this time point. Despite this limitation, we have shown that high yields of pDMB02-GFP can be produced during constant-temperature growth at 30°C without a temperature shift. This is particularly advantageous for production-scale runs, as it reduces the complexity of the process and allows the culture to achieve a higher final cell density. In addition, the mutant plasmid pDMB-ATG seems to perform better at 42°C, making it the more attractive vector if a process with a temperature shift is desired.

### **3.3.5 Plasmid quality**

For biopharmaceutical applications, it is important to assess the quality of the plasmid DNA produced in addition to the yield. While there is some debate over the differences in immunogenicity of the various plasmid isoforms (supercoiled, nicked, and linear), the FDA currently recommends that plasmid DNA biopharmaceuticals contain predominantly the supercoiled isoform (Klinman et al., 2010). Gel electrophoresis analysis of samples of pDMB02-GFP and pDMB-ATG collected from cultures with and without a temperature shift show a high percentage of supercoiled DNA (Figure 3-7). Also, the trends in plasmid quantity are consistent with the specific yield measured for these samples (Table 3-1 and Table 3-2).

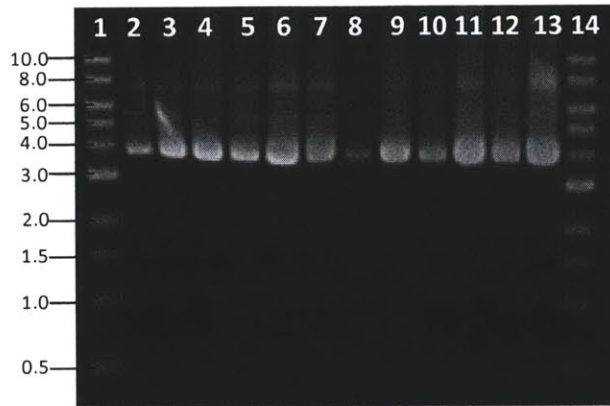


**Figure 3-7.** Agarose gel electrophoresis of pDMB02-GFP and pDMB-ATG produced in DH5 $\alpha$  with and without a mid-exponential phase temperature shift from 30°C to 42°C. **Lane 1:** DNA ladder with DNA size in kilobases (kb) indicated to the left of the image, **Lane 2:** pDMB02-GFP t=2 hr 30°C, **Lane 3:** pDMB02-GFP t=2 hr 42°C, **Lane 4:** pDMB02-GFP t=4 hr 30°C, **Lane 5:** pDMB02-GFP t=4 hr 42°C, **Lane 6:** pDMB02-GFP t=8 hr 30°C, **Lane 7:** pDMB02-GFP t=8 hr 42°C, **Lane 8:** pDMB-ATG t=2 hr 30°C, **Lane 9:** pDMB-ATG t=2 hr 42°C, **Lane 10:** pDMB-ATG t=4 hr 30°C, **Lane 11:** pDMB-ATG t=4 hr 42°C, **Lane 12:** pDMB-ATG t=8 hr 30°C, **Lane 13:** pDMB-ATG t=8 hr 42°C, **Lane 14:** DNA ladder. Times indicate hours after the temperature shift.

These data show that neither the elevated temperature nor the start codon mutation had a negative impact on plasmid quality. Thus, pDMB02-GFP and pDMB-ATG are capable of producing not only high yields of plasmid DNA, but high quality product as well.

### 3.4 Conclusions

In this work, we have described construction of a new DNA vaccine vector, pDMB02-GFP, containing the runaway R1 origin of replication. Our new vector produced high yields of high quality plasmid DNA during constant-temperature culture at 30°C. The runaway R1 replicon has been reported to result in a temperature-dependent loss of copy number control, with higher copy numbers at higher temperatures. However, while we observed some temperature-induced amplification of pDMB02-GFP shortly after a temperature shift, at longer times, the yield at 30°C was often higher than that at 42°C. Using RNA and protein expression measurements, we demonstrated that RepA protein availability may be limiting pDMB02-GFP yield at 42°C. To increase RepA protein levels, we constructed a second vector, pDMB-ATG, in which the start codon of *repA* was changed from the sub-optimal GTG to ATG. RepA was

detected in cultures of DH5 $\alpha$ [pDMB-ATG] up to 8 hours after a temperature shift and was accompanied by enhanced temperature-dependent plasmid amplification.

Overall, we have developed a new set of high-yielding DNA vaccine vectors that are well suited to processes run at low temperatures (pDMB02-GFP) as well as processes that include a temperature shift (pDMB-ATG). Future work to systematically vary the expression of RepA and to determine the resulting effects on specific yield will guide additional efforts to maximize plasmid production. Furthermore, the mechanistic insight into the factors limiting R1 replication gained in this work can serve as the basis of scale-up studies to investigate R1-based DNA vaccine vectors under industrially-relevant conditions.

# Chapter 4

---

## Scale up of R1-based vector production

### Abstract

The recent renewed interest in plasmid-based biopharmaceuticals has led to an increased demand for high-yield, economic processes for plasmid DNA (pDNA) production. At the bioreactor scale, plasmid DNA is typically produced in *E. coli* using a fed-batch fermentation strategy. Successful scale up requires leveraging both an understanding of plasmid and host physiology as well as systematic investigation of process parameters. In this work, we have scaled up production of a DNA vaccine vector containing the runaway R1 replicon, pDMB02-GFP, from 50-mL shake flasks to 2-L bioreactors in *E. coli* DH5 $\alpha$ . Based on results in shake flasks, we chose to cultivate DH5 $\alpha$ [pDMB02-GFP] at a constant temperature of 30°C. We modified an existing culture medium with respect to carbon source, hydrolysate source, and concentration of MgSO<sub>4</sub>·7H<sub>2</sub>O. Using this medium at the 2-L-scale, we found that high growth rates were correlated to low plasmid specific yields. To remedy this, we implemented a growth rate control strategy by reducing dissolved oxygen levels and were able to produce 5.1 mg/g DCW of pDMB02-GFP. Overall, this work has led to an understanding of some of the key aspects of successful scale up of R1-based vector production.

## 4.1 Introduction

As discussed in previous chapters, there has recently been increased interest in plasmid-based DNA vaccines and gene therapies. With this interest comes increased demand for high-yield, economical processes for the production of high-quality plasmid DNA (pDNA). In an industrial setting, the vector and host are typically defined before scale-up studies begin; however, there are still many scale-up decisions that can significantly impact process productivity.

Plasmid DNA is often produced in a fed-batch process to allow for controlled accumulation of high cell densities. Depending on the replicon, a temperature shift may be used to induce plasmid amplification after sufficient biomass is produced. In fed-batch processes, substrate is typically added at a constant rate or using an exponential algorithm that allows control of growth rate at a constant value; the latter strategy often results in higher productivity (Carnes et al., 2006). Fed-batch fermentations have also been shown to result in an increase in the content of supercoiled plasmid over batch fermentations, possibly due to lower growth rate and reduced exposure to stationary-phase growth conditions (O'Kennedy et al., 2003). While many of the high-yielding plasmid production processes in the literature use fed-batch fermentations (Carnes et al., 2006; Danquah and Forde, 2008; Listner et al., 2006b; Williams et al., 2009b), there has been some investigation of high cell density batch processes for plasmid production (Soto et al., 2011).

Process scale can also impact strain physiology and gene expression; facts that are particularly evident in reports comparing genetic engineering strategies across scales. For instance, Ow et al. (2009) observed that knocking out the global regulator *fruR* in *E. coli* DH5 $\alpha$  only resulted in improved plasmid specific yield in an exponential fed-batch culture, not a batch cultivation. Also, Williams et al. (2009b) saw that the impact on plasmid yield of overexpressing DNA replication enzymes or primosomal components varied significantly between batch test-tube scale and fed-batch fermenter scale cultures; in some cases, a mutation was detrimental at one scale and favorable at another.



An additional aspect of plasmid production that is often considered during scale-up studies is medium design. O’Kennedy et al. (2000) found that using a semi-defined versus a rich medium in shake flasks reduced genomic DNA contamination of alkaline lysates, and that modulating the C:N ratio could induce 10-fold changes in plasmid specific yield. Other shake flask studies systematically investigated different carbon and nitrogen sources and quantified their effects on volumetric and specific yields (Xu et al., 2005; Zheng et al., 2007). A medium has been designed specifically for plasmid DNA production using a stoichiometric model (Wang et al., 2001). A modified version of this medium with an optimized C:N ratio that also excluded expensive nucleosides and amino acids has been used for high-yield production of pUC-based DNA vaccine vectors in fed-batch, pilot-scale cultures (Danquah and Forde, 2008).

While all of the studies discussed above used ColE1-based plasmids they still may be able to inform design of a bioreactor-scale process for R1-based vector production. There are many reports in the literature of process development for R1 vectors (Ansoerge and Kula, 2000; Hoffmann et al., 1987; Kidwell et al., 1996; Morino et al., 1988), but the goal of these reports was to maximize recombinant protein production, and the process parameters required to maximize plasmid production may be significantly different.

In this chapter, we demonstrate scale up of production of DH5 $\alpha$ [pDMB02-GFP] from 50-mL shake flask cultures to 2-L bioreactors in a semi-defined medium at 30°C. We report our modifications to the medium described by Listner et al. (2006a) with respect to carbon source, hydrolysate source, and MgSO<sub>4</sub>·7H<sub>2</sub>O concentration. Despite initial low yields in fed-batch and batch cultures, we were ultimately able to produce 5.1 mg/g DCW of pDMB02-GFP using a growth rate control strategy during batch fermentation.

## 4.2 Materials and Methods

### 4.2.1 Plasmid and strain

This study used *E. coli* DH5 $\alpha$  [F  $\phi$ 80*lacZ* $\Delta$ M15  $\Delta$ (*lacZYA-argF*)U169 *deoR recA1 endA1 hsdR17*(r<sub>k</sub><sup>-</sup>, m<sub>k</sub><sup>+</sup>) *phoA supE44 thi-1 gyrA96 relA1*  $\lambda$ ] as a host for the plasmid pDMB02-GFP (5668 bp). The construction and features of pDMB02-GFP are described in detail in Section 3.2.1.

### 4.2.2 Preparation of working seed banks

Frozen working seed banks of DH5 $\alpha$ [pDMB02-GFP] were prepared by transforming subcloning-efficiency, chemically-competent DH5 $\alpha$  (Invitrogen; Carlsbad, CA) with purified plasmid. Positive transformants were selected on LB/agar plates containing 25  $\mu$ g/mL kanamycin. After overnight incubation at 30°C, a single colony was used to inoculate 3 mL of LB medium containing 25  $\mu$ g/mL kanamycin. The culture was incubated overnight at 30°C. The next day, 500  $\mu$ L of overnight culture was used to inoculate 50 mL of LB medium containing 25  $\mu$ g/mL kanamycin in a 250-mL shake flask. The culture was incubated at 30°C until mid-exponential phase (OD<sub>600</sub> approximately equal to 0.5), at which time 900  $\mu$ L of culture was added to 900  $\mu$ L of cold 30% (v/v) glycerol in a cryogenic vial and immediately stored at -80°C. Working seed bank vials were discarded after two freeze-thaw cycles.

### 4.2.3 Culture medium

A semi-defined culture medium was adapted from Listner et al. (2006a). The basal medium contained 3 g/L (NH<sub>4</sub>)<sub>2</sub>SO<sub>4</sub>, 3.5 g/L K<sub>2</sub>HPO<sub>4</sub>, 3.5 g/L KH<sub>2</sub>PO<sub>4</sub>, 10 g/L yeast extract, and 10 g/L Bacto peptone (BD; Franklin Lakes, NJ). Difco Select Soytone (BD) was used in place of Bacto peptone for some cultures as part of the medium development experiment described in the text. 8.3 mL/L seed supplement solution, 1 mL/L trace elements solution, and 25  $\mu$ g/mL kanamycin were added as supplements to the basal medium. Unless otherwise noted, 5 g/L glycerol was added to the medium as

well. The seed supplement solution typically contained 60 g/L  $\text{MgSO}_4 \cdot 7\text{H}_2\text{O}$  and 24 g/L thiamine hydrochloride, except in experiments that systematically varied the concentration of  $\text{MgSO}_4 \cdot 7\text{H}_2\text{O}$  as described in the text. The trace elements solution contained 16.2 g/L  $\text{FeCl}_3$ , 2 g/L  $\text{ZnCl}_2$ , 2 g/L  $\text{CoCl}_2 \cdot 6\text{H}_2\text{O}$ , 2 g/L  $\text{Na}_2\text{MoO}_4 \cdot 2\text{H}_2\text{O}$ , 1 g/L  $\text{CaCl}_2 \cdot 2\text{H}_2\text{O}$ , 1.27 g/L  $\text{CuCl}_2 \cdot 2\text{H}_2\text{O}$ , and 0.5 g/L  $\text{H}_3\text{BO}_3$  dissolved in 1.2 N hydrochloric acid. The pH of the basal medium was adjusted to 7.1 using NaOH.

#### 4.2.4 Shake flask cultures

For medium development purposes, shake flask cultures were prepared using various combinations of hydrolysate source and  $\text{MgSO}_4 \cdot 7\text{H}_2\text{O}$  concentration (Table 4-1). All other components of the semi-defined medium were as described in Section 4.2.3. Cultures were mixed and aerated by agitation at 250 rpm unless stated otherwise.

**Table 4-1.** Combinations of hydrolysate source and  $\text{MgSO}_4 \cdot 7\text{H}_2\text{O}$  concentration tested during development of semi-defined medium.

| Hydrolysate | [ $\text{MgSO}_4 \cdot 7\text{H}_2\text{O}$ ] |
|-------------|---|
| Bacto       | 2 g/L   |
| Bacto       | 1 g/L   |
| Bacto       | 0.5 g/L                                       |
| Soy         | 2 g/L   |
| Soy         | 1 g/L   |
| Soy         | 0.5 g/L                                       |

3-mL seed cultures containing each medium composition (Table 4-1) were inoculated with 0.4% DH5 $\alpha$ [pDMB02-GFP] working seed bank. A culture prepared in LB medium was also included, and all seed cultures contained 25  $\mu\text{g}/\text{mL}$  kanamycin. Seed cultures were incubated overnight at 30°C. The next day, 50-mL shake flask cultures containing each of the medium compositions were inoculated in duplicate to an initial  $\text{OD}_{600} = 0.03$  with seed cultures that were in late-exponential or early-stationary growth phase. Cultures were incubated at 30°C for a total of 24 hours. After 10 hours of incubation, a

bolus of glycerol was added to each culture (with the exception of the LB cultures) to a final concentration of 5 g/L.

In a separate experiment, shake flask cultures were run using the final medium composition (Section 4.2.3). For these cultures, the seed was prepared by inoculating 5 mL of semi-defined medium (including 5 g/L glycerol) with 0.4% DH5 $\alpha$ [pDMB02-GFP] working seed bank and incubating the culture overnight at 30°C. All other cultures conditions were the same as those described above, except no additional glycerol was added to the cultures.

#### **4.2.5 Fed-batch bioreactor cultures**

Fed-batch bioreactor cultures were performed using a Labfors 3 bioreactor (Infors; Bottmingen, Switzerland) with a 5.0 L maximum working volume. The bioreactor was equipped with a D140 OxyProbe dissolved oxygen sensor (Broadley-James; Irvine, CA) and an F-695 FermProbe pH electrode (Broadley-James). To prepare the bioreactor inoculum, 3 mL of semi-defined medium was inoculated with 0.4% seed bank and grown overnight at 30°C. The next day, two cultures, each containing 100 mL of semi-defined medium, were inoculated with 1 mL of overnight culture in a 500-mL baffled shake flask and incubated overnight at 30°C. 3.5 L of basal cultivation medium were autoclaved in the reactor.

On the day of inoculation, medium supplements (including 5 g/L glycerol) and 0.2 mL Antifoam 204 (Sigma-Aldrich; St. Louis, MO) were added, and the reactor was inoculated to an initial OD<sub>600</sub> of 0.05 using the overnight seed cultures. The reactor was run in batch mode at 30°C until all of the batched glycerol was consumed, as evidenced by a sudden increase in dissolved oxygen. At this time, feeding of a solution containing 321.4 g/L glycerol and 79.3 g/L yeast extract began at a flow rate of 0.54 mL/min. The entire run time was 30 hours.

Dissolved oxygen was controlled at 35% using a cascade to agitation (400 rpm to 850 rpm), and air was provided at a flow rate of 0.7-0.9 vvm. pH was controlled at 7.10  $\pm$  0.05 using 4 M NaOH and

2.25 M H<sub>3</sub>PO<sub>4</sub>. Antifoam was manually added in 0.2-mL increments as needed. Online data was logged using IRIS fermenter log and control software (Infors). Samples were taken periodically to measure OD<sub>600</sub> offline using a DU800 Spectrophotometer (Beckman Coulter; Indianapolis, IN). Samples for glycerol, acetate, and plasmid DNA concentration measurements were stored at -30°C until analysis.

#### **4.2.6 Batch bioreactor cultures**

Batch bioreactor cultures were performed using a Labfors 3 bioreactor (Infors) with a 2.3 L maximum working volume. The bioreactor was equipped with a D140 OxyProbe dissolved oxygen sensor (Broadley-James) and an F-695 FermProbe pH electrode (Broadley-James). To prepare the bioreactor inoculum, 3 mL of semi-defined medium was inoculated with 0.4% seed bank and grown overnight at 30°C. The next day, 100 mL of semi-defined medium was inoculated with 1 mL of overnight culture in a 500-mL baffled shake flask and incubated overnight at 30°C. 2.0 L of basal cultivation medium were autoclaved in the reactor.

On the day of inoculation, medium supplements (including 5 g/L glycerol) and 0.2 mL Antifoam 204 (Sigma-Aldrich) were added, and the reactor was inoculated to an initial OD<sub>600</sub> of 0.03 using overnight seed culture. The reactor was run in batch mode at 30°C. Dissolved oxygen was controlled at various setpoints, as described in the text, using a cascade to agitation (250 rpm to 850 rpm), and air was provided at a flow rate of 1 vvm. pH was controlled at 7.10 ± 0.05 using 4 M NaOH and 2.25 M H<sub>3</sub>PO<sub>4</sub>. Data logging, OD<sub>600</sub> measurements, and sample storage were performed as described in Section 4.2.5.

#### **4.2.7 Measurement of glycerol and acetate concentrations**

Glycerol and acetate concentrations in culture supernatants were determined using an Agilent 1200 Series HPLC (Agilent Technologies; Santa Clara, CA) equipped with an Aminex HPX-87H column

(Bio-Rad; Hercules, CA). A 5 mM sulfuric acid mobile phase was run at 0.6 mL/min for 25 minutes at 50°C. Glycerol and acetate peaks were detected by refractive index at approximate retention times of 13.4 and 15.2 minutes, respectively.

#### **4.2.8 Measurement of plasmid DNA specific yield**

Plasmid DNA was quantified from crude lysates prepared from  $OD_{600} = 10$  cell pellets using the method described by Listner et al. (2006a). The lysis method was modified slightly: cell pellets were harvested by centrifugation at  $5000 \times g$  for 15 minutes, the 37°C incubation took place with 250 rpm shaking, and 5  $\mu$ L of 10 mg/mL RNase A solution was used per mL of lysate. The pDNA content of the lysates was measured using a Gen-Pak FAX anion-exchange column (Waters Corporation; Milford, MA) on an Agilent 1100 Series HPLC system (Agilent Technologies). Three buffers were used: Buffer A (25 mM Tris-HCl, 1 mM EDTA, pH 8.0), Buffer B (25 mM Tris-HCl, 1 mM EDTA, 1 M NaCl, pH 8.0), and Buffer C (0.04 M  $H_3PO_4$ ). The LC method was run at a constant flow rate of 0.75 mL/min and consisted of the following steps: (1) linear ramp from 70%:30% A:B to 34%:66% A:B over 10 min., (2) 100% B for 5 min., (3) 100% C for 4.5 min., and (4) 70%:30% A:B for 10 min. Plasmid DNA eluted at a retention time of approximately 11.5 min as detected by absorbance at 260 nm. A standard curve of pVAX1-GFP (2  $\mu$ g/mL to 50  $\mu$ g/mL) was prepared using pDNA purified using the Hi-Speed QIAfilter Plasmid Maxi Kit (Qiagen; Valencia, CA) and quantified using a NanoPhotometer (Implen; Westlake Village, CA). The standard curve was used to calculate the  $\mu$ g of pDNA per mL of lysate prepared from each pellet. Specific yield was calculated using the correlation that 1  $OD_{600}$  unit = 0.4 g DCW/L culture.

## 4.3 Results and Discussion

### 4.3.1 Process medium design

To scale up production of the R1-based DNA vaccine vectors from the shake flask to bioreactor scale, we began by choosing a culture medium better suited to a high-density fed-batch process than LB. After reviewing the literature, we chose to work with the semi-defined medium described by Listner et al. (2006a) While a comprehensive medium optimization study was beyond the scope of this project, several alterations were made to the published medium formulation to improve its performance in our applications. Glycerol was used instead of glucose as the primary carbon source, as glycerol is often the substrate of choice for plasmid DNA production due to a recent increase in availability as well as the potential for reduced acetate secretion. To make our work as industrially-relevant as possible, we aimed to replace the Bacto peptone used in our laboratory with a non-animal-derived soy hydrolysate, specifically, Difco Select Soytone (BD). Another aspect of medium development that we pursued was varying the concentration of  $\text{MgSO}_4 \cdot 7\text{H}_2\text{O}$  to prevent formation of a precipitate that was often observed. This precipitate did not appear to impact cell growth, but was troublesome in micro-scale bioreactor experiments (Chapter 2) as precipitate particles often blocked the optical sensors and interfered with measurements. After calculating the amount of magnesium and sulfur required to achieve the cell densities typically obtained in the bioreactors, we determined that the magnesium concentration could be reduced at least four-fold without depriving the cells of required elements.

To test the re-designed medium, shake flask cultures of DH5 $\alpha$ [pDMB02-GFP] were run in both the Bacto- and soy-based media along with LB.  $\text{MgSO}_4 \cdot 7\text{H}_2\text{O}$  was included at concentrations of 2 g/L – the concentration cited in Listner et al. (2006a), 1 g/L, and 0.5 g/L. The semi-defined medium was supplemented with 5 g/L glycerol, while the LB contained no additional carbon source. We did not observe any significant differences in the growth curves between the Bacto- and soy-based media (Figure 4-1A). However, the cultures containing Select Soytone attained a slightly higher cell density by

the 9.5-hr time point. The final cell densities of cultures in both semi-defined media were comparable, and significantly higher than the cultures grown in LB due to the presence of glycerol as an additional carbon source (Figure 4-1B). Reducing the concentration of  $\text{MgSO}_4 \cdot 7\text{H}_2\text{O}$  to 0.5 g/L did not significantly impact growth rate or final cell density.

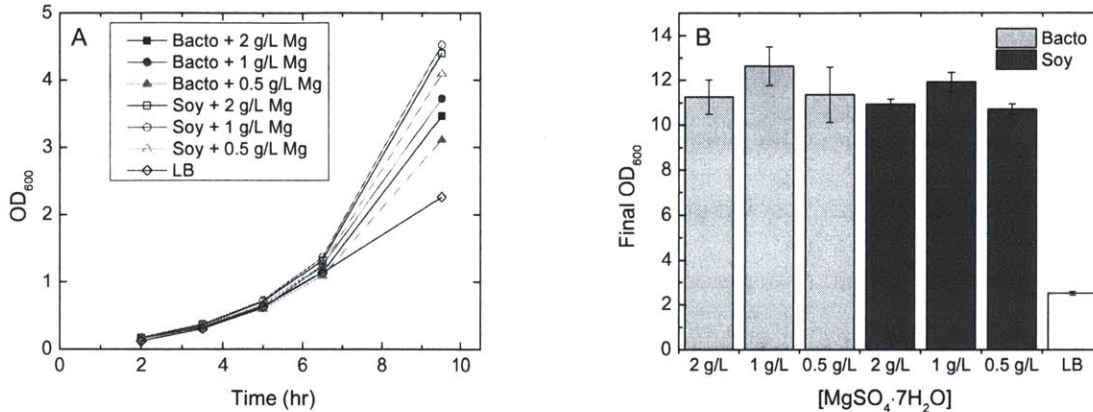


**Figure 4-1.** (A) Growth curves and (B) final OD<sub>600</sub> (cell density after 24 hours of incubation at 30°C) for cultures of DH5α[pDMB02-GFP] in semi-defined medium containing either Bacto or soy peptone along with varying concentrations of  $\text{MgSO}_4 \cdot 7\text{H}_2\text{O}$  in shake flasks. Growth of cultures in LB medium with no glycerol is also shown. OD<sub>600</sub> values are reported as the average of two replicates. For (A), the standard deviations are not shown because all were less than 0.13 OD<sub>600</sub> units. The error bars in (B) represent one standard deviation.

The maximum plasmid yield was about the same for both peptones, but the kinetics of plasmid accumulation differed somewhat (Figure 4-2). This was especially evident at 6.5 hours when there was no detectable plasmid in the soy peptone cultures, while the Bacto peptone cultures contained about 2 mg pDNA/g DCW. Reducing the concentration of  $\text{MgSO}_4 \cdot 7\text{H}_2\text{O}$  to 0.5 g/L did not impact plasmid yield and prevented precipitate formation. Interestingly, the plasmid yields in semi-defined media were similar to those in LB, suggesting that the presence of a carbon source in addition to those found in the rich medium components didn't increase plasmid yields. However, the glycerol-supplemented cultures reached much higher final cell densities than the LB culture (Figure 4-1B), resulting in higher volumetric plasmid productivity.



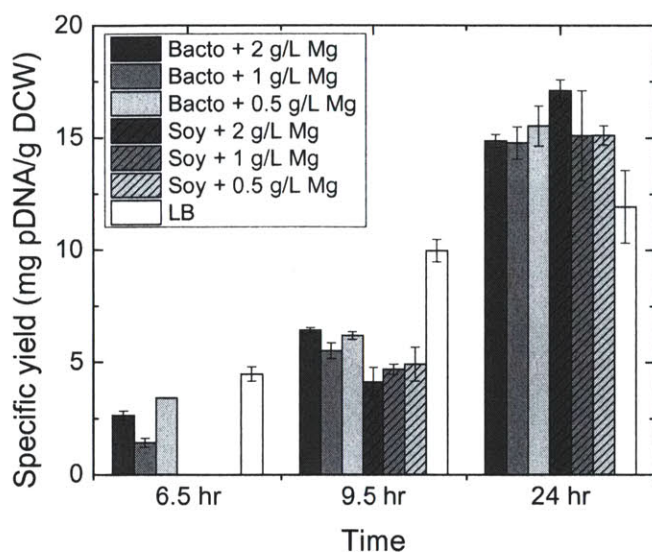


**Figure 4-2.** Specific yield of pDMB02-GFP in semi-defined medium containing either Bacto or soy peptone along with varying concentrations of  $MgSO_4 \cdot 7H_2O$  in shake flask scale culture. LB medium with no glycerol was also included. Cultures were grown at 30°C for 24 hours; the flasks containing semi-defined medium were supplemented with 5 g/L glycerol at the start of the experiment and 10 hours after inoculation. Error bars represent one standard deviation calculated from two replicate cultures.

While the maximum plasmid yield was about the same for both peptones, there were some differences in the glycerol utilization and acetate production profiles of the Bacto and soy peptones (Table 4-2). Despite nearly identical growth curves, cultures containing soy peptone consumed glycerol more slowly and produced more acetate than those containing Bacto peptone. These differences may be due to the fact that soy peptones have a significantly higher concentration of carbohydrates than Bacto peptones (336.2 mg/g vs. 6.29 mg/g; (BD Biosciences, 2006)); these carbohydrates have not been further characterized by the manufacturer beyond their total concentration.

**Table 4-2.** Glycerol and acetate concentrations measured in the supernatants of cultures containing either Bacto or soy peptones and various concentrations of  $\text{MgSO}_4 \cdot 7\text{H}_2\text{O}$

| Peptone | [ $\text{MgSO}_4 \cdot 7\text{H}_2\text{O}$ ]<br>(g/L) | Glycerol (g/L) |       | Acetate (g/L) |       |
|---------|--|----------------|-------|---------------|-------|
|         |  | 9.5 hr         | 24 hr | 9.5 hr        | 24 hr |
| Bacto   | 2  | 3.5            | 0     | 0.2           | 0     |
|         | 1  | 3.4            | 0     | 0.2           | 0     |
|         | 0.5  | 3.7            | 0     | 0.2           | 0     |
| Soy     | 2  | 4.0            | 0.3   | 0.7           | 0.6   |
|         | 1  | 3.7            | 1.1   | 0.8           | 0.2   |
|         | 0.5  | 3.7            | 2.3   | 0.8           | 0.3   |

After evaluating the results shown above, we decided to proceed with the medium containing Bacto peptone to avoid the potential for increased acetate production and to ensure that the higher carbohydrate content of the soy-based medium would not interfere with glycerol feeding strategies pursued at the bench scale.

#### 4.3.2 Scale up challenges

Based on the high yields of pDMB02-GFP observed during constant-temperature culture at 30°C in shake flasks, we chose to pursue a constant-temperature process at the bench scale as well. However, challenges were encountered during scale-up. In particular, we observed that DH5 $\alpha$ [pDMB02-GFP] grew at a faster rate and produced significantly less plasmid DNA at the bench scale. In a fed-batch fermentation at 30°C with an initial specific feed rate of approximately 3 g glycerol/L/hr there was a 1.7-fold increase in growth rate accompanied by a 20-fold decrease in specific pDNA yield compared to batch shake flask cultures (Table 4-3). Feeding at 3 g glycerol/L/hr resulted in high oxygen demand, and as such, the DO setpoint of 35% could not be maintained after the start of feeding.

**Table 4-3.** Summary of maximum values of specific growth rate ( $\mu_{\max}$ ), doubling time ( $t_D$ ),  $OD_{600}$ , specific yield, and volumetric yield observed under various culture conditions at shake flask and bioreactor scales.

|                            | $\mu_{\max}$<br>( $\text{hr}^{-1}$ ) | $t_D$<br>(hr) | Max<br>$OD_{600}$ | Max sp. yield<br>(mg/g DCW) | Max vol. yield<br>(mg/L) |
|----------------------------|--------------------------------------|---------------|-------------------|-----------------------------|--------------------------|
| <b>Shake flask (batch)</b> | 0.33                                 | 2.1           | 8.8               | 14.2                        | 50.3                     |
| <b>Fed-batch</b>           | 0.56                                 | 1.2           | 57.7              | 0.7                         | 13.0                     |
| <b>Batch (35% DO)</b>      | 0.49                                 | 1.4           | 13.5              | 0.8                         | 3.6                      |
| <b>Batch (10% DO)</b>      | 0.56                                 | 1.2           | 15.3              | 0.3                         | 0.7                      |

Since the conditions encountered in shake flasks clearly facilitated plasmid production, we ran several batch fermentations to attempt to replicate these conditions. 2-L batch cultures were run with dissolved oxygen setpoints of 35% and 10%. The lower setpoint was investigated in order to better replicate the conditions in shake flasks, where oxygen transfer is likely slower than that achieved in the stirred-tank vessels. Neither condition resulted in improved specific yield; increased growth rate compared to shake flask cultures was still observed (Table 4-3).

#### 4.3.3 Batch bioreactor with growth rate control

For the bioreactor experiments described above, we cannot definitively determine whether the faster growth rate caused the lower yield, or vice versa. However, there is evidence in the literature that slower growth rates may favor increased plasmid production, both for pMB1/ColE1 (Lin-Chao and Bremer, 1986; Seo and Bailey, 1985) and R1 plasmids (Engberg and Nordstrom, 1975; Siegel and Ryu, 1985). With this in mind, we pursued a strategy to control the growth rate by limiting dissolved oxygen availability, rather than allowing the cultures to grow unrestricted until glycerol was exhausted, as was the case in the experiments described above. To achieve this, we began a batch fermentation by only aerating the culture via air sparging, then slowly increased the agitation as the cell density increased. The culture grew at maximum growth rate for approximately the first 5 hours of culture, after which we were able to control the specific growth rate near  $0.11 \text{ hr}^{-1}$  (Figure 4-3).

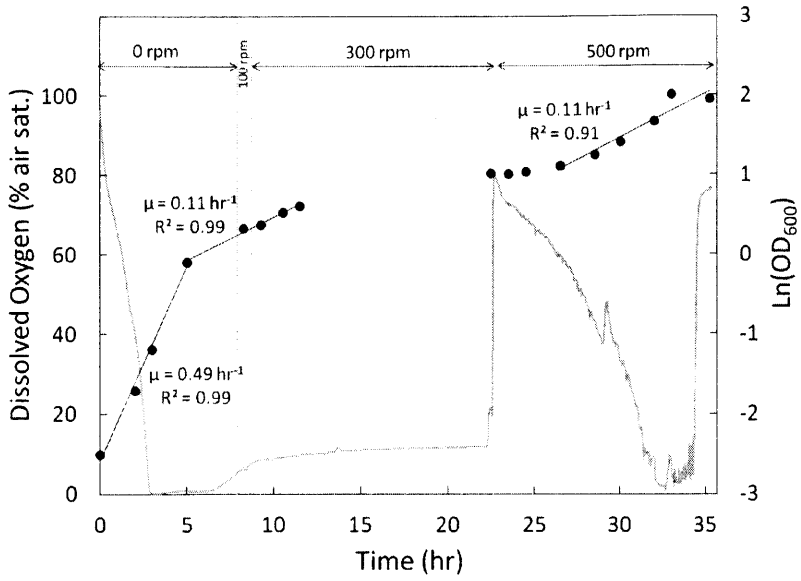


**Figure 4-3.** Dissolved oxygen (gray line) and growth (●) profiles from a batch culture of DH5α[pDMB02-GFP]. The agitation rate was increased gradually throughout the run as indicated at the top of the figure.

This growth rate control strategy resulted in a marked increase in specific and volumetric yields of pDMB02-GFP compared to the values observed in batch cultures with un-restricted growth rate (Figure 4-4). The specific yield peaked after 26.5 hours, reaching a maximum value of 5.1 mg/g DCW, while the volumetric yield peaked later in the culture after the additional biomass accumulation that resulted from the final increase in agitation.

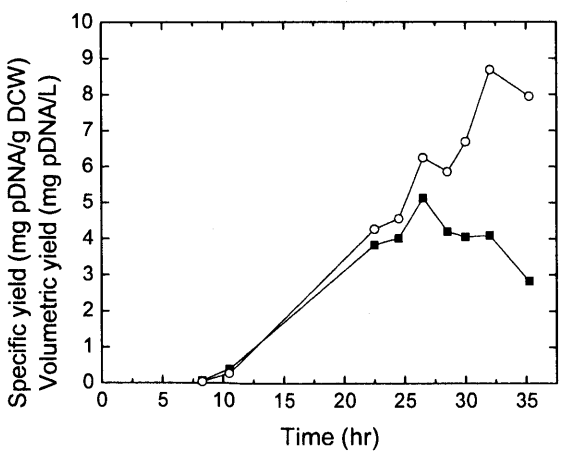


**Figure 4-4.** Specific yield (■) and volumetric yield (○) from a batch culture of DH5α[pDMB02-GFP] with controlled growth rate.

Although the specific yield obtained in the growth-rate-controlled batch run was lower than that observed in shake flasks (Table 4-3) it was on par with yields observed previously for DH5 $\alpha$ [pDMB02-GFP] under suboptimal conditions (Section 3.3.1). Thus, growth rate control is a viable strategy for maintaining the productivity of R1-based DNA vaccine vectors during scale up. As part of future work in this area, growth rate control via exponential, substrate-limited feeding may allow for both increased plasmid yield and higher biomass accumulation. These experiments may also provide insight into whether reduced growth rate or low dissolved oxygen is the true cause of increased specific yield. In addition, we have found that R1-based plasmids are sensitive to the growth phase of seed cultures; specifically that late stationary phase seeds can result in reduced culture productivity (Section 3.3.2). With this in mind, optimization of the seed train used for the bioreactor-scale studies is also a promising strategy for improving plasmid production.

#### **4.4 Conclusions**

In this chapter, we have demonstrated scale up of production of the R1-based DNA vaccine vector, pDMB02-GFP, from the shake flask (50 mL) to bioreactor (2 L) scale. Based on results in shake flasks, we chose to run all cultures at a constant 30°C. All scale up experiments used *E. coli* DH5 $\alpha$  as the host strain, and a semi-defined medium with glycerol as the primary carbon source. Initially, we observed that the growth rate increased by an average of 1.6-fold on scale up. This growth rate increase was accompanied by a 24-fold decrease in specific yield, on average, compared to shake flask cultures. By controlling the growth rate using reduced dissolved oxygen levels we were able to improve the specific yield to 5.1 mg/g DCW. While this is still lower than the specific yields typically observed in shake flasks, it represents an approximately 9-fold improvement over our initial scale up experiments. Future work in this area aims to leverage the knowledge gained during process development of a pUC-based DNA vaccine vector (Chapter 2) and the molecular-level insights gained during characterization of

pDMB02-GFP (Chapter 3) to continue to improve the performance of R1-based DNA vaccine vectors at an industrially-relevant scale.

# Chapter 5

---

## Conclusions & Recommendations

### Abstract

To conclude my thesis, I have summarized the major findings of each chapter. I have also included a discussion of recommendations for future work.

## 5.1 Summary

The growing interest in plasmid-based DNA vaccines and gene therapies brings with it the need for high-yield, rationally-designed pDNA production processes. In this thesis, I sought to meet this need in several ways, as described below.

- In Chapter 2, my collaborators and I developed a 1-mL fed-batch microbioreactor device capable of online monitoring and control of dissolved oxygen, pH, and temperature, as well as continuous monitoring of cell density. We used the micro-device to scale down production of a pUC-based DNA vaccine vector (pVAX1-GFP) and demonstrate the utility of the device as a process design tool. We showed that plasmid copy number as well as glycerol and acetate profiles were comparable across scales as long as key process parameters such as dissolved oxygen were held constant. We also discovered that conditions of high acetate and low dissolved oxygen may favor increased pVAX1-GFP copy number.
- In Chapter 3, I constructed a new DNA vaccine vector containing the runaway R1 replicon. The runaway mutant of the R1 replicon contains mutations that confer the phenotype of increased plasmid copy number at high temperature (42°C). However, my runaway R1-based DNA vaccine vector, pDMB02-GFP, produced the highest specific yields (approximately 19 mg pDNA/g DCW) during constant-temperature culture at 30°C. Analysis of RNA and protein levels of the R1 replication initiation protein, RepA, showed that a temperature shift from 30°C to 42°C induced expression of *repA* mRNA, as expected from the published mechanism of R1 replication. However, RepA protein was not detectable by Western blot after 8 hours at 42°C, suggesting a protein limitation on plasmid yield. I constructed a second DNA vaccine vector, pDMB-ATG, by mutating the RepA start codon from GTG to ATG. The mutant plasmid showed lower plasmid yields at 30°C and higher plasmid yields at 42°C compared to pDMB02-GFP, accompanied by detectable RepA protein after 8 hours at 42°C.
- In Chapter 4, I investigated the scale up of pDMB02-GFP production in *E. coli* DH5α from shake flasks (50 mL) to bioreactors (2 L). First, I developed a semi-defined medium by



evaluating both animal- and plant-derived hydrolysates. I found that hydrolysate source did not significantly impact growth rate or final cell density, but ultimately decided to use animal-derived Bacto peptone because it contained lower concentrations of carbohydrates and resulted in less acetate production. Initial scale up efforts using both fed-batch and batch strategies at 30°C resulted in a 24-fold decrease in specific yield accompanied by a 1.6-fold increase in specific growth rate compared to shake flasks. In a subsequent batch fermentation, I controlled the growth rate at roughly  $0.1 \text{ hr}^{-1}$  by modulating agitation to reduce the dissolved oxygen concentration. This resulted in a maximum pDMB02-GFP specific yield of 5.1 mg/g DCW – a significant improvement over the initial scale up experiments.

## 5.2 Recommendations for future work

Ph.D. thesis research is never truly finished. There are endless ways to refine and extend the research conducted during a thesis project. Here, I outline several proposed directions for future work in developing new tools for the production of plasmid DNA biopharmaceuticals.

In Chapter 2, my colleagues and I demonstrated that 1-mL fed-batch microbioreactors can effectively reproduce a bench-scale, temperature-induced pDNA production process. The microreactors are inexpensive to fabricate and operate and can be disposed after a single use. However, to truly harness the high-throughput power of micro-scale devices the next step in this work must be to multiplex the devices so that many cultures can be run in parallel under varying conditions. This work is being actively pursued by Pharyx, Inc. ([www.pharyx.com](http://www.pharyx.com)), a start-up company from Prof. Rajeev Ram's laboratory at MIT. As the microreactor technology continues to mature, a more refined and robust user interface will increase their usefulness as well.

Another aspect of micro-scale bioprocessing that should be pursued in the future is the development of companion, micro-scale analytics. I developed a qPCR assay to measure plasmid copy number from  $\mu\text{L}$ -scale culture volumes, but this analysis was still limited by the frequency of sampling,

i.e. collection of too many samples could lead to significant changes in the culture volume. Analytics that provide online analysis of metabolites and product concentrations would be an ideal complement to micro-scale technology. In one promising area of work, Zanzotto et al. (2006) investigated the use of luminescent and fluorescent reporters for online monitoring of gene expression, and found that the high surface area to volume ratio of microscale devices makes them well suited to this type of analysis. Finally, there has also been recent work on designing scaled-down versions of downstream purification trains (Titchener-Hooker et al., 2008) which may eventually allow scale down of both the upstream and downstream stages of a bioprocess. Scale down of the complete process can facilitate high-throughput analysis of the impact of process conditions on the final product.

In Chapter 3, I described construction and characterization of new DNA vaccine vectors containing the runaway R1 origin of replication. One potential area of future work is design of a strain specifically suited to production of these vectors. It has been shown in the literature that host strain can significantly impact plasmid yield (Yau et al., 2008), and my own preliminary data have shown that R1 plasmid yield varies with host strain. In addition, current plasmid production processes result in yields that are much lower than the theoretical maximum, and it has been shown that strain engineering may be able to close this gap (Appendix A). To remove confounding strain effects from my analyses of R1 replication, I chose to use *E. coli* DH5 $\alpha$  exclusively in this thesis. DH5 $\alpha$  is commonly used for plasmid production at the bioreactor scale, but recent work in our laboratory suggests that *de novo* construction of strains specifically suited for plasmid production (using wild-type *E. coli* MG1655 as the parent strain) can increase plasmid yields (Gonçalves GAL et al., *in preparation*). The strain engineering work by Gonçalves et al. focused on engineering metabolism to redirect flux toward plasmid DNA intermediates. Future strain engineering work could start with transcriptomic or flux analysis of strains carrying R1 plasmids to identify additional targets for beneficial flux redirection.

Another potential way to improve the R1-based DNA vaccine vectors designed in this thesis would be to reduce their size. The R1 origin of replication and associated regulatory elements are larger than the pUC origin (approximately 2.5 kb versus 0.7 kb, respectively). Smaller vectors are desirable both because vector size may limit maximum titer and because smaller vectors typically give higher transgene expression (Kay et al., 2010). R1 vector size could be reduced by production of minicircles or use of a selection system that does not require a plasmid-based sequence (see discussion in Section 1.1.3). Minicircles are especially promising – a recent report on an improved method for minicircle production and isolation suggests that these small vectors may soon be a viable (and desirable) alternative to pDNA containing bacterial sequences (Kay et al., 2010).

Chapter 4 discussed scale up of R1-based vector production and the associated challenges. Future work in this area can leverage the knowledge gained during the microbioreactor studies. As shown in Chapter 2, microbioreactors can accurately replicate a bench-scale pDNA production process at the 1-mL scale and can also provide additional process insight. This insight, combined with multiplexed microreactors, could provide a very useful platform for analysis of R1-based plasmid production. From the results presented in Chapter 4, it seems that growth rate and possibly dissolved oxygen are key parameters in R1 vector production. Multiple microreactors run in parallel would be a very effective method to evaluate the impact of these process parameters on plasmid copy number.

# References

---

- Akerlund T, Nordström K, Bernander R. 1995. Analysis of cell size and DNA content in exponentially growing and stationary-phase batch cultures of *Escherichia coli*. *J Bacteriol* 177:6791-6797.
- Alexeeva S, Hellingwerf KJ, Teixeira de Mattos MJ. 2002. Quantitative assessment of oxygen availability: Perceived aerobiosis and its effect on flux distribution in the respiratory chain of *Escherichia coli*. *J Bacteriol* 184:1402-1406.
- Ansorge MB, Kula M. 2000. Production of recombinant L-leucine dehydrogenase from *Bacillus cereus* in pilot scale using the runaway replication system *E. coli*[pIET98]. *Biotechnol Bioeng* 68:557-562.
- Bareither R, Pollard D. 2011. A review of advanced small-scale parallel bioreactor technology for accelerated process development: Current state and future need. *Biotechnol Prog* 27:2-14.
- BD Biosciences. 2006. BD Bionutrients Technical Manual: Advanced Bioprocessing. BD Biosciences. 68 p.
- Betts JI, Baganz F. 2006. Miniature bioreactors: Current practices and future opportunities. *Microb Cell Fact* 5:21.
- Bi X, Liu LF. 1996. A replicational model for DNA recombination between direct repeats. *J Mol Biol* 256:849-858.
- Bipatnath M, Dennis PP, Bremer H. 1998. Initiation and velocity of chromosome replication in *Escherichia coli* B/r and K-12. *J Bacteriol* 180:265-273.
- Boyd AC, Popp F, Michaelis U, Davidson H, Davidson-Smith H, Doherty A, McLachlan G, Porteous DJ, Seeber S. 1999. Insertion of natural intron 6a-6b into a human cDNA-derived gene therapy vector for cystic fibrosis improves plasmid stability and permits facile RNA/DNA discrimination. *J Gene Med* 1:312-321.
- Butler VA. 1996. Points to consider on plasmid DNA vaccines for preventive infectious disease indications. Center for Biologics Evaluation and Research, Food and Drug Administration. Docket 96N-0400.
- Carnes AE, Hodgson CP, Williams JA. 2006. Inducible *Escherichia coli* fermentation for increased plasmid DNA production. *Biotechnol Appl Biochem* 45:155-166.
- Cayley S, Lewis BA, Guttman HJ, Record Jr MT. 1991. Characterization of the cytoplasm of *Escherichia coli* K-12 as a function of external osmolarity: Implications for protein-DNA interactions in vivo. *J Mol Biol* 222:281-300.
- Chen JH, Yeh HT. 1997. The seventh copy of IS1 in *Escherichia coli* W3110 belongs to the IS1A (IS1E) type which is the only IS1 type that transposes from chromosome to plasmids. *Proc Natl Sci Council Repub China B* 21:100-105.

- Chen ZY, He CY, Kay MA. 2005. Improved production and purification of minicircle DNA vector free of plasmid bacterial sequences and capable of persistent transgene expression *in vivo*. *Hum Gene Ther* 16:126-131.
- Ciccolini LAS, Shamlou PA, Titchener-Hooker NJ, Ward JM, Dunnill P. 1998. Time course of SDS-alkaline lysis of recombinant bacterial cells for plasmid release. *Biotechnol Bioeng* 60:768-770.
- Cooke GD, Cranenburgh RM, Hanak JAJ, Dunnill P, Thatcher DR, Ward JM. 2001. Purification of essentially RNA free plasmid DNA using a modified *Escherichia coli* host strain expressing ribonuclease A. *J Biotechnol* 85:297-304.
- Cranenburgh RM, Hanak JA, Williams SG, Sherratt DJ. 2001. *Escherichia coli* strains that allow antibiotic-free plasmid selection and maintenance by repressor titration. *Nucleic Acids Res* 29:E26.
- Cranenburgh RM, Lewis KS, Hanak JA. 2004. Effect of plasmid copy number and lac operator sequence on antibiotic-free plasmid selection by operator-repressor titration in *Escherichia coli*. *J Mol Microbiol Biotechnol* 7:197-203.
- Cunningham DS, Koepsel RR, Ataai MM, Domach MM. 2009. Factors affecting plasmid production in *Escherichia coli* from a resource allocation standpoint. *Microb Cell Fact* 8:27.
- Danquah M, Forde G. 2008. Development of a pilot-scale bacterial fermentation for plasmid-based biopharmaceutical production using a stoichiometric medium. *Biotechnol Bioprocess Eng* 13:158-167.
- Darquet AM, Cameron B, Wils P, Scherman D, Crouzet J. 1997. A new DNA vehicle for nonviral gene delivery: Supercoiled minicircle. *Gene Ther* 4:1341-1349.
- Dryselius R, Nekhotiaeva N, Nielsen PE, Good L. 2003. Antibiotic-free bacterial strain selection using antisense peptide nucleic acid. *BioTechniques* 35:1060-1064.
- Durfee T, Nelson R, Baldwin S, Plunkett III G, Burland V, Mau B, Petrosino JF, Qin X, Muzny DM, Ayele M, Gibbs RA, Csorgo B, Posfai G, Weinstock GM, Blattner FR. 2008. The complete genome sequence of *Escherichia coli* DH10B: Insights into the biology of a laboratory workhorse. *J Bacteriol* 190:2597-2606.
- El-Attar LMR, Scott S, Goh S, Good L. 2012. A pestivirus DNA vaccine based on a non-antibiotic resistance *Escherichia coli* essential gene marker. *Vaccine* 30:1702-1709.
- Engberg B, Nordström K. 1975. Replication of R-factor R1 in *Escherichia coli* K-12 at different growth rates. *J Bacteriol* 123:179-186.
- Ferreira GNM, Monteiro GA, Prazeres DMF, Cabral JMS. 2000. Downstream processing of plasmid DNA for gene therapy and DNA vaccine applications. *Trends Biotechnol* 18:380-388.

- Funke M, Buchenauer A, Mokwa W, Kluge S, Hein L, Mueller C, Kensy F, Buechs J. 2010. Bioprocess control in microscale: Scalable fermentations in disposable and user-friendly microfluidic systems. *Microb Cell Fact* 9:86.
- Giraldo-Suárez R, Fernández-Tresguerres E, Díaz-Orejas R, Malki A, Kohiyama M. 1993. The heat-shock DnaK protein is required for plasmid R1 replication and it is dispensable for plasmid ColE1 replication. *Nucleic Acids Res* 21:5495-5499.
- Givskov M, Stougaard P, Light J, Molin S. 1987. Identification and characterization of mutations responsible for a runaway replication phenotype of plasmid R1. *Gene* 57:203-211.
- Goh S, Good L. 2008. Plasmid selection in *Escherichia coli* using an endogenous essential gene marker. *BMC Biotechnol* 8:61.
- Gonçalves GAL, Bower DM, Prazeres DMF, Monteiro GA, Prather KLJ. 2012. Rational engineering of *Escherichia coli* strains for plasmid biopharmaceutical manufacturing. *Biotechnol J* 7:251-261.
- Gross CA. 1996. Function and regulation of the heat shock proteins. In: Neidhardt FC, editor. *Escherichia coli* and *Salmonella*: Cellular and molecular biology. Washington, DC: ASM Press. p 1382-1399.
- Hagg P, de Pohl JW, Abdulkarim F, Isaksson LA. 2004. A host/plasmid system that is not dependent on antibiotics and antibiotic resistance genes for stable plasmid maintenance in *Escherichia coli*. *J Biotechnol* 111:17-30.
- Hanke T, McMichael AJ. 2000. Design and construction of an experimental HIV-1 vaccine for a year-2000 clinical trial in Kenya. *Nat Med* 6:951-955.
- Hodgson CP, Williams JA. 2006. Improved strains of *E. coli* for plasmid DNA production. WO 2006/026125 A2
- Hoffmann I, Widstrom J, Zeppezauer M, Nyman PO. 1987. Overproduction and large-scale preparation of deoxyuridine triphosphate nucleotidohydrolase from *Escherichia coli*. *Eur J Biochem* 164:45-51.
- Horn NA, Meek JA, Budahazi G, Marquet M. 1995. Cancer gene therapy using plasmid DNA: Purification of DNA for human clinical trials. *Hum Gene Ther* 6:565-573.
- Isett K, George H, Herber W, Amanullah A. 2007. Twenty-four-well plate miniature bioreactor high-throughput system: Assessment for microbial cultivations. *Biotechnol Bioeng* 98:1017-1028.
- Islam RS, Tisi D, Levy MS, Lye GJ. 2008. Scale-up of *Escherichia coli* growth and recombinant protein expression conditions from microwell to laboratory and pilot scale based on matched  $k_{1a}$ . *Biotechnol Bioeng* 99:1128-1139.
- Kay MA, He C, Chen Z. 2010. A robust system for production of minicircle DNA vectors. *Nat Biotech* 28:1287-1289.

- Kidwell J, Valentin H, Dennis D. 1995. Regulated expression of the *Alcaligenes eutrophus pha* biosynthesis genes in *Escherichia coli*. *Appl Environ Microbiol* 61:1391-1398.
- Kidwell J, Kolibachuk D, Dennis D. 1996. High-level expression of *lacZ* under control of the *tac* or *trp* promoter using runaway replication vectors in *Escherichia coli*. *Biotechnol Bioeng* 50:108-114.
- Klinman DM, Klaschik S, Tross D, Shiota H, Steinhagen F. 2010. FDA guidance on prophylactic DNA vaccines: Analysis and recommendations. *Vaccine* 28:2801-2805.
- Kozak M. 1987. An analysis of 5'-noncoding sequences from 699 vertebrate messenger RNAs. *Nucleic Acids Res* 15:8125-8148.
- Kozak M. 2005. Regulation of translation via mRNA structure in prokaryotes and eukaryotes. *Gene* 361:13-37.
- Kutzler MA, Weiner DB. 2008. DNA vaccines: ready for prime time? *Nat Rev Genet* 9:776-788.
- Lee C, Kim J, Shin SG, Hwang S. 2006a. Absolute and relative QPCR quantification of plasmid copy number in *Escherichia coli*. *J Biotechnol* 123:273-280.
- Lee HL, Boccazzi P, Ram RJ, Sinskey AJ. 2006b. Microbioreactor arrays with integrated mixers and fluid injectors for high-throughput experimentation with pH and dissolved oxygen control. *Lab Chip* 6:1229-1235.
- Lee HLT, Boccazzi P, Gorret N, Ram RJ, Sinskey AJ. 2004. *In situ* bioprocess monitoring of *Escherichia coli* bioreactions using Raman spectroscopy. *Vib Spectrosc* 35:131-137.
- Lee KS, Boccazzi P, Sinskey AJ, Ram RJ. 2011. Microfluidic chemostat and turbidostat with flow rate, oxygen, and temperature control for dynamic continuous culture. *Lab Chip* 11:1730-1739.
- Legmann R, Schreyer HB, Combs RG, McCormick EL, Russo AP, Rodgers ST. 2009. A predictive high-throughput scale-down model of monoclonal antibody production in CHO cells. *Biotechnol Bioeng* 104:1107-1120.
- Light J, Riise E, Molin S. 1985. Transcription and its regulation in the basic replicon region of plasmid R1. *Mol Gen Genet* 198:503-508.
- Lin-Chao S, Bremer H. 1986. Effect of the bacterial growth rate on replication control of plasmid pBR322 in *Escherichia coli*. *Mol Gen Genet* 203:143-149.
- Lin-Chao S, Chen W, Wong T. 1992. High copy number of the pUC plasmid results from a Rom/Rop-suppressible point mutation in RNA II. *Mol Microbiol* 6:3385-3393.
- Listner K, Bentley LK, Chartrain M. 2006a. A simple method for the production of plasmid DNA in bioreactors. In: Saltzman WM, et al., editors. *DNA Vaccines: Methods and Protocols*. Totowa, NJ: Humana Press. p 295-309.

- Listner K, Bentley L, Okonkowski J, Kistler C, Wnek R, Caparoni A, Junker B, Robinson D, Salmon P, Chartrain M. 2006b. Development of a highly productive and scalable plasmid DNA production platform. *Biotechnol Prog* 22:1335-1345.
- Livak K, Schmittgen T. 2001. Analysis of relative gene expression data using real-time quantitative PCR and the  $2^{-\Delta\Delta CT}$  method. *Methods* 25:402-408.
- Luders S, Fallet C, Franco-Lara E. 2009. Proteome analysis of the *Escherichia coli* heat shock response under steady-state conditions. *Proteome Sci* 7:36.
- Mairhofer J, Grabherr R. 2008. Rational vector design for efficient non-viral gene delivery: Challenges facing the use of plasmid DNA. *Mol Biotechnol* 39:97-104.
- Mairhofer J, Pfaffenzeller I, Merz D, Grabherr R. 2008. A novel antibiotic free plasmid selection system: Advances in safe and efficient DNA therapy. *Biotechnol J* 3:83-89.
- Mairhofer J, Cserjan-Puschmann M, Striedner G, Nöbauer K, Razzazi-Fazeli E, Grabherr R. 2010. Marker-free plasmids for gene therapeutic applications—Lack of antibiotic resistance gene substantially improves the manufacturing process. *J Biotechnol* 146:130-137.
- Masai H, Arai K. 1988. RepA protein- and oriR-dependent initiation of R1 plasmid replication: Identification of a *rho*-dependent transcription terminator required for *cis*-action of *repA* protein. *Nucleic Acids Res* 16:6493-6514.
- Mayrhofer P, Blaesen M, Schleef M, Jechlinger W. 2008. Minicircle-DNA production by site specific recombination and protein-DNA interaction chromatography. *J Gene Med* 10:1253-1269.
- Mizutani S, Iijima S, Kobayashi T. 1986. Fed-batch culture of *Escherichia coli* harboring a runaway-replication plasmid. *J Chem Eng Jpn* 19:111-116.
- Moore JP, Klasse PJ, Dolan MJ, Ahuja SK. 2008. AIDS/HIV. A STEP into darkness or light? *Science* 320:753-755.
- Morino T, Morita M, Seya K, Sukenaga Y, Kato K, Nakamura T. 1988. Construction of a runaway vector and its use for a high-level expression of a cloned human superoxide dismutase gene. *Appl Microbiol Biotechnol* 28:170-175.
- Neidhardt FC, Umbarger HE. 1996. Chemical composition of *Escherichia coli*. In: Neidhardt FC, editor. *Escherichia coli and Salmonella: Cellular and molecular biology*. Washington, DC: ASM Press. p 13-16.
- Nikaido H. 1996. Outer membrane. In: Neidhardt FC, editor. *Escherichia coli and Salmonella: Cellular and molecular biology*. Washington, D.C.: ASM Press. p 29-47.
- Nordström K, Uhlin BE. 1992. Runaway-replication plasmids as tools to produce large quantities of proteins from cloned genes in bacteria. *Nat Biotechnol* 10:661-666.



- Nordström K. 2006. Plasmid R1—Replication and its control. *Plasmid* 55:1-26.
- O’Kennedy RD, Baldwin C, Keshavarz-Moore E. 2000. Effects of growth medium selection on plasmid DNA production and initial processing steps. *J Biotechnol* 76:175-183.
- O’Mahony K, Freitag R, Hilbrig F, Müller P, Schumacher I. 2007. Strategies for high titre plasmid DNA production in *Escherichia coli* DH5 $\alpha$ . *Process Biochem* 42:1039-1049.
- O’Kennedy RD, Ward JM, Keshavarz-Moore E. 2003. Effects of fermentation strategy on the characteristics of plasmid DNA production. *Biotechnol Appl Biochem* 37:83-90.
- Okonkowski J, Kizer-Bentley L, Listner K, Robinson D, Chartrain M. 2005. Development of a robust, versatile, and scalable inoculum train for the production of a DNA vaccine. *Biotechnol Prog* 21:1038-1047.
- Oliveira PH, Lemos F, Monteiro GA, Prazeres DM. 2008. Recombination frequency in plasmid DNA containing direct repeats - predictive correlation with repeat and intervening sequence length. *Plasmid* 60:159-165.
- Oliveira PH, Prazeres DMF, Monteiro GA. 2009. Deletion formation mutations in plasmid expression vectors are unfavored by runaway amplification conditions and differentially selected under kanamycin stress. *J Biotechnol* 143:231-238.
- Oliveira P, Prather K, Prazeres D, Monteiro G. 2010. Analysis of DNA repeats in bacterial plasmids reveals the potential for recurrent instability events. *Appl Microbiol Biotechnol* 87:2157-2167.
- Ongkudon CM, Pickering R, Webster D, Danquah MK. 2011. Cultivation of *E. coli* carrying a plasmid-based Measles vaccine construct (4.2 kbp pcDNA3F) employing medium optimisation and pH-temperature induction techniques. *Microb Cell Fact* 10:16.
- Ow DS, Lee RM, Nissom PM, Philp R, Oh SK, Yap MG. 2007. Inactivating FruR global regulator in plasmid-bearing *Escherichia coli* alters metabolic gene expression and improves growth rate. *J Biotechnol* 131:261-269.
- Ow DS, Nissom PM, Philp R, Oh SK, Yap MG. 2006. Global transcriptional analysis of metabolic burden due to plasmid maintenance in *Escherichia coli* DH5 $\alpha$  during batch fermentation. *Enzyme Microb Technol* 39:391-398.
- Ow DS, Yap MG, Oh SK. 2009. Enhancement of plasmid DNA yields during fed-batch culture of a *fruR*-knockout *Escherichia coli* strain. *Biotechnol Appl Biochem* 52:53-59.
- Panula-Perala J, Siurkus J, Vasala A, Wilmanowski R, Casteleijn MG, Neubauer P. 2008. Enzyme controlled glucose auto-delivery for high cell density cultivations in microplates and shake flasks. *Microb Cell Fact* 7:31.
- Pedelacq JD, Cabantous S, Tran T, Terwilliger TC, Waldo GS. 2006. Engineering and characterization of a superfolder green fluorescent protein. *Nat Biotechnol* 24:79-88.

- Phue JN, Lee SJ, Trinh L, Shiloach J. 2008. Modified *Escherichia coli* B (BL21), a superior producer of plasmid DNA compared with *Escherichia coli* K (DH5alpha). *Biotechnol Bioeng* 101:831-836.
- Phue JN, Noronha SB, Hattacharyya R, Wolfe AJ, Shiloach J. 2005. Glucose metabolism at high density growth of *E. coli* B and *E. coli* K: Differences in metabolic pathways are responsible for efficient glucose utilization in *E. coli* B as determined by microarrays and Northern blot analyses. *Biotechnol Bioeng* 90:805-820.
- Pogliano J. 2002. Dynamic cellular location of bacterial plasmids. *Curr Opin Microbiol* 5:586-590.
- Posfai G, Plunkett III G, Feher T, Frisch D, Keil GM, Umenhoffer K, Kolisnychenko V, Stahl B, Sharma SS, de Arruda M, Burland V, Harcum SW, Blattner FR. 2006. Emergent properties of reduced-genome *Escherichia coli*. *Science* 312:1044-1046.
- Prather KL, Edmonds MC, Herod JW. 2006. Identification and characterization of IS1 transposition in plasmid amplification mutants of *E. coli* clones producing DNA vaccines. *Appl Microbiol Biotechnol* 73:815-826.
- Prazeres DMF, Ferreira GNM. 2004. Design of flowsheets for the recovery and purification of plasmids for gene therapy and DNA vaccination. *Chem Eng Process* 43:609-624.
- Remaut E, Tsao H, Fiers W. 1983. Improved plasmid vectors with a thermoinducible expression and temperature-regulated runaway replication. *Gene* 22:103-113.
- Ribeiro SC, Oliveira PH, Prazeres DM, Monteiro GA. 2008. High frequency plasmid recombination mediated by 28 bp direct repeats. *Mol Biotechnol* 40:252-260.
- Saade F, Petrovsky N. 2012. Technologies for enhanced efficacy of DNA vaccines. *Expert Rev Vaccines* 11:189-209.
- Sardesai NY, Weiner DB. 2011. Electroporation delivery of DNA vaccines: Prospects for success. *Curr Opin Immunol* 23:421-429.
- Schapper D, Alam MNHZ, Szita N, Eliasson Lantz A, Gernaey KV. 2009. Application of microbioreactors in fermentation process development: A review. *Anal Bioanal Chem* 395:679-695.
- Schneider D, Duperchy E, Depeyrot J, Coursange E, Lenski R, Blot M. 2002. Genomic comparisons among *Escherichia coli* strains B, K-12, and O157:H7 using IS elements as molecular markers. *BMC Microbiol* 2:18.
- Seo J, Bailey JE. 1985. Effects of recombinant plasmid content on growth properties and cloned gene product formation in *Escherichia coli*. *Biotechnol Bioeng* 27:1668-1674.
- Siegel R, Ryu DDY. 1985. Kinetic study of instability of recombinant plasmid pPLc23trpAl in *E. coli* using two-stage continuous culture system. *Biotechnol Bioeng* 27:28-33.

- Siurkus J, Panula-Perala J, Horn U, Kraft M, Rimseliene R, Neubauer P. 2010. Novel approach of high cell density recombinant bioprocess development: Optimisation and scale-up from microlitre to pilot scales while maintaining the fed-batch cultivation mode of *E. coli* cultures. *Microb Cell Fact* 9:35.
- Soto R, Caspeta L, Barrón B, Gosset G, Ramírez OT, Lara AR. 2011. High cell-density cultivation in batch mode for plasmid DNA production by a metabolically engineered *E. coli* strain with minimized overflow metabolism. *Biochem Eng J* 56:165-171.
- Soubrier F, Cameron B, Manse B, Somarriba S, Dubertret C, Jaslin G, Jung G, Caer CL, Dang D, Mouvault JM, Scherman D, Mayaux JF, Crouzet J. 1999. pCOR: A new design of plasmid vectors for nonviral gene therapy. *Gene Ther* 6:1482-1488.
- Soubrier F, Laborderie B, Cameron B. 2005. Improvement of pCOR plasmid copy number for pharmaceutical applications. *Appl Microbiol Biotechnol* 66:683-688.
- Summers D. 1998. Timing, self-control and a sense of direction are the secrets of multicopy plasmid stability. *Mol Microbiol* 29:1137-1145.
- Sundararaj S, Guo A, Habibi-Nazhad B, Rouani M, Stothard P, Ellison M, Wishart DS. 2004. The CyberCell Database (CCDB): A comprehensive, self-updating, relational database to coordinate and facilitate *in silico* modeling of *Escherichia coli*. *Nucleic Acids Res* 32:D293-D295.
- Szpirer CY, Milinkovitch MC. 2005. Separate-component-stabilization system for protein and DNA production without the use of antibiotics. *BioTechniques* 38:775-781.
- Titchener-Hooker NJ, Dunnill P, Hoare M. 2008. Micro biochemical engineering to accelerate the design of industrial-scale downstream processes for biopharmaceutical proteins. *Biotechnol Bioeng* 100:473-487.
- Tolmachov O, Palaszewski I, Bigger B, Coutelle C. 2006. RecET driven chromosomal gene targeting to generate a RecA deficient *Escherichia coli* strain for Cre mediated production of minicircle DNA. *BMC Biotechnol* 6:17.
- Twiss E, Coros AM, Tavakoli NP, Derbyshire KM. 2005. Transposition is modulated by a diverse set of host factors in *Escherichia coli* and is stimulated by nutritional stress. *Mol Microbiol* 57:1593-1607.
- Uhlin BE, Molin S, Gustafsson P, Nordström K. 1979. Plasmids with temperature-dependent copy number for amplification of cloned genes and their products. *Gene* 6:91-106.
- Vandermeulen G, Marie C, Scherman D, Preat V. 2011. New generation of plasmid backbones devoid of antibiotic resistance marker for gene therapy trials. *Mol Ther* 19:1942-1949.
- Vester A, Hans M, Hohmann H, Weuster-Botz D. 2009. Discrimination of riboflavin producing *Bacillus subtilis* strains based on their fed-batch process performances on a millilitre scale. *Appl Microbiol Biotechnol* 84:71-76.

- Vidal L, Pinsach J, Striedner G, Caminal G, Ferrer P. 2008. Development of an antibiotic-free plasmid selection system based on glycine auxotrophy for recombinant protein overproduction in *Escherichia coli*. *J Biotechnol* 134:127-136.
- Wang Z, Le G, Shi Y, Węgrzyn G. 2001. Medium design for plasmid DNA production based on stoichiometric model. *Process Biochem* 36:1085-1093.
- Williams JA, Carnes AE, Hodgson CP. 2009a. Plasmid DNA vaccine vector design: Impact on efficacy, safety and upstream production. *Biotechnol Adv* 27:353-370.
- Williams JA, Luke J, Langtry S, Anderson S, Hodgson CP, Carnes AE. 2009b. Generic plasmid DNA production platform incorporating low metabolic burden seed-stock and fed-batch fermentation processes. *Biotechnol Bioeng* 103:1129-1143.
- Wolfe AJ. 2005. The acetate switch. *Microbiol Mol Biol Rev* 69:12-50.
- Xu ZN, Shen WH, Chen H, Cen PL. 2005. Effects of medium composition on the production of plasmid DNA vector potentially for human gene therapy. *J Zhejiang Univ Sci B* 6:396-400.
- Yau SY, Keshavarz-Moore E, Ward J. 2008. Host strain influences on supercoiled plasmid DNA production in *Escherichia coli*: Implications for efficient design of large-scale processes. *Biotechnol Bioeng* 101:529-544.
- Zanzotto A, Boccazzi P, Gorret N, Van Dyk TK, Sinskey AJ, Jensen KF. 2006. *In situ* measurement of bioluminescence and fluorescence in an integrated microbioreactor. *Biotechnol Bioeng* 93:40-47.
- Zhao JB, Wei DZ, Tong WY. 2007. Identification of *Escherichia coli* host cell for high plasmid stability and improved production of antihuman ovarian carcinoma x antihuman CD3 single-chain bispecific antibody. *Appl Microbiol Biotechnol* 76:795-800.
- Zheng S, Friehs K, He N, Deng X, Li Q, He Z, Xu C, Lu Y. 2007. Optimization of medium components for plasmid production by recombinant *E. coli* DH5 $\alpha$  pUK21CMV $\beta$ 1.2. *Biotechnol Bioprocess Eng* 12:213-221.
- Zielenkiewicz U, Ceglowski P. 2001. Mechanisms of plasmid stable maintenance with special focus on plasmid addiction systems. *Acta Biochim Pol* 48:1003-1023.
- Zor T, Selinger Z. 1996. Linearization of the Bradford protein assay increases its sensitivity: Theoretical and experimental studies. *Anal Biochem* 236:302-308.

# Appendix A

---

## Theoretical yield of plasmid DNA

As increasingly higher yields of plasmid DNA are produced, it is important to understand whether or not the reported yields are approaching a theoretical maximum or if there is room for further improvement. A recent article by Cunningham et al. (2009) used metabolic flux analysis to estimate the maximum theoretical yield of a 3.3 kb plasmid in *E. coli*. They found that the optimal conditions for plasmid DNA production were zero pyruvate kinase (Pyk) flux, no antibiotic resistance marker production, no acetate production, and expression of a nicotinamide nucleotide transhydrogenase to produce NADPH from NADH. Under these conditions, the predicted yield of plasmid DNA was 592 mg/g dry cell weight. The highest specific yield reported in the literature is 51 mg/g DCW (Williams et al., 2009b), and values on this order were predicted by the Cunningham model when fluxes representative of plasmid-bearing *E. coli* JM101 were used. Hence, it may be possible to achieve a 10-fold improvement in specific yield using metabolic and genetic engineering strategies.

However, there may be a limitation in the amount of physical space available to plasmid DNA in the cell at the high theoretical yields predicted by the Cunningham model. We calculated the approximate cellular volume occupied by 592 mg/g dry cell weight using estimates of *E. coli* cell volume and chromosome size. The volume of the *E. coli* cytoplasm ( $V_{cyto}$ ) fluctuates with medium osmolality, but at 0.28 osm (near optimal value for *E. coli* growth)  $V_{cyto}$  has been estimated to be  $6.3 \times 10^{-10}$   $\mu\text{L}$  per cell (Cayley et al., 1991). About 1% of this volume is occupied by DNA in cells without plasmid (Sundararaj et al., 2004), so the volume occupied by the genome(s) is approximately:

$$V_{gDNA} = 0.01 \times V_{cyto} = 0.01 \times 6.3 \times 10^{-10} \mu\text{L} = 6.3 \times 10^{-12} \mu\text{L}$$

The number of chromosomes in an *E. coli* cell varies considerably with growth rate and phase, but for this analysis we assumed two chromosomes per cell. The volume occupied by a DNA base pair in the cell was calculated by dividing  $V_{gDNA}$  by the number of basepairs (n) in two *E. coli* chromosomes:

$$\frac{Volume}{bp} = \frac{V_{gDNA}}{2n} = \frac{6.3 \times 10^{-12} \mu L}{2(4.69 \times 10^6 bp)} = 6.72 \times 10^{-19} \frac{\mu L}{bp}$$

The maximum specific yield of 592 mg/g reported by Cunningham et al. (2009) corresponds to about 48,500 copies/cell or  $1.60 \times 10^8$  bp/cell using the conversion factors of  $3.0 \times 10^{-13}$  g dry weight per cell (Neidhardt and Umbarger, 1996), a basepair molecular weight of 660 g/mol, and the plasmid size of 3337 bp. Combining this copy number with the volume/bp calculation shown above, the volume occupied by the plasmids is about  $1.08 \times 10^{-10}$   $\mu$ L. This corresponds to about 17% of the cytoplasmic volume of the cell. Since 70% of a plasmid-free *E. coli* cytoplasm is occupied by water (Neidhardt and Umbarger, 1996), it could be argued that occupying 17% of the cytoplasm with pDNA would not be detrimental enough to the cell to limit pDNA production. Occupation of cytoplasmic volume by pDNA would, however, reduce the free volume of water in the cell due to an increase in bound water via hydration of the plasmid molecules, which could negatively impact other molecular interactions in the cell.

# Appendix B

## Plasmid feature maps

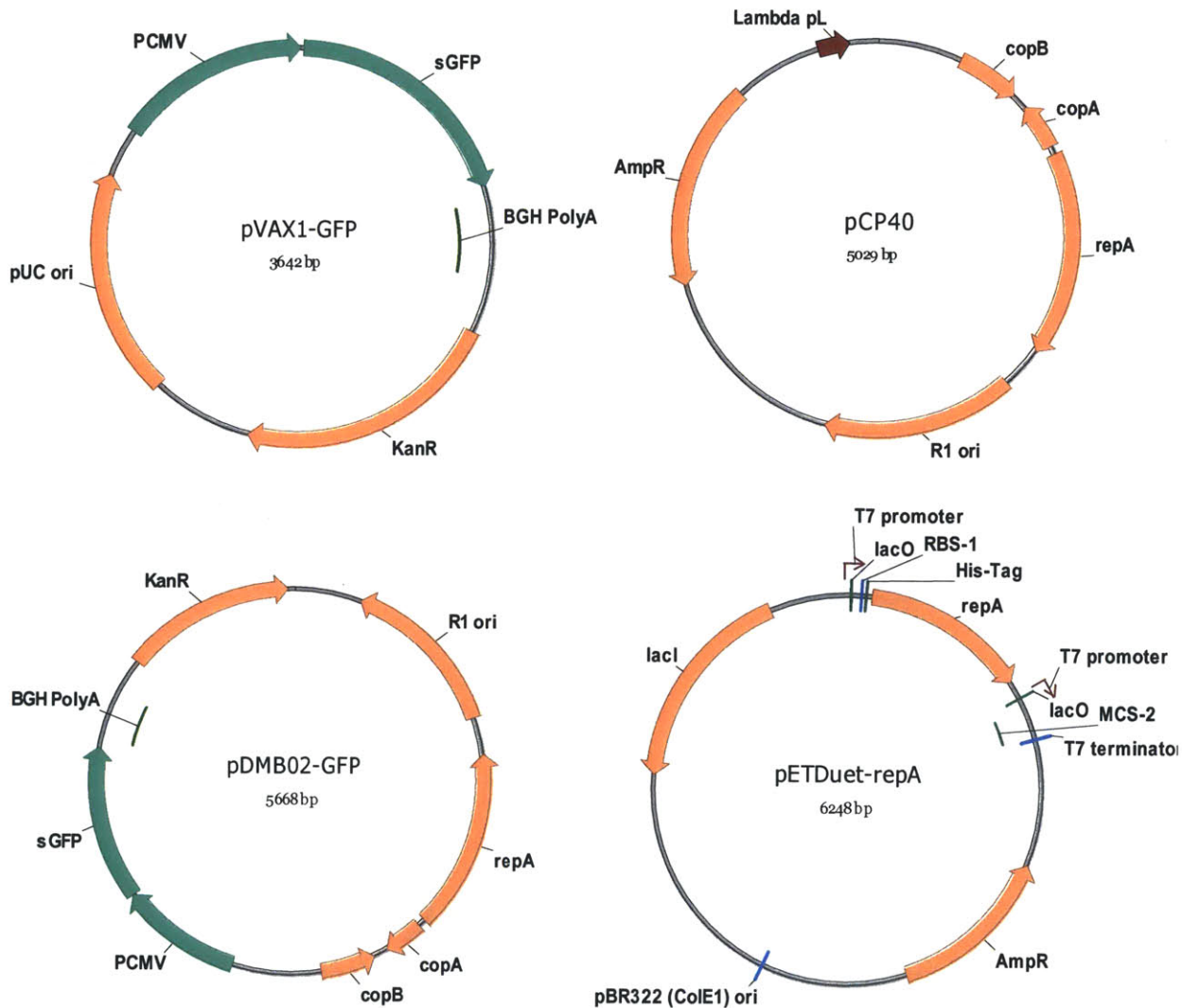


**Figure B-1:** Plasmid feature maps. pVAX1-GFP is a pUC-based DNA vaccine vector used in the microbioreactor studies described in Chapter 2, as well as for comparison to the R1-based DNA vaccine vectors described in Chapter 3. pCP40 (Remaut et al., 1983) was used in Chapter 3 as the source of the runaway R1 replicon. pDMB02-GFP is the runaway R1-based DNA vaccine vector that was constructed and characterized in Chapters 3 and 4. A derivative of pDMB02-GFP with a GTG-to-ATG mutation in the start codon of *repA* was also constructed (feature map not shown). Finally, pETDuet-*repA* was constructed by cloning *repA* into the expression vector pETDuet-1 (EMD Millipore; feature map not shown) to overexpress RepA protein as a positive control for the Western blots in Chapter 3.

**Table B-1:** Abbreviations used in plasmid feature maps

| <b>Abbreviation</b>                     | <b>Feature description</b>   |
|---|--|
| PCMV                                    | Human cytomegalovirus immediate-early promoter/enhancer              |
| BGH PolyA                               | Bovine growth hormone polyadenylation signal                         |
| sGFP                                    | Gene encoding superfolder green fluorescent protein                  |
| KanR                                    | Gene conferring kanamycin resistance                                 |
| pUC ori<br>pBR322 (ColE1) ori<br>R1 ori | Plasmid origins of replication                                       |
| Lambda pL                               | Phage lambda major leftward promoter                                 |
| AmpR                                    | Gene conferring ampicillin resistance ( <i>bla</i> )                 |
| copB                                    | Repressor of <i>repA</i> promoter (R1 ori)                           |
| copA                                    | Antisense RNA repressor of <i>repA</i> (R1 ori)                      |
| repA                                    | Replication initiation protein (R1 ori)                              |
| T7 promoter                             | Promoter responsive to T7 RNA polymerase                             |
| lacO                                    | <i>lac</i> operator (binding site for <i>lacI</i> )                  |
| lacI                                    | Gene encoding <i>lac</i> repressor (binds to <i>lacO</i> site)       |
| RBS-1                                   | Ribosome binding site for first multiple cloning site in Duet vector |
| His-Tag                                 | 6X Histidine tag   |
| MCS-2                                   | Second multiple cloning site in Duet vector                          |